FINAL TECHNICAL REPORT

Development of a Simplified Reliability-Based Method for Liquefaction Evaluation

USGS Grant Number: 02HQGR0058

M. Gutierrez, J. M. Duncan, C. Woods and M. Eddy
Civil and Environmental Engineering
Virginia Polytechnic Institute & State University
200 Patton Hall, Blacksburg, VA 24061

NEHRP Element: PT

Research supported by the U.S. Geological Survey (USGS), Department of the Interior, under USGS award number: M. Gutierrez and J.M. Duncan, 02HQGR0058. The views and conclusions contained in this document are those of the authors and should not be interpreted as necessarily representing the official policies, either expressed or implied, of the U.S. Government.

December 10, 2003

NON-TECHNICAL SUMMARY

Despite major uncertainties, evaluation of liquefaction potential of soils is still routinely carried out deterministically in practice. This is attributed to the lack of familiarity among geotechnical engineers, who perform most liquefaction evaluations, of the concepts and procedures in reliability theory, and the lack of data to carry out probabilistic analyses. A review of probabilistic liquefaction evaluation procedures also reveals that there is currently no comprehensive approach that accounts for all sources of uncertainties in liquefaction evaluations. Usually, only seismic demand is analyzed stochastically while analysis of seismic capacity is carried out deterministically. Moreover, available probabilistic methods do not take into consideration recent improvements in the state-of-the-art in liquefaction evaluation. The objective of the study summarized in this report is to develop a simplified reliability-based method for liquefaction evaluation. In the absence of attenuation relationships, determination of seismic demand is based on the USGS National Seismic Hazard Map together with a procedure to account for local site effects on ground surface acceleration. The proposed method clearly delineates the magnitudes of the uncertainties that arise from seismic sources, local site effects, liquefaction criteria and evaluation procedures, and variability in parameters.

Key Words: Liquefaction, Site Effects, Probabilistic Seismic Hazard, Amplification

ABSTRACT

Despite major uncertainties, evaluation of liquefaction potential of soils is still routinely carried out deterministically in practice. Methods for probabilistic and statistical liquefaction risk analysis have been available for more than two decades, but their use has been limited to critical facilities. This is attributed to the lack of familiarity among geotechnical engineers, who perform most liquefaction evaluations, of the concepts and procedures in reliability theory, and the perceived lack of data to carry out with probabilistic analyses. A review of probabilistic liquefaction evaluation procedures also reveals that there is currently no comprehensive approach that accounts for all sources of uncertainties in liquefaction evaluations. Usually, only seismic demand is analyzed stochastically while analysis of seismic capacity is carried out deterministically. Moreover, available probabilistic methods do not take into consideration recent improvements in the state-of-the-art in liquefaction evaluation.

This report present a reliability-based method for liquefaction evaluation based on the Seed and Idriss "simplified procedure" for deterministic liquefaction evaluation (using SPT and CPT results), and the Taylor Series Reliability Method to determine the probability of liquefaction at a given site. The Taylor Series method is easy to use and employs parameters that are familiar to geotechnical engineers. Determination of seismic demand is based on the USGS National Seismic Hazard Map together with simple procedures to account for local site effects on ground surface acceleration. The method clearly delineates the magnitudes of the uncertainties that arise from seismic sources, local site effects, liquefaction criteria and evaluation procedures, and variability in parameters.

The uncertainties in the variables, model assumptions, and procedures involved in the "simplified procedure" for liquefaction evaluation are catalogued and analyzed. A database of parameters required in the "simplified procedure" and a range of coefficients of variation (*COV*'s) for these parameters are established. The recommend *COV*'s can be used in the absence of project or site-specific data on the uncertainty of the different parameters required in the "simplified procedure." The reliability-based procedure is implemented in an Excel worksheet. Application to example case studies illustrates the use of the proposed liquefaction evaluation procedure.

The procedure outlined in this report can be used to reduce losses from earthquakes in the US by improving current procedures for probabilistic liquefaction evaluation, and making such procedures accessible to practicing engineers. By providing a measure of the risk of liquefaction, engineers can make better decisions on measures to mitigate liquefaction based on the degree of uncertainty and the consequences of liquefaction. By using the proposed procedure, engineers will be able to evaluate the parameters that contribute significantly to the uncertainty and devise means to reduce the uncertainty in the evaluation. Also, by making probabilistic procedures easily available to engineers, it is hoped that estimates of probability of liquefaction can be combined with increasing data and case histories on the consequences of liquefaction to provide an improved measure of liquefaction risk and improved procedures for liquefaction evaluation.

Acknowledgement

Assistance, valuable comments and discussions from Prof. I.M. Idriss, University of California, Davis, are gratefully acknowledged.

TABLE OF CONTENTS

1. BACKGROUND 1
1.1 Introduction 1
1.2 Objectives and Relevance to NEHRP Priorities 4

2. REVIEW OF PREVIOUS STUDIES 6

3. METHODS AND PROCEDURES 12
3.1 Probability of Liquefaction 12
3.2 Procedures for Estimating Variability 12
3.3 Determination of Conditional Probability of Liquefaction, P_L 14

4. SEISMIC DEMAND 17
4.1 Required Parameters to Determine Seismic Demand 17
4.2 Determination of *PGA* and *SA* from the USGS Seismic Hazard Web Page 17
4.3 Determination of M_w and *ED* from the USGS Seismic Hazard Web Page 20
4.4 Determination of Amplification Factors, F_a 22

5. ENVIRONMENTAL FACTORS 29
5.1 Dry and Moist Unit Weights 30
5.2 Buoyant Unit Weights 34
5.3 Percentage of Fines, *FC* 36

6. CYCLIC STRESS RATIO (CSR) PARAMETERS 39
6.1 Depth Reduction Factor, r_d 39
6.2 Magnitude Scaling Factor, *MSF* 44
6.3 Overburden Correction Factor, K_σ , for SPT Analysis 45
6.4 Overburden Correction Factor, K_σ , for CPT Analysis 50
6.5 Correction Factor for Sloping Ground, K_α 52

7. CYCLIC RESISTANCE RATIO (CRR) FOR SPT DATA 53
7.1 Overburden Correction Factor, C_N 54
7.2 Energy Correction Factor, C_E 57
7.3 Rod Length Correction Factor, C_R 58
7.4 Sampler Correction Factor, C_S 60
7.5 Borehole Diameter Correction Factor, C_B 60
7.6 Summary 61

8. CRR FOR CPT DATA 63
8.1 CPT Tip Resistance, q_c, and Sleeve Resistance, f_s 65
8.2 Nonlinear Stress Exponent, *n* 66
8.3 Overburden Correction Factor, C_Q 67
8.4 CPT Grain Characteristics Correction Factor, K_c 69

9. EXCEL IMPLEMENTATION 71

10. SUMMARY AND CONCLUSIONS 74

11. REFERENCES 78

APPENDIX A – SPT AND CPT EXCEL WORKSHEETS 83

APPENDIX B– EXAMPLE PROBLEMS 84

1 - BACKGROUND

1.1 – Introduction

The most commonly used method to evaluate liquefaction potential of a site is the "simplified procedure" originally developed by Seed and Idriss (1971). The method has been modified and improved on several occasions since it was developed. The current "simplified procedure" calculates the factor of safety, *FS*, against liquefaction in terms of the cyclic stress ratio, *CSR* (the demand), and the cyclic resistance ratio, *CRR* (the capacity), according to:

$$FS = \left(\frac{CRR_{7.5}}{CSR} \right) MSF \cdot K_{\sigma} \cdot K_{\alpha} \qquad (1\text{-}1)$$

where $CRR_{7.5}$ is the cyclic resistance ratio for magnitude 7.5 earthquakes, *MSF* is the magnitude scaling factor, K_{σ} is the overburden correction factor, and K_{α} is the correction factor for sloping ground. *CSR* is estimated using the Seed and Idriss (1971) equation:

$$CSR = 0.65 \left(\frac{a_{\max}}{g} \right) \left(\frac{\sigma_{vo}}{\sigma'_{vo}} \right) r_d \qquad (1\text{-}2)$$

where a_{max} is the peak horizontal acceleration at the ground surface generated by the earthquake, g is acceleration due to gravity, σ_{vo} and σ'_{vo} are the total and effective overburden stresses, respectively, and r_d is the stress reduction coefficient. The three most routinely used methods to evaluate the liquefaction resistance, *CRR*, are: 1) using the Standard Penetration Test (SPT), 2) using the Cone Penetration Test (CPT), and 3) using seismic shear wave velocity, V_s. A review of the current state-of-practice in liquefaction evaluation based on the simplified procedure is given in Youd and Idriss et. al. (2001).

The two main issues in the development of probabilistic methods for liquefaction risk analysis based on the simplified procedure are: 1) the uncertainty in demand particularly the maximum acceleration a_{max}, and the earthquake magnitude, M_w, required to estimate the magnitude scaling factor *MSF*, and 2) the uncertainty in the capacity *CRR*. For the latter, the uncertainties are due to the natural variability of soil and geotechnical properties, in-situ testing procedures, and most importantly, the simplified method. Probabilistic liquefaction analysis has often been treated from the separate points of view of seismologists, geotechnical engineers and experts in probability and statistics. Rarely has probabilistic liquefaction analysis been treated as a multi-disciplinary problem. Based on the two categories of uncertainty described above, Table 1.1 lists the parameters which have been identified as sources of uncertainty within the simplified liquefaction analysis. The contribution of each parameter to the overall uncertainty of the analysis is discussed in the indicated sections.

Table 1.1 - Parameters Identified as Part of the Simplified Liquefaction Analysis

PARAMETERS	SECTION
Seismic Parameters	
Ground Acceleration, a_{max}	4
Magnitude, M_w	4
Epicentral Distance, *ED*	4
Site Amplification Factors, F_a	4
Environmental Parameters	
Unit Weight of Soil, γ	5
Buoyant Unit Weight of Soil, γ_b	5
Fines Content, *FC*	5
CSR Parameters	
Depth Reduction Factor, r_d	6
Magnitude Scaling Factor, *MSF*	6
Overburden Correction Factor, K_σ	6
Sloping Ground Correction Factor, K_α	6
CRR Parameters for SPT	
SPT *N*-value	7
SPT *N*-value Correction Factors, C_N, C_E, C_B, C_R, and C_S	7
Percentage of Fines, *FC*	7
CRR Parameters for CPT	
CPT q_c and f_s-value	8
Linear Stress Exponent, *n*	8
CPT Correction Factors, C_Q and K_c	8
CPT Soil Behaviour Type Index, I_c	8

As discussed in Section 2, several models for probabilistic seismic demand have been developed, and usually analysis of capacity is carried out deterministically in conjunction with probabilistic analysis of the ground shaking (e.g., Youd and Perkins 1978, Atkinsons et al. 1984, Todorovska 1998). Procedures that evaluate probabilistic seismic capacity often deal only with specific aspects of the liquefaction evaluation. For instance, the procedures of Liao et al. (1988), and Youd and Noble (1997) deal mainly with the statistical and probabilistic analysis and probabilistic analyses of field data based on SPT measurements. Probabilistic *CRR* vs. SPT blow count curves have been developed that are more rigorous in delineating liquefaction and non-liquefaction in terms of probabilities than the original deterministic simplified procedure. However, other important uncertainties have not been included in probabilistic liquefaction evaluation. In addition to the need to statistically analyze the data used in the *CRR* vs. SPT blow count criterion (or CPT and V_s-based criteria), there are significant uncertainties in the empirical correction factors that are used in the procedure.

Another important source of uncertainty is the natural variability of soil properties. This variability is manifested mainly in the scatter in the SPT blow count. This variability has

been accounted in the liquefaction potential mapping of San Francisco, California by Kavazanjian et al. (1985) and of Charleston, South Carolina by Elton and Jadj-Hamou (1990). In comparison, Liao et al. (1988) use the minimum SPT blow count measured in granular layers as the critical blow count for their analysis. In terms of SPT blow counts alone, it appears that there is a lack of consistent treatment of uncertainties in dealing with probabilistic liquefaction evaluation.

Current probabilistic liquefaction criteria are based mainly on the SPT, although other tests like CPT and V_s measurements are increasingly being used. With the increasing CPT and V_s database, it is now possible to establish probabilistic liquefaction criteria for CPT and V_s measurements as well, and for combinations of test results from different in situ tests.

Finally with the publication of the USGS, National Seismic Hazard Map and its availability on the internet, it is now possible for practicing engineers to perform probabilistic seismic hazard evaluations for routine projects. This possibility should be exploited in the development of a simple probabilistic liquefaction evaluation procedure.

Despite the significant uncertainties in the different variables involved in the above method, liquefaction risk in practice is still rooted in deterministic analysis. Methods for probabilistic and statistical liquefaction risk analysis have been proposed since the late 1970's, but they are complex, and they have been used mainly for important projects and critical facilities. While there have been tremendous strides in the development of probabilistic seismic demand and risk analysis in other fields, application of probabilistic liquefaction analysis is still beyond the normal practice of most geotechnical engineers. Reliability calculations provide a means of evaluating the combined effects of uncertainties, and a means of distinguishing between conditions where uncertainties are particularly high or particularly low. Reliability analyses also provide a logical framework for choosing factors of safety that are appropriate for the degree of uncertainty and the consequences of failure.

Duncan (2000) discussed the reasons why reliability analysis has not been used in routine geotechnical practice. First, reliability theory involves terms and concepts that are not familiar to most geotechnical engineers. Second, it is commonly perceived that using reliability theory would require more data, time, and effort than are available in most circumstances. These concerns need to be addressed if probabilistic liquefaction evaluation procedures are to be more widely used in practice.

From the above discussions, it can be seen that there are several motivations for the development of a simplified reliability-based liquefaction evaluation procedure. These are:

1) Probabilistic methods need to be simplified and made easier to use.
2) A comprehensive probabilistic method that accounts for uncertainty in demand, uncertainty in the procedures for the liquefaction evaluation, and uncertainties in field geotechnical data needs to be developed.

3) Existing probabilistic methods need to be updated to account for new data and for improvements in the existing deterministic "simplified procedure" for liquefaction analysis.
4) Probabilistic methods need to be developed for SPT and CPT based procedures or from combinations of in situ test procedures, and
5) Probabilistic methods need to be made widely accessible to practicing engineers by using current advances in information technology.

1.2 - Objectives and Relevance to NEHRP Priorities

The main goal of the project described in this report is to develop a simplified reliability-based method to evaluate the liquefaction potential of soils. The project aims to reduce losses from earthquakes by improving current procedures for probabilistic liquefaction evaluation, and by making such procedures widely accessible to practicing engineers. In conjunction with traditional factors of safety, the reliability-based method presented in this report will provide measures of liquefaction risk, from which engineers can make better decisions on devising measures to mitigate liquefaction or to reduce the uncertainty in the evaluation.

The specific goals of the research described in this report are:

1) To develop a procedure that is easy to use and that employs concepts and parameters that are familiar to geotechnical engineers.
2) To clearly delineate and systematically analyze the magnitudes of the uncertainties involved in liquefaction evaluation that arise from different sources. These sources are: a) the seismic demand (source, magnitude and recurrence of earthquakes), b) the effects of local site conditions on seismic demand, c) the models and procedures used in the liquefaction criteria, and d) the variability in the parameters used in the evaluation procedure.
3) To link the procedure to an existing and broadly available web-based procedure for predicting seismic demand using the USGS National Seismic Hazard Map.
4) To implement the latest improvements and advances in field evaluation of soil liquefaction resistance (including the use of cone penetration test (CPT) and shear-wave velocity measurement) in the reliability-based procedure, in addition to the use of Standard Penetration (SPT) data.
5) To make the procedure generally available by providing a user-friendly computer code implementing the procedure.
6) To demonstrate the validity and value of the proposed procedure by applying it to cases of liquefaction and by comparing it with existing probabilistic liquefaction evaluation procedures.

The project addresses a topic that has been identified as a critical issue in several recent workshops and conferences on mitigation of earthquake geohazards. The project is in line

with the USGS Research Priorities for FY 2002, mainly Element I (Products for Earthquake Loss Reduction), and the topical area PT (Processes, Laboratory and Theoretical), which include basic and applied research that has potential for reducing earthquake hazard in many geographical areas. The research will address two of the tasks listed in the Research Priorities for FY 2002 in this topical area. These tasks are:

1) "*Collect field data and conduct laboratory experiments to improve understanding of the processes leading to liquefaction, lateral spreading, and slope failure during earthquakes*", and

2) "*Analyze existing data to identify the parameters and ground motion that control damage to structures, and investigate soil structure interaction*."

2 - REVIEW OF PREVIOUS STUDIES

In recent years, several studies have been conducted relating to probabilistic evaluation of soil liquefaction. The following tables summarize several previous studies that were reviewed as part of the current research.

Table 2.1- Fardis and Veneziano (1981)

REFERENCE
Fardis, M. N. and Veneziano, D. (1981), "Statistical Analysis of Sand Liquefaction," J. Geotech. Geoenvir. Engrg. ASCE, 107(10), 1361-1377.
TYPE OF STUDY
This study presents a statistical method of analyzing liquefaction potential of sands using the results of 192 published cyclic simple-shear tests.
PRINCIPAL FINDINGS
• In-situ liquefaction behavior of sand depends on grain size characteristics, relative density, soil structure, and previous static and dynamic stress history. • Bayesian regression is used as opposed to standard regression techniques because standard techniques cannot be used to estimate the coefficients used in this method from observed values because of the unreliability of laboratory determinations of relative density, D_r. • A model is determined based on laboratory conditions which account for uncertainties caused by effect of sample preparation, effect of system compliance, and stress non-uniformities. • This model is then converted to one applicable to field conditions after considering effect of in situ soil structure and multi-directionality of motion. • This model is only applicable to uniform, medium clean sands, because of the types of sand in the available data set.

Table 2.2 - Fardis and Veneziano (1982)

REFERENCE
Fardis, M. N. and Veneziano, D. (1982), "Probabilistic Analysis of Deposit Liquefaction," J. Geotech. Geoenvir. Engrg., ASCE, 108(3), 395-417.
TYPE OF STUDY
This study presents a probabilistic method of liquefaction analysis of horizontally layered sand deposits subject to vertically propagating seismic S waves.
PRINCIPAL FINDINGS
• The study presents three models for liquefaction analysis which are one-dimensional, and differ in the fact that they either neglect or include pore pressure diffusion and soil stiffness reduction. • Uncertainties with several parameters such as soil liquefaction resistance, cyclic stress-strain law, spatial variation of N-value and D_r and permeability and compressibility are discussed. • Method was as good a predictor of probability of liquefaction based on historical data.

Table 2.3- NRC Committee on Earthquake Engineering (1985)

REFERENCE
NRC (1985), "Liquefaction of Soils During Earthquakes," Report No. CETS-EE-001, National Research Council (NRC), Washington D.C.
TYPE OF STUDY
The study presents a general overview of probabilistic evaluation of potentially liquefiable soils. It presents a basic backbone for probabilistic evaluation and for quantifying some of the various uncertainties that can arise in liquefaction evaluation.
PRINCIPAL FINDINGS
• Probabilistic evaluations are tools to augment, but not replace, the assessment of risk by human judgment. • Overall probability of liquefaction is obtained by multiplying "conditional probability of liquefaction" (all loading conditions) by the probability of earthquake occurrence. • The basic model for probabilistic liquefaction evaluation is to integrate the following: conditional probability of liquefaction times probability distribution of soil resistance parameters times overall rate of earthquake occurrence. • Provides a general overview of methods of determining seismic activity rates, load parameters, and site characterization problems. • Suggests model uncertainties are a result of simplifications and assumptions made by the engineer. • Probabilistic methods are good because liquefaction risk can be compared in equivalent terms with other forms of risk to a structure.

Table 2.4 - Liao, Veneziano, and Whitman (1988)

REFERENCE
Liao, S.C., Veneziano, D. and Whitman, R. V. (1988), "Regression Models for Evaluating Liquefaction Probability," J. Geotech. Geoenvir. Engrg., ASCE, 114(4), 389-411.
TYPE OF STUDY
Presents a study in which four models were developed to analyze probability of liquefaction based on the data from 278 case studies from past earthquakes.
PRINCIPAL FINDINGS
• Study uses methods of statistical regression to quantify the probability of liquefaction as a function of given diagnostic parameters (distance to earthquake, a_{max}, *CSRN* (normalized *CSR*), depth of groundwater table, *GWT*, σ_{vo} and σ'_{vo}, corrected and field SPT *N*-values, fines content, *FC*, clay content, *CC*, gravel content, *GC*, and grain size at 50% passing, D_{50}). Models used goodness of fit statistics to produce probability contours. • The four models developed include two local models, where probability of liquefaction P_L is based on *CSRN* and $(N_1)_{60}$, and two source models in which P_L is based on epicentral distance *ED*, earthquake magnitude M_w, and $(N_1)_{60}$. Each of the two sets of models was developed for sands with fines and without fines where 12% was the critical value for fines content, *FC*. Each model had contours of P_L from 1% to 95%. • Study implies that SPT values do not always increase with increasing fines content. It also concludes that *FC* is the only gradation effect that significantly influences liquefaction potential. • Uses Iwasaki and Kawashima attenuation models to obtain acceleration based on M_w and *ED* for the *CSRN*-values which are used.

Table 2.5 - Hwang and Lee (1991)

REFERENCE
Hwang, H. H. M. and Lee, C. S. (1991), "Probabilistic Evaluation of Liquefaction Potential," Center for Earthquake Research and Information, Technical Report NCEER-91-0025, Memphis State University, Memphis, TN.
TYPE OF STUDY
Presents a probabilistic method of assessing the liquefaction potential of a site using SPT data from the President's Island, Memphis, Tennessee as an example.
PRINCIPAL FINDINGS
• The study uses a liquefaction potential probability matrix and a fragility curve based on moment magnitude to determine the probabilities of no, minor, moderate, and major liquefaction. • Includes uncertainties in both site parameters and seismic parameters to determine various earthquake-site models. • The Fourier Acceleration amplitude spectrum (non-linear site response analysis) is used to determine ground motions for each case. Synthetic horizontal time histories are generated based on a given spectrum. • A Factor of Safety based on SPT *N*-values is calculated in order to calculate a probability of liquefaction index, P_L, which measures the severity of liquefaction. • The shear stresses calculated by this method are close to those obtained by using the simplified method. • For earthquakes with magnitudes M_w>7.5, the P_L calculated by the method is much larger than that obtained by the simplified method, whereas the opposite is true for earthquakes with M_w<6.5. The results for an earthquake with M_w=7.0 are comparable.

Table 2.6 - Rahman and El Zahaby (1997)

REFERENCE
Rahman, M. S. and El Zahaby, K. M. (1997), "Probabilistic Liquefaction Risk Analysis Including Fuzzy Variables," Soil Dynamics and Earthquake Engineering., 16(1), 63-79.
TYPE OF STUDY
The study presents a probabilistic method of evaluating liquefaction potential at a site, based on a list of 12 fuzzy variables.
PRINCIPAL FINDINGS
• The paper presents a framework for incorporating fuzzy variables characterized by non-statistical uncertainty into probabilistic liquefaction risk analysis. • The fuzzy variables include such parameters as soil density, *N*-value, low permeability layers, depth, layer thickness, type of deposit, ground water table *GWT*, gradation, and grain size. • The fuzzy variables that are applicable to the site are graded from A to E, with A being the most important. The variables are then transformed into a fuzzy number which is a weighted average of all sites being evaluated. • The uncertainty of the fuzzy number, called entropy in this instance, is the measure of the uncertainty of a random variable. • The probability of liquefaction is then calculated using the uncertainties previously calculated from the transformed fuzzy numbers using integration.

Table 2.7 - Juang, Rosowsky, and Tang (1999)

REFERENCE
Juang, C. H., Rosowsky, D. V. and Tang, W. H. (1999), "Reliability-Based Method for Assessing Liquefaction Potential of Soils," J. Geotech. Geoenvir. Engrg., ASCE, 125(8), 684-689.
TYPE OF STUDY
Presents a probabilistic method of assessing the liquefaction potential of sandy soils based on a case study of CPT data from Moss Landing in Monterey Bay, California. *(Spreadsheet Available for CPT Data)*
PRINCIPAL FINDINGS
• The cyclic shear stress ratio *CSR* is calculated using Seed and Idriss' method with r_d as a non-random variable and maximum surface acceleration a_{max}, earthquake magnitude M_w, total vertical stress σ_{vo}, and effective vertical stress σ'_{vo} being treated as random variables. Each variable was assigned a coefficient of variation, *COV*. The cyclic resistance ratio *CRR* for this paper was determined with Robertson and Wride's method. • A reliability index, β, was determined for each case, with all random variables being assumed to be normally distributed. The reported values used for the variables in this example were taken to be mean values. The distribution of β values could be fit well using the Rayleigh distribution. • The probability of liquefaction was determined at each point, and the results indicated that probabilistic analysis does not yield an advantage over the deterministic method. (i.e. a site with a P_L of 0.008 had liquefied.) • The authors used the following coefficients of variation for the described reliability study: $a_{max} \rightarrow 0.15$, $M \rightarrow 0.05$, $\sigma_v \rightarrow 0.10$, $\sigma'_v \rightarrow 0.15$, $q_c \rightarrow 0.15$, $f_s \rightarrow 0.20$, *CRR* model → 0.10

Table 2.8 - Whitman (2000)

REFERENCE
Whitman, R. V. (2000), "Organizing and Evaluating Uncertainty in Geotechnical Engineering," J. Geotech. Geoenvir. Engrg., ASCE, 126(7), 583-593.
TYPE OF STUDY
The paper presents an outline as to the types of uncertainty present in Geotechnical Engineering and presents some basic ideas as to how to evaluate them.
PRINCIPAL FINDINGS
• Different analyses can be used for the 4 stages of a project: 1) site evaluation and characterization; 2) design evaluation; 3) decision making; 4) construction control. • Data scatter and systematic errors are the primary sources of uncertainty in site evaluation. • When evaluating risk, it is important to realize that not all procedures are appropriate for all projects, and that model error is a major source of evaluation uncertainty. • Multiplying the probability of an earthquake occurrence with the P_L given the earthquake will give an overall probability of liquefaction (based on Liao et al. 1988). A time averaged probability can then be computed by adding the probabilities of different M_w values. • Data concerning the consequences of liquefaction can potentially be combined into an analysis leading to the probability of some damaging amount of movement. • Probabilistic methods should be used together with traditional evaluation methods, rather than separately.

Table 2.9 - Juang, Chen, and Jiang (2001)

REFERENCE
Juang, C.H., Chen, C.J. and Jiang, T. (2001), "Probabilistic Framework for Liquefaction Potential by Shear Wave Velocity," J. Geotech. Geoenvir. Engrg., ASCE, 127(8), 670-678.
TYPE OF STUDY
This study presents two ideas. First, a new method of determining *CRR* is determined using a database of 225 cases. Secondly, a probabilistic method of evaluating liquefaction potential is developed based upon the *FS* calculated deterministically.
PRINCIPAL FINDINGS
• The paper discusses the current methods of evaluating liquefaction potential of soils based on the results of V_s tests. • A new equation for the *CRR* of a site was developed using a database containing information from 26 earthquakes and in situ measurements from over 70 sites, resulting in 225 case studies. • The new *CRR* equation was developed using a neural network to find points on the unknown liquefaction boundary curve. • A single clean-sand equivalence curve was established where clean sand has a fines content, $FC \leq 5\%$. • A mapping function to determine P_L, based on the deterministically calculated *FS* was obtained through regression of (FS, P_L) pairs. • The mapping function approach is based on the deterministic method and the field data used. The empirical data equation for *CRR* must be used along with the associated *CSR* equation.

Table 2.10 - Lew (2001)

REFERENCE
Lew, M. (2001), "Guidelines for Analyzing and Mitigating Soil Liquefaction," Proc. the Ohio River Valley Soils Seminar XXXII, Louisville, KY, October 24.
TYPE OF STUDY
Presents and overview of liquefaction analysis of soils including preliminary screening methods, field investigation methods, determination of ground motions for analysis using the USGS website, and methods of mitigation liquefaction hazard.
PRINCIPAL FINDINGS
• The main objective of the paper is to inform practitioners about the present state-of-practice in liquefaction analysis and mitigation. • Provides an outline of a screening procedure to be used to determine if a site needs an in-depth liquefaction analysis. • The outline of in-situ testing used in liquefaction analysis is the same as the methods outlined in the 1997 NCEER proceedings, but recommends that all sites are evaluated for liquefaction to a depth of at least 50 feet below grade. • Outlines the determination of ground motions based on the output of the USGS Geohazards website. This discussion includes the description of the difference between deterministic and probabilistic methods of determining ground motion. • Discusses hazard assessment in terms of types of possible failures and the consequences of each kind.

Table 2.11 - Juan, Jiang, and Andrus (2002)

REFERENCE
Juang, C.H., Jiang, T. and Andrus, R. D. (2002), "Assessing Probability-Based Methods for Liquefaction Potential Evaluation," J. Geotech. Geoenvir. Engrg., ASCE, 128(7), 580-589.
TYPE OF STUDY
This study presents an assessment of existing and new probabilistic methods for liquefaction potential evaluation, with emphasis being placed on comparison of probabilities of liquefaction calculated with two different approaches, logistic regression and Bayesian mapping.
PRINCIPAL FINDINGS
• The methods and procedures for probabilistic analysis presented by this paper can be applied to all simplified methods. • The equation for determining liquefaction probability established through logistic regression has nothing to do with any deterministic methods. • Liquefaction probabilities interpreted from Bayesian mapping functions are comparable with those interpreted from the results of logistic regression. • Bayesian mapping preserves the characteristics of a particular deterministic method under consideration and provides an easy transition from *FS* design to P_L design, thus it is the preferred approach. • All deterministic methods should be calibrated so that the calculated *FS* can readily be mapped to the probability of liquefaction, and thus the *FS* for design can be readily selected based on a specified level of risk.

3 - METHODS AND PROCEDURES

3.1 Probability of Liquefaction

Probability of liquefaction is calculated from the joint probability of the conditional probability of liquefaction, P_L, and the probability distribution of the earthquake load parameters:

$$P(FS=1) \approx \lambda T \int_{\Omega} \int_{\Psi} P(FS=1|\Omega,\Psi) \cdot g(\Psi) d\Psi d\Omega \qquad (3\text{-}1)$$

where $P(FS=1)$=probability of liquefaction, $P(FS=1|\Omega,\Psi)=P_L$ =conditional probability of liquefaction (i.e., probability of liquefaction given all other loading conditions for the evaluation of liquefaction), $g(\Psi)$=probability distribution of the earthquake load parameters (accounts for uncertainty in earthquake magnitude, distance, acceleration and amplification), λ=overall rate of occurrence (e.g., number of earthquakes per year) from all potential seismic sources within the vicinity of the project site, T=time period, $\Psi=\Psi(a_{\max}, M_w, ED)$= vector of load parameters $\Omega=\Omega((N_1)_{60}, F_c, ...)$= vector of liquefaction resistance parameters

The latest version of the "simplified procedure", as embodied in the “NCEER Report” (Youd and Idriss et al. 2001) will be used as the basis for the probabilistic procedure. The parameters involved in the "simplified procedure" will be treated as random variables. For most parameters, a normal distribution will be assumed, with each parameter having a mean value (or most likely value) and a standard deviation, although the assumption of normally distributed variables will not be a requirement. Model and procedural uncertainties will also be accounted for in the reliability-based approach. The uncertainties in the seismic demand parameters will be treated separately using the USGS National Seismic Hazard Map with a newly developed procedure to account for local site effects on ground surface acceleration. The procedure will be developed for SPT and CPT tests.

3.2 – Procedures for Estimating Variability

In calculating the standard deviation of a parameter for use in a probabilistic analysis, several methods can be used as outlined by Duncan (2000). These methods include computing the standard deviation from available data, using previously published values, and the “Three-Sigma Rule” by Dai and Wang (1992).

In determining the standard deviation for the different parameters that are involved in the Simplified Method of Liquefaction Evaluation, the “Three-Sigma Rule” is the method primarily used. This rule uses the fact that 99.73% of all values for a normally distributed parameter fall within three standard deviations of the average. Thus the average plus three standard deviations and the average minus three standard deviations represent rare extremes that are realized less than 0.3% of the time. In practical terms, these can be

viewed as the "highest conceivable value" and "lowest conceivable value." The "Three-Sigma Rule" uses estimates of these extreme values to estimate the standard deviation as follows:

$$\sigma = \left(\frac{HCV - LCV}{6} \right) \tag{3-2}$$

where σ = standard deviation, *HCV* = highest conceivable value, and *LCV* = lowest conceivable value.

In a discussion of Duncan (2000), Christian and Baecher (2001) pointed out the difficulty of estimating sufficiently wide extremes for a given parameter. As a result of this, the highest and lowest conceivable values might not actually be being used, causing error in the calculation. One way of addressing this issue is by using a value smaller than 6 in the denominator, as shown by equation (3-3), since using values which were not actually the *HCV* and *LCV* would account for less than 99.73% of the values in the sample.

$$\sigma = \left(\frac{HCV - LCV}{N_n} \right) \tag{3-3}$$

where N_n is the value of denominator based on sample size. Christian and Baecher (2001) point to work by Burlington and May (1970), which suggests that standard deviation is a function of sample size for smaller samples. Table 3.1 provides values to use as N_n in equation (3-3) for smaller samples.

Table 3.1 - Standard Deviations Based on Sample Size (Burlingtion and May, 1970)

n	N_n	N	N_n
2	1.1	9	3.0
3	1.7	10	3.1
4	2.1	11	3.2
5	2.3	12	3.3
6	2.5	20	3.7
7	2.7	30	4.1
8	2.9		

Note: n is the sample size, and N_n is the value of the denominator in equation (3-3).

Once the standard deviation of a parameter has been established, the final step is to calculate the *COV* for each parameter. This is done using the following formula:

$$COV = \left(\frac{\sigma}{Average} \right) \tag{3-4}$$

in which the denominator is simply the average of the sample.

This calculation is used in determining how much a given parameter contributes to the overall uncertainty of the entire analysis.
Additional methods of determining the standard deviation as proposed by Duncan (2000) include:

- Direct calculation from data - if sufficient data are available, the standard deviation can be obtained from the following equation:

$$\sigma = \sqrt{\frac{\Sigma(x_i - \bar{x})}{N-1}} \tag{3-5}$$

  where $\bar{x}$ is the average value, x_i is the ith value of the parameter, and N is the number of data.

- From published values - there is now an increasing database on the variability of many geotechnical engineering parameters and in situ tests. *COV* values of several geotechnical parameters and in situ tests are given in Duncan (2000). For instance, the *COV* for SPT blow count N is estimated to be from 15-45% (Harr 1984, Kulhawy 1992). Given the *COV* and $\bar{x}$, the σ of a parameter can be calculated as:

$$\sigma = COV \cdot \bar{x} \tag{3-6}$$

3.3 – Determination of Conditional Probability of Liquefaction, P_L

The conditional P_L is calculated using the Taylor Series Reliability Method (Wolff 1994; USACE 1997, 1998; Duncan 2000). In this method, conditional P_L is evaluated using the following steps:

1) Calculate the most likely value of factor of safety, F_{MLV}, using the best estimate of the values of all the parameters required in equations (1-1) and (1-2).

2) Estimate the standard deviations of the quantities involved in equations (1-1) and (1-2). Methods for estimating the standard deviations are discussed above.

3) For each of the parameters i, calculate the factors of safety F_i^+ and F_i^- corresponding to the best estimate of the parameter i increased by one standard deviation and decreased by a similar magnitude, respectively. In calculating F_i^+ and F_i^-, all the other variables are kept at their most likely values.

4) Using the Taylor series technique, estimate the standard deviation and coefficient of variation of the factor of safety, σ_F, using the formula:

$$\sigma_F = \sqrt{\left(\frac{\Delta F_1^2}{2}\right) + \left(\frac{\Delta F_2^2}{2}\right) + \left(\frac{\Delta F_3^2}{2}\right) + \ldots + \left(\frac{\Delta F_n^2}{2}\right)} \tag{3-7}$$

and

$$V_F = \frac{\sigma_F}{F_{MLV}} \tag{3-8}$$

in which $\Delta F_i = F_i^+ - F_i^-$, and n is number of variables involved in the calculation of P_L and V_F is the coefficient of variation of the factor of safety.

5) Using F_{MLV} and V_F, the conditional probability of liquefaction is determined assuming a log-normal distribution of the factor of safety. This requires the calculation of a log-normal reliability index, β_{LN}, using the formula:

$$\beta_{LN} = \frac{\ln\left(\frac{F_{MLV}}{\sqrt{1+V_F^2}}\right)}{\sqrt{\ln\left(1+V_F^2\right)}} \tag{3-9}$$

6) Using β_{LN}, the conditional probability of liquefaction, $P_L = P\left(FS = 1 \middle| \Omega, \Psi\right)$, can be determined using tables for standard cumulative normal distribution, which can be found in textbooks in probability and reliability, or calculated from built-in statistical functions in Excel. The standard cumulative normal distribution can also be programmed directly. Using Excel, Duncan (2000) has developed a table giving values of probability as function of F_{MLV} and V_F.

A note should be given on the determination of *COV*'s of parameters which vary linearly against another variable. It can be shown that using suitable transformations, a constant *COV* can be obtained for these parameters over their entire range of values. Consider for instance, the stress reduction factor, r_d, whose average, $-1\cdot\sigma$ and $+1\cdot\sigma$ values can be approximated by linear functions up to a certain depth, z:

$$\left(r_d\right)_{ave} = 1 - a\cdot z\,,\ \left(r_d\right)_{-\sigma} = 1 - b\cdot z\ \ ,\ \left(r_d\right)_{+\sigma} = 1 - c\cdot z$$

where a, b and c are constants. Using equations (3-2) and (3-4), the *COV* of r_d can be calculated as:

$$\mathrm{COV}\left(r_d\right) = \frac{(b-c)z}{\left(1 - a\cdot z\right)6} \tag{3-10}$$

As can be seen, *COV* (r_d) varies linearly with z. On the other hand, the *COV* of 1- r_d can be shown to be constant:

$$COV(1 - r_d) = \frac{(b - c)z}{c \cdot z} = \frac{b - c}{a \cdot 6} \tag{3-11}$$

Note that the approach can also give a reasonably constant *COV* even if the parameter varies non-linearly. Thus, all the parameters involved in the simplified method will be given constant *COV's* corresponding to the average value even if *COV* is not constant. The advantage of using a constant *COV* is that the variability of different parameters can be more conveniently compared with a single constant *COV* for each parameter. Using the three procedures discussed above, *COV*'s are obtained for the different parameters required in the "simplified procedure." These *COV*'s should be used only as initial estimates in the absence of any data. Users of the proposed procedure should use more reliable *COV*'s whenever they can be obtained.

4 - SEISMIC DEMAND

4.1- Required Parameters to Determine Seismic Demand

The following seismic parameters are required to determine the seismic demand, *CSR*, for a site:

1) Maximum acceleration, a_{max}
2) Moment magnitude, M_w
3) Epicentral distance, *ED*
4) Site amplification factors, F_a

The "1996 NCEER and 1998 NCEE/NSF Workshops on Evaluation of Liquefaction Resistance" (Youd and Idriss et al. 2001) lists the following methods for determining seismic demand parameters, in order of preference:

1) Using empirical attenuation correlations of a_{max} with M_w, *ED* from the source (hypocentral distance in Western US, WUS), and local site conditions.
2) Performing site response analysis for soft sites and soil profiles not compatible with available attenuation relationships. A suite of plausible earthquake records from earthquakes with similar magnitudes, distance, etc. should be used in the analysis.
3) Using empirical amplification factors.

4.2 - Determination of Peak Ground and Spectral Accelerations from the USGS Seismic Hazard Web Page

The determination of the probabilistic seismic demand parameters from the USGS Seismic Hazard Web Page is based on the USGS National Seismic Hazard Map (Frankel et al. 1997). This procedure uses the peak ground acceleration (*PGA*), the spectral acceleration (*SA*) and the de-aggregation matrices provided in the USGS Geohazards web page (http://geohazards.cr.usgs.gov/eq/). The web page provides only soft rock *PGA* and *SA* which must be converted to surface acceleration $a_{\max}$ to account for local site effects. The uncertainties due to local site effects are treated separately from the uncertainties due to seismic source, magnitude and recurrence. The soft rock *PGA* and *SA* and the magnitude M_w for the design earthquake are, therefore, treated as "non-random" variables in the determination of the maximum ground surface acceleration $a_{\max}$ and the magnitude scaling factor *MSF*. Conversion of the *PGA* and *SA* data to $a_{\max}$ and the method to account for the uncertainties in local site effects are discussed below.

The seismic demand parameters $a_{\max}$ and M_w based on the procedure described below are used in the determination of the conditional probability of liquefaction. In calculating the conditional probability of liquefaction, the uncertainties in M_w due to local site effects and the uncertainties in *MSF* are included in the calculation of the standard deviation σ_F

and the coefficient of variation of the factor of safety V_F . The conditional probability of liquefaction is then multiplied by the probability of exceedance (*PE*) corresponding to the *PGA* and *SA* values used in determining $a_{\max}$ and M_w. The USGS web page provides *PGA* and *SA* values at three periods (0.2, 0.3 and 1.0 sec) with 10%, 5% and2% probability of exceedance *PE* in 50 years (Frankel et al., 1997). These *PE*'s correspond to return times of approximately 500, 1000 and 2500 years, and annual frequencies of exceedance of $2.1 \cdot 10^{-3}$, $1.03 \cdot 10^{-3}$ and $4.04 \cdot 10^{-4}$, respectively.

The following is a brief description of the steps in the determination of the peak ground and spectral accelerations using the USGS National Seismic Hazard Map:

1) Access the web page: http/geohazards.cr.usgs/gov/eq (Shown in Figure 4.1).
2) If the Latitude/Longitude of the site is known click on "Hazard by Lat/Lon." Otherwise click on "Hazard by Zip Code." Enter the Latitude/Longitude or Zip Code of the area. A table (an example is shown in Table 4.1) will appear which provides the following information:
   - The input zip-code
   - The latitude and longitude of site
   - The distance to the nearest grid point.
   - Ground motion hazard values expressed as a percent of the acceleration of gravity (%*g*).

Notes on the values provided by the USGS Website:

- The seismological parameters from the USGS Seismic Hazard Web Page should be used only for projects where specific local seismological parameters are not available, or for making preliminary liquefaction evaluation where such information is available. The use of the USGS Seismic Hazard Web Page is consistent with the 1998 HEHRP provisions.

- The following ground motion values are provided by the USGS website:

  PGA = Peak Ground Acceleration for:
  - $SA_{0.2}$ = 0.2 second period (or 5 Hz frequency) spectral acceleration
  - $SA_{0.3}$ = 0.3 second period (or 3.33 Hz frequency) spectral acceleration
  - $SA_{1.0}$= 1.0 second period (or 1 Hz frequency) spectral acceleration

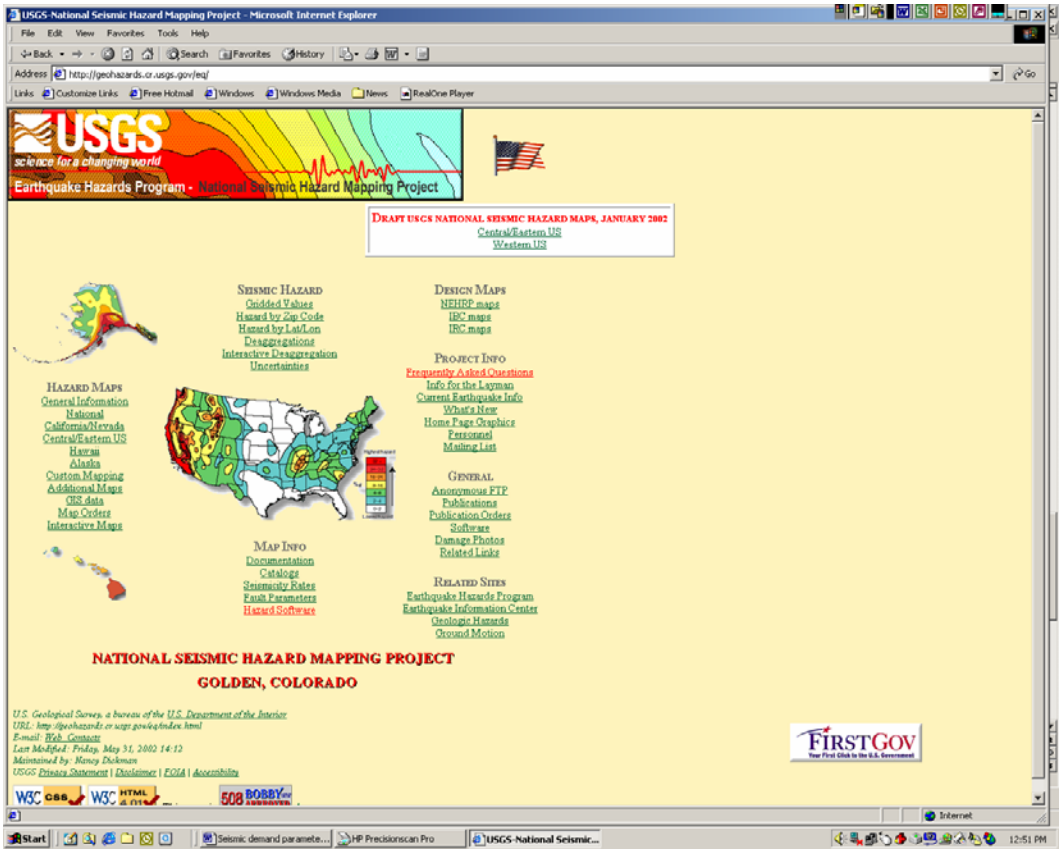

Figure 4.1 - USGS Website (http://geohazards.cr.usgs.gov/eq)

- The ground motion values are provided in terms of the following hazard levels:

  PE = probability of exceedence:
  - 10% *PE* in 50 yrs ≈ 500-year earthquake (use for typical structures)
  - 5% *PE* in 50 yrs ≈ 1000-year earthquake
  - 2% *PE* in 50 yrs ≈ 2500-year earthquake

- The latitude and longitude associated with each zip code is the average of the northern and southern most latitudes and the average of the eastern and western most longitudes of the zip code area. This location is not necessarily the Post Office location or the centroid of the zip code area.

- Note that ground motion hazards are determined at the nearest point on a grid of points 1/10 of a degree apart on which earthquake ground motions have been calculated covering the 48 adjacent US states.

- Ground motion values are calculated for 'firm rock' sites which correspond to a V_s of 760 m/s in the top 30m. Amplification/de-amplification due to different soil sites is discussed below.

Table 4.1 - Example of an Output from the USGS Earthquake Hazard Web Page

```
The input zip-code is 24060.
   ZIP CODE                        24060
   LOCATION                        37.2312 Lat.  -80.4159 Long.
   DISTANCE TO NEAREST GRID POINT  3.7392 kms
   NEAREST GRID POINT              37.2 Lat.  -80.4 Long.
   Probabilistic ground motion values, in %g, at the Nearest Grid point are:
               10%PE in 50 yr   5%PE in 50 yr   2%PE in 50 yr
      PGA        5.391438         9.686434       19.432100
   0.2 sec SA   11.927370        19.331141       37.480820
   0.3 sec SA    9.590293        15.736790       27.547449
   1.0 sec SA    3.998297         6.285469       10.984450
   - - - - - - - - - - - - - - - - - - - - - - - - - - - - - - - -
```

4.3 - Determination of the Earthquake Magnitude, M_w, and epicentral distance, ED, from the USGS Seismic Hazard Web Page

The proposed procedure for determining earthquake magnitude M_w and epicentral distance *ED* is not new. It is commonly used by seismologists in quantifying the mean magnitude of the seismic event that causes a ground-motion exceedance at a chosen return period. The mean magnitude M_w is obtained by de-aggregating the results from the USGS Seismic Hazard web page (McGuire and Shedlock 1981; Frankel et al. 1997). The magnitude M_w is required to estimate the magnitude scaling factor *MSF*. A brief outline of the procedures to determine M_w and *ED* from the USGS Seismic Hazard Web Page is given below:

1) Return to the web page: http/geohazards.cr.usgs/gov/eq.
2) Click on "Deaggregations."
3) In the second paragraph, click on the link for either the CEUS map or the WUS map depending on whether the site is located in the Central-Eastern or Western US, respectively.
4) On the map, click on the closest city to the site of interest.
5) Four matrices will be generated corresponding to the *PGA*, $SA_{0.2}$, $SA_{0.3}$ and $SA_{1.0}$ for 10% *PE* in 50 yrs. Table 4.2 gives an example of the deaggregation matrix for $SA_{1.0}$ with 10% *PE* in 50 yrs.
6) Download the matrices for the *PGA* and $SA_{1.0}$. Only these two matrices will be used in the deaggregation procedure since the *PGA* and spectral acceleration at 1.0 second reasonably bound the frequency range for most soil deposits.
7) Using the deaggregation matrix for the *PGA*, calculate the weighted average for the mean moment magnitude $(M_w)_{PGA}$ and the mean distance ED_{PGA}:

$$(M_w)_{PGA} = \frac{1}{100}\left(5.0\sum D_{M\,5.0} + 5.5\sum D_{M\,5.5} + 6.0\sum D_{M\,6.0} + ... + 7.5\sum D_{M\,7.5}\right) \quad (4\text{-}1)$$

$$ED_{PGA} = \frac{1}{100}\left(25\sum D_{D25} + 50\sum D_{D50} + 75\sum D_{D75} + ... + 625\sum D_{M\,625}\right) \quad (4\text{-}2)$$

where

$D_{M\,5.0}$ = numbers in the column under heading "5.0" in the deaggregation matrix.
$D_{M\,5.5}$ = numbers in the column under heading "5.5" in the deaggregation matrix.
….
$D_{M\,7.5}$ = numbers in the column under heading "7.5" in the deaggregation matrix.

D_{D25} = numbers in the rows with the heading "25" in the deaggregation matrix.
D_{D50} = numbers in the rows with the heading "50" in the deaggregation matrix.
…
D_{D625} = numbers in the rows with the heading "625" in the deaggregation matrix.

8) Using the deaggregation matrix for the 1.0 Spectral Acceleration, calculate the weighted average for the mean moment magnitude $(M_w)_{1.0s}$ and the mean distance $ED_{1.0s}$. The calculations are similar to those used for $(M_w)_{PGA}$ and ED_{PGA} in Step 7.

9) Calculate the mean values of M_w and ED from the corresponding values for the PGA and $SA_{1.0}$.

$$M = \frac{(M_w)_{PGA} + (M_w)_{1.0s}}{2} \quad (4\text{-}3)$$

$$ED = \frac{ED_{PGA} + ED_{1.0s}}{2} \quad (4\text{-}4)$$

Notes on the de-aggregation procedure:

- The seismological parameters from the USGS Seismic Hazard Web Page should be used only for projects where specific local seismological parameters are not available, or for making preliminary liquefaction evaluation where such information is available. The use of the USGS Seismic Hazard Web Page is consistent with the 1998 NEHRP provisions.

- The numbers in the matrices represent the relative contributions of the corresponding ED and M_w pair to the seismic hazard of the site having the indicated probability of exceedence PE in 50 yrs. For example, 0.192% of the seismic hazard at the site is attributed to an M_w = 5.5 earthquake having an ED = 100 km. The sum of all the

numbers in the matrix equals 100%. The matrix may be viewed as a surface, with the mean elevation of the surface corresponding to the mean hazard.

- The deaggregation determination of M_w and *ED* from the USGS seismic hazard web page is based on a widely-used and well-established procedure of probabilistic seismic hazard evaluation originally developed by McGuire and Shedlock (1981).

- The deaggregation procedure should be used with care if the deaggregation matrix shows the site is dominated by two separate events (i.e., a bi-modal distribution). In such a case, the deaggregation matrix will have two large numbers corresponding to distinctly different M_w and *ED* pairs and the mean values may not correspond to a likely event.

Table 4.2 - Example USGS Deaggregation Table from USGS Earthquake Hazard Web Page

Deaggregated Seismic Hazard PE = 2% in 50 years 1.0 hz (1.0 s)
Richmond VA 37.567 deg N 77.433 deg W SA= 0.07820 g

M<=	5.0	5.5	6.0	6.5	7.0	7.5
d<= 25.	1.206	3.448	4.087	2.636	1.037	0.629
50.	0.216	1.592	3.831	3.991	2.028	1.384
75.	0.038	0.513	2.012	3.107	2.043	1.622
100.	0.009	0.192	1.091	2.205	1.724	1.531
125.	0.003	0.091	0.666	1.584	1.375	1.309
150.	0.001	0.049	0.425	1.145	1.076	1.097
175.	0.001	0.026	0.270	0.833	0.861	0.947
200.	0.000	0.016	0.187	0.657	0.758	0.891
225.	0.000	0.011	0.143	0.565	0.717	0.901
250.	0.000	0.008	0.125	0.548	0.753	1.014
275.	0.000	0.006	0.109	0.530	0.787	1.135
300.	0.000	0.005	0.091	0.487	0.777	1.202
325.	0.000	0.003	0.071	0.414	0.707	1.170
350.	0.000	0.002	0.048	0.313	0.572	1.009
375.	0.000	0.001	0.034	0.245	0.478	0.895
400.	0.000	0.001	0.026	0.203	0.423	1.477
425.	0.000	0.001	0.019	0.165	0.358	3.562
450.	0.000	0.000	0.015	0.138	0.302	4.902
475.	0.000	0.000	0.012	0.116	0.260	4.494
500.	0.000	0.000	0.010	0.107	0.247	3.409
525.	0.000	0.000	0.000	0.000	0.000	2.917
550.	0.000	0.000	0.000	0.000	0.000	2.049
575.	0.000	0.000	0.000	0.000	0.000	1.593
600.	0.000	0.000	0.000	0.000	0.000	0.787
625.	0.000	0.000	0.000	0.000	0.000	0.095

D_{D100}

$D_{M5.5}$

4.4 - Determination of Amplification Factors, F_a

The following methods have been developed for determining the amplification factor, *Fa*, needed to convert the *PGA* to surface acceleration, a_{max}, of a site:

1) Using amplification curves (e.g., Seed and Idriss 1982, Idriss 1990, 1991, Girsang and Gutierrez 2001) – see Figs. 4.2 to 4.4.
2) Perform site response analysis.
3) Use NEHRP amplification factors.

Conversion of the *PGA* and *SA* data from the USGS National Seismic Hazard Map to maximum surface acceleration a_{max} should be ideally based on site response analysis. If such analysis is not possible, simple procedures have been recently developed at Virginia Tech to provide quick estimates of a_{max} based on local site conditions (Green, 2001). The proposed procedure is intended for use in sites where detailed seismologic information is not available, and for making preliminary estimates where such information is available. The *PGA* and *SA*, obtained by inputting a site's zip code or latitude/longitude in the USGS web page, is converted to maximum ground surface acceleration based on the observed relationship between the characteristics of the rock outcrop motions and the peak accelerations of uniform soil profiles (i.e., soil profiles having constant shear wave velocity with depth).

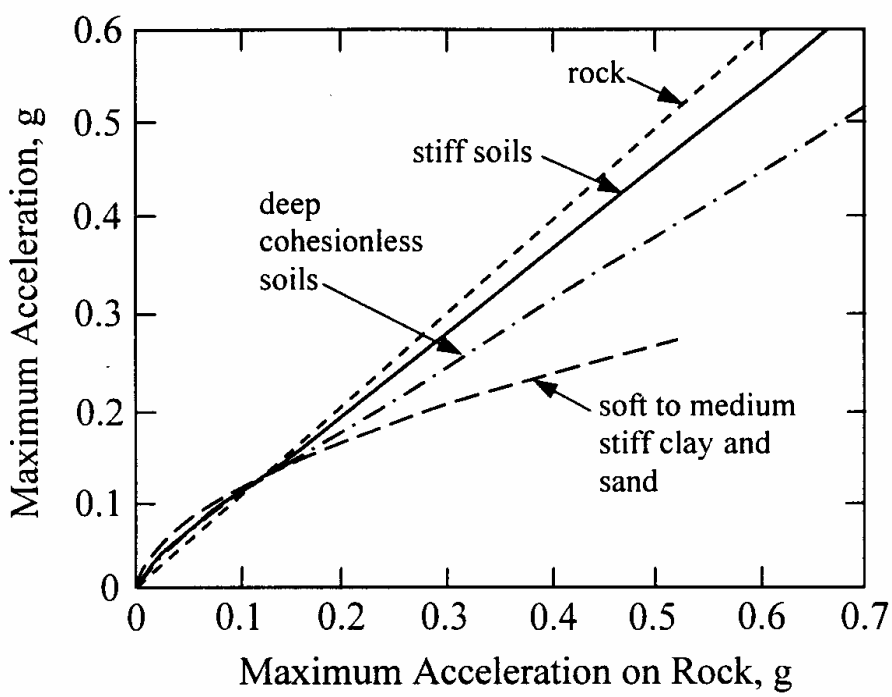

Figure 4.2 – Amplification Factors as Function of Site Conditions and Amplitude of Rock Acceleration (Seed and Idriss, 1982)

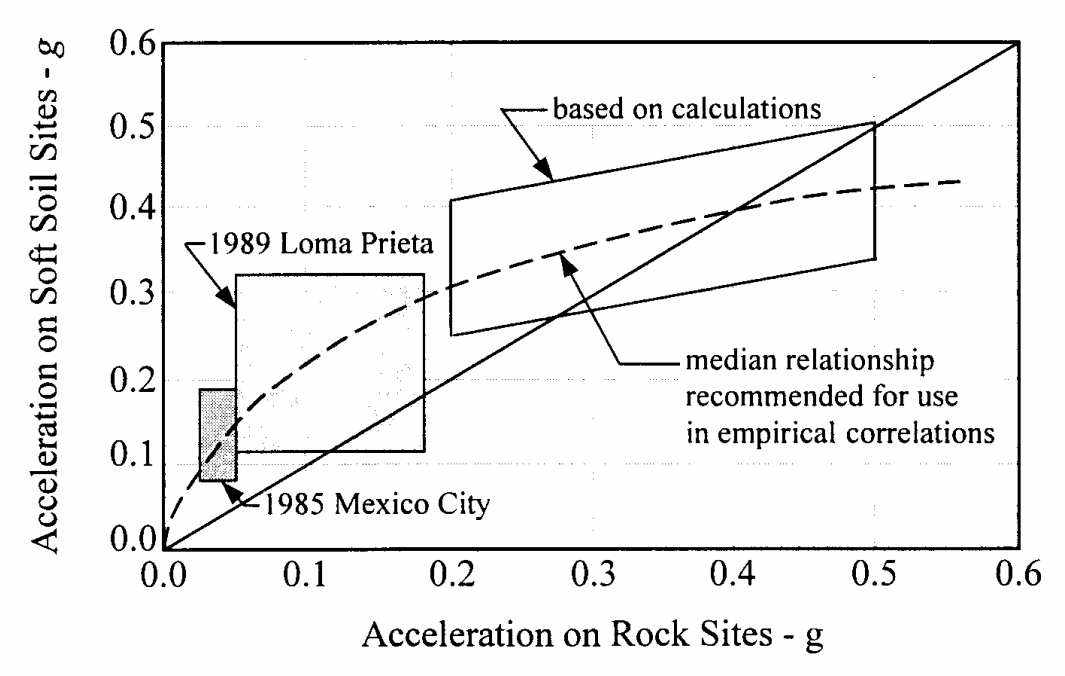

Figure 4.3– Amplification Factors for Soft-Soil Sites (Idriss 1990, 1991)

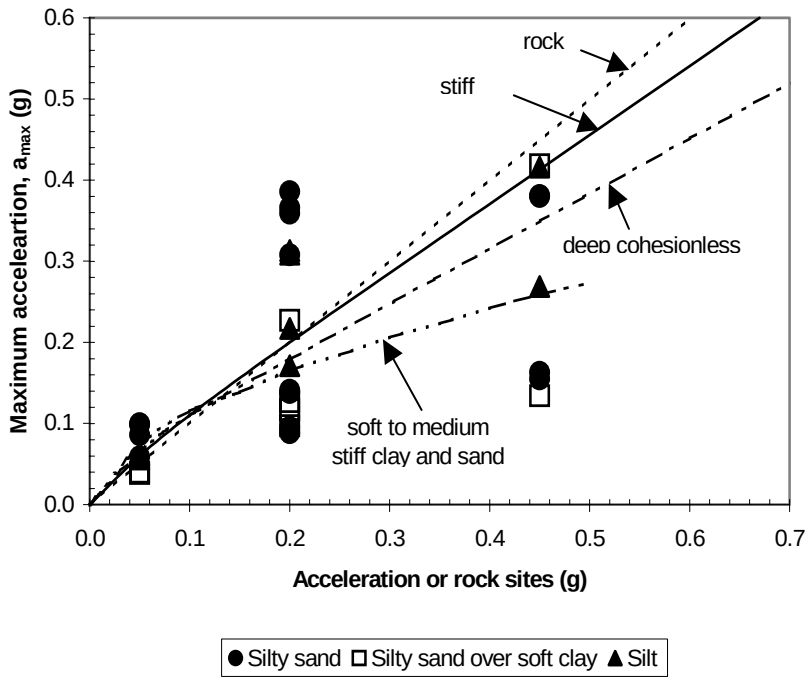

Figure 4.4 – Amplification Factors for Soft Soil Sites from Site Response Analysis with Pore Pressure Accumulation (Girsang and Gutierrez, 2001)

The following is a brief outline of procedures to convert the *PGA* and *SA* data from the USGS National Seismic Hazard Map to maximum surface acceleration $a_{\max}$

1) Using the average shear wave velocity, average undrained shear strength and average SPT *N*-values of the site, classify the site according to the 1998 NEHRP provisions. The NEHRP site categories are given in Table 4.3.

Table 4.3 - NEHRP Site Class Definitions (ICBO, 2003)

SITE CLASS	SOIL PROFILE NAME	AVERAGE PROPERTIES IN TOP 100 feet, AS PER SECTION 1615.1.5		
		Soil shear wave velocity, $\bar{v}_s$, (ft/s)	Standard penetration resistance, $\bar{N}$	Soil undrained shear strength, $\bar{s}_u$, (psf)
A	Hard rock	$\bar{v}_s > 5{,}000$	Not applicable	Not applicable
B	Rock	$2{,}500 < \bar{v}_s \leq 5{,}000$	Not applicable	Not applicable
C	Very dense soil and soft rock	$1{,}200 < \bar{v}_s \leq 2{,}500$	$\bar{N} > 50$	$\bar{s}_u \geq 2{,}000$
D	Stiff soil profile	$600 \leq \bar{v}_s \leq 1{,}200$	$15 \leq \bar{N} \leq 50$	$1{,}000 \leq \bar{s}_u \leq 2{,}000$
E	Soft soil profile	$\bar{v}_s < 600$	$\bar{N} < 15$	$\bar{s}_u < 1{,}000$
E	—	Any profile with more than 10 feet of soil having the following characteristics: 1. Plasticity index $PI > 20$; 2. Moisture content $w \geq 40\%$, and 3. Undrained shear strength $\bar{s}_u < 500$ psf		
F	—	Any profile containing soils having one or more of the following characteristics: 1. Soils vulnerable to potential failure or collapse under seismic loading such as liquefiable soils, quick and highly sensitive clays, collapsible weakly cemented soils. 2. Peats and/or highly organic clays ($H > 10$ feet of peat and/or highly organic clay where H = thickness of soil) 3. Very high plasticity clays ($H > 25$ feet with plasticity index $PI > 75$) 4. Very thick soft/medium stiff clays ($H > 120$ ft)		

For SI: 1 foot = 304.8 mm, 1 square foot = 0.0929 m², 1 pound per square foot = 0.0479 kPa.

In this table, the average shear wave velocity $\bar{V}_s$, average undrained shear strength $\bar{s}_u$, and average SPT *N*-value, $\bar{N}$, are calculated as follows:

$$\bar{V}_s = \frac{\sum_{i=1}^{n} d_i}{\sum_{i=1}^{n} \frac{d_i}{V_{si}}}, \qquad \bar{s}_u = \frac{\sum_{i=1}^{k} d_i}{\sum_{i=1}^{k} \frac{d_i}{s_{ui}}}, \qquad \bar{N} = \frac{\sum_{i=1}^{m} d_i}{\sum_{i=1}^{m} \frac{d_i}{N_i}} \tag{4-5}$$

where:

n = number of soil layers

k = number of cohesive soil layers

m = number of cohesionless soil layers

d_i = thickness of soil layer

V_{si} = shear wave velocity of a soil layer (in ft/s)

s_{ui} = undrained shear strength of a cohesive soil layer (in psf), not to exceed 5000 psf

N_i = SPT *N*-value of a cohesionless soil layer

d_i = thickness of a soil layer (in ft), not to exceed 100 ft.

Note that the total thickness $\sum d_i$ should also not exceed 100 ft.

2) Using the site classification and the spectral acceleration for 0.2 s and 1.0 ($SA_{0.2}$ and $SA_{1.0}$) obtained from the USGS Seismic Hazard Web Page, determine the site amplification factors F_a and F_v from Tables 4.4 and 4.5.

Table 4.4 -Site Amplification Factor F_a as Function of Site Class and Short Period Spectral Acceleration $S_s = SA_{0.2}$ of the site (ICBO, 2003)

SITE CLASS	MAPPED SPECTRAL RESPONSE ACCELERATION AT SHORT PERIODS				
	$S_S \leq 0.25$	$S_S = 0.50$	$S_S = 0.75$	$S_S = 1.00$	$S_S \geq 1.25$
A	0.8	0.8	0.8	0.8	0.8
B	1.0	1.0	1.0	1.0	1.0
C	1.2	1.2	1.1	1.0	1.0
D	1.6	1.4	1.2	1.1	1.0
E	2.5	1.7	1.2	0.9	Note b
F	Note b	Note b	Note b	Note b	Note b

a. Use straight line interpolation for intermediate values of mapped spectral acceleration at short period, S_S.
b. Site-specific geotechnical investigation and dynamic site response analyses shall be performed to determine appropriate values.

3) Calculate the a_{max} using F_a from Table 4.4, F_v from Table 4.5, and $SA_{0.2}$ and $SA_{1.0}$ from Table 4.1.

a) Using an empirical relationship developed by Martin (2000):

$$a_{\max} = 0.0606 \frac{(F_a SA_{0.2})^2}{F_v SA_{1.0}} + 0.267 F_a SA_{0.2} \tag{4-6}$$

Table 4.5 - Site Amplification Factor F_v as Function of Site Class and the Long Period Spectral Acceleration $S_1 = SA_{1.0}$ of the Site (ICBO, 2003).

SITE CLASS	MAPPED SPECTRAL RESPONSE ACCELERATION AT 1 SECOND PERIOD				
	$S_1 \leq 0.1$	$S_1 = 0.2$	$S_1 = 0.3$	$S_1 = 0.4$	$S_1 \geq 0.5$
A	0.8	0.8	0.8	0.8	0.8
B	1.0	1.0	1.0	1.0	1.0
C	1.7	1.6	1.5	1.4	1.3
D	2.4	2.0	1.8	1.6	1.5
E	3.5	3.2	2.8	2.4	Note b
F	Note b	Note b	Note b	Note b	Note b

a. Use straight line interpolation for intermediate values of mapped spectral acceleration at 1-second period, S_1.
b. Site-specific geotechnical investigation and dynamic site response analyses shall be performed to determine appropriate values.

b) Using an empirical relationship developed by Green (2001):

$$a_{\max} = F_a pga \approx F_a \frac{SA_{0.2}}{2.5} \tag{4-7}$$

Note that $S_s/2.5$ is approximately the rock outcrop *PGA* (Dobry et al., 2000). Equation (4-7) is shown graphically in Fig. 4.5.

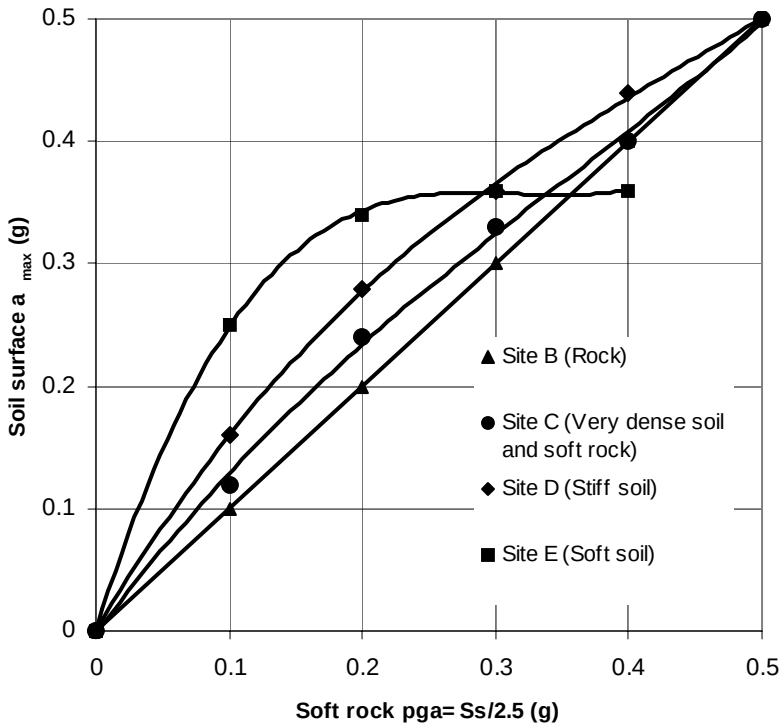

Fig. 4.5 - Surface $a_{\max}$ as function of soft rock *PGA* and NEHRP site class.

There is currently very little data on the variability of F_a for specific site conditions. An example of the variability of the relationship between surface and rock acceleration is given in Fig. 4.6, which is taken from Golesorkhi (1989). Based on the results of Golesorkhi (1989), and Idriss (1990 and 1991), a preliminary estimate of the COV for F_a is about 52.5%. Results of Golesorkhi (1989) indicate that F_a is only dependent on the rock site characteristics and the soft rock *PGA* and only to less extent to the earthquake magnitude M_w.

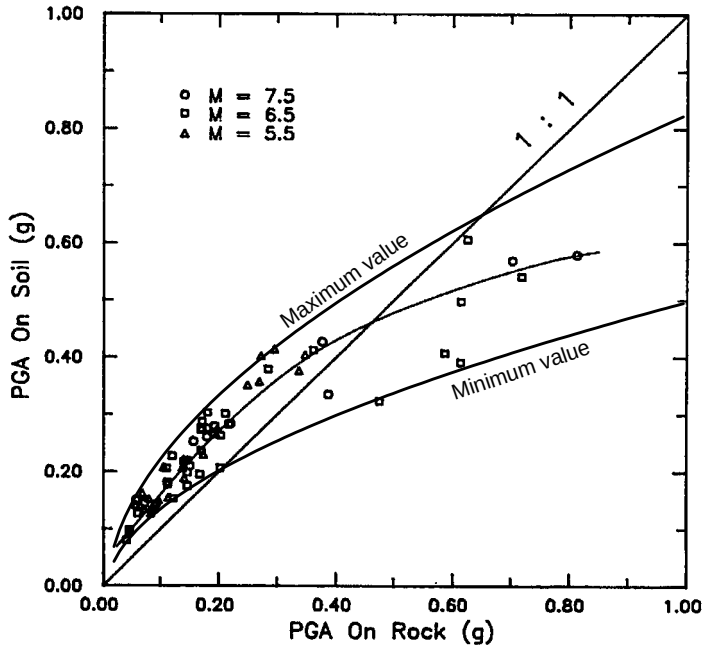

Fig. 4.6 – Variability in soil amplification (Golesorkhi, 1989).

5 - ENVIRONMENTAL FACTORS

In the NCEER 1997 Liquefaction Evaluation Procedure, there are two instances where calculations involving the unit weight of the soils are performed. First, when determining the *CSR* of the soil for each depth being evaluated, both the total and effective vertical stress σ_{vo} and σ'_{vo} at that point are required. Secondly, when evaluating liquefaction potential based on the results of Standard Penetration Test (SPT) results, a correction factor, C_N, is applied to correct the SPT *N*-value to an overburden pressure of 1 tsf, which requires the effective stress at that point.

Data from four United States Bureau of Reclamation dams was used to estimate the standard deviation and coefficient of variation for the dry, moist, and buoyant unit weights of soils. Results of both in-place density tests and relative density tests from Casitas Dam, Bradbury Dam, Mormon Island Dam, and Bully Creek Dam were obtained and analyzed for various soil groups at each site. Two of the dams, Bradbury Dam and Bully Creek Dam, contained enough data to calculate a *COV* for different soil groups based upon their unified soil classifications. The other two dams, Casitas and Mormon Island did not have sufficient data to separate the soils into groups. The soils which were grouped together during this procedure included GP and GW, SM and ML, and SP and SW.

Table 5.1 summarizes the number of test results available for use in calculating the standard deviation for the above mentioned soil types:

Table 5.1 - Summary of Available Test Results for Determining the *COV* of Soil Unit Weight.

Dam	In-Place Density Tests	Relative Density Tests
Casitas Dam	5	4
Bradbury Dam	3	17
Mormon Island Dam	12	0
Bully Creek	12	7

Using the data presented in the following tables, separate standard deviation, σ, values and *COV*'s were calculated for dry unit weights, moist unit weights, and buoyant unit weights. All σ values were calculated using the "Three-Sigma Rule" as outlined by Dai and Wang (1992), but using the values recommended by Christian and Baecher (2001) for the denominator of the standard deviation equation. All *COV*'s were calculated according to the methods discussed by Duncan (2000). The following sections outline the procedures used in calculating these parameters for the varying unit weights of soil.

5.1 - Dry and Moist Unit Weights

Using the data presented in Tables 5.2 through 5.9, standard deviation and *COV* values were calculated for each of the four above-mentioned dams. The results of these calculations are as follows:

Table 5.2 - Casitas Dam Test Results (from USBR, 1999)

Material	Dry Unit Weight (pcf)	Moisture Content %	Moist Unit Weight (pcf)	Relative Density (%)
SM	96.3	6.7	102.8	71.9
SP-SM	94.9	4.3	99.0	62.1
SM	100.6	12.1	112.8	N/A
SW-SM	96.5	6.0	102.3	71.4
SM	110.0	17.1	128.8	N/A
GM	109.0	9.9	119.8	N/A
SM	104.0	8.3	112.6	94.1
SM	95.9	16.0	111.2	N/A
SP-SM	103.9	8.5	112.7	N/A

Table 5.3 - *COV* Calculations for Casitas Dam

	Dry Unit Weight (pcf)		Moist Unit Weight (pcf)	
Average	101.2		111.3	
Lowest	94.9		99.0	
Highest	110.0		128.8	
N_n	2.97	*COV*	2.97	*COV*
Std. Dev.	5.08	5.0%	10.04	9.0%

In Table 5.3, the coefficient of variation for the dry unit weight was calculated as follows:

$$Average = 101.2\text{pcf}$$

$$\sigma = \frac{(HCV - LCV)}{N_n} = \frac{(110.0\,pcf - 94.9\,pcf)}{2.97} = 5.08\text{pcf}$$

$$COV = \frac{\sigma}{average} = \frac{5.08}{101.2} = 5.0\%$$

The calculation demonstrated above for *COV* was performed consistently for the following dams, for both the dry and moist unit weight.

It should be noted when reviewing the *COV* calculations shown above that the recommended value of the N_n is based upon Christian and Baecher (2001).

Table 5.4 - Mormon Island Auxilary Dam Test Results (from USBR)

Mormon Island Auxiliary Dam	
Material	Dry Unit Weight (pcf)
Foundation Gravel (Dredged Alluvium)	129
	128
	125
	125
	117
	116
	116
	115
	111
	111
	110
	107

Table 5.5 - *COV* Calculations for Mormon Island Auxillary Dam

	Dry Unit Weight	
Average	117.5	
Lowest	107	
Highest	129	
N_n	3.258	*COV*
σ	6.75	6.0%

As mentioned above, two of the dams, Bradbury and Bully Creek Dam had enough data to break up the *COV* determinations into groupings based upon unified soil classifications. Tables 5.6 and 5.7 contain raw data and the calculations of coefficient of variation for the different soil groupings at Bradbury Dam, while tables 5.8 and 5.9 contain all pertinent data and calculations for Bully Creek Dam.

Table 5.6 - Bradbury Dam Test Results (from USBR, 1997)

Bradbury Dam				
Material	Dry Unit Weight (pcf)	Moisture Content %	Moist Unit Weight (pcf)	Relative Density (%)
GP	87.2	18.1	103.0	44.3
GP	119.1	6.2	126.5	32.7
GW	119.8	6.2	127.2	75.2
GW	107.6	13.3	121.9	35.2
GW	111.5	5.4	117.5	19.4
ML	89.4	27.0	113.5	N/A
ML	92.8	28.3	119.1	N/A
SM	74.6	38.0	102.9	N/A
SM	89.9	20.8	108.6	72.9
SM	97.9	13.0	110.6	84.9
SM	90.0	N/A	N/A	72.0
SM	97.0	N/A	N/A	84.0
SP	100.7	8.4	109.2	33.0
SP	98.9	5.2	104.0	62.9
SP	117.4	5.9	124.3	73.6
SP	101.0	N/A	N/A	34.0
SP	119.0	N/A	N/A	74.0
SP	117.0	N/A	N/A	72.0
SW	118.5	6.6	126.3	58.2
SW	118.0	N/A	N/A	56.0

Table 5.7 - *COV* Calculations for Bradbury Dam

GP-GW

	Dry Unit Weight		Moist Unit Weight	
Average	109		119.2	
Lowest	87.2		103	
Highest	119.8		127.2	
N_n	2.326	*COV*	2.326	*COV*
σ	14	13.00%	10.4	9.00%

ML-SM

Average	90.2		111	
Lowest	74.6		102.9	
Highest	97.9		119.1	
N_n	2.704	*COV*	2.326	*COV*
σ	8.62	10.00%	6.93	6.00%

SP-SW

Average	111.3		116	
Lowest	98.9		104	
Highest	119		126.3	
N_n	2.847	*COV*	2.059	*COV*
σ	7.06	6.00%	10.82	9.00%

Table 5.8 - Bully Creek Dam Test Results (from USBR, 1998)

Material	Dry Unit Weight (pcf)	Bully Creek Dam Moisture Content %	Moist Unit Weight (pcf)	Relative Density (%)
CL	90.4	25.4	113.4	N/A
GM	77.6	11.4	86.4	N/A
GP	114.2	3.4	118.1	23
GP-GM	119.7	5.5	126.3	44
GW	118	2.6	121.1	38
GW	108.5	5.3	114.3	N/A
GW	128.9	5.5	136	52
GW-GM	124.6	3.3	128.7	71
ML	80.3	14.7	92.1	N/A
ML	72.1	17.4	84.6	N/A
ML	75.1	16.4	87.4	N/A
ML	84.8	29.3	109.6	N/A
ML	88.3	16.4	102.8	N/A
SM	80.8	14.1	92.2	N/A
SM	74.1	11.4	82.5	8
SM	67.7	16.1	78.6	N/A
SM	83.5	36.7	114.1	N/A
SM	84.9	25	106.1	N/A
SP-SM	87.3	6.7	93.1	8

Table 5.9 - *COV* Calculations for Bully Creek Dam

GP-GW

	Dry Unit Weight		Moist Unit Weight	
Average	119.0		124.1	
Lowest	108.5		114.3	
Highest	128.9		136.0	
N_n[1]	2.534	*COV*	2.534	*COV*
σ.[2]	8.05	7.0%	8.58	7.0%

SM-ML

Average	79.9		94.9	
Lowest	67.7		78.6	
Highest	88.3		114.1	
N_n	3.173	*COV*	3.173	*COV*
σ	6.49	8.0%	11.20	12.0%

Table 5.10 summarizes the results of the *COV* calculations performed above for both dry and moist unit weights of soils.

Table 5.10 - *COV* Summary for Dry and Moist Unit Weights of Soils

Material	*COV* for γ_d	*COV* for γ_m
GP – GW	7-13%	7-9%
SM – ML	5-10%	6-12%
SP – SW	6%	9%

5.2 - Buoyant Unit Weights

The *COV* for buoyant unit weight was calculated using the same data as above for the moist unit weights. The standard deviation obtained from the moist unit weight data of the four dams was held constant while the average value used in the denominator of the *COV* calculation differed by the unit weight of water. The same groupings based upon soil classifications were also used. Table 5.11 contains the data used in obtaining the *COV* for moist unit weight, as well as the calculations performed to obtain a *COV* for the buoyant unit weight of soils.

Table 5.11 – *COV* Calculations for Buoyant Unit Weight

Moist Unit Weight	(pcf)	Buoyant Unit Weight	(pcf)
Average	111.3	Average	48.9
Low	99.0	Low	36.6
High	128.8	High	66.4
		N_n	2.97
		σ	10.04
		COV	21.0%

Table 5.12 – continued from previous page.

Bradbury Dam

	Moist Unit Weight (pcf)		Buoyant Unit Weight (pcf)	
GP-GW	Average	119.2	Average	56.8
	Low	103.0	Low	40.6
	High	127.2	High	64.8
			N_n	2.326
			σ	10.42
			COV	18.0%
SM-ML	Average	111.0	Average	48.6
	Low	102.9	Low	40.5
	High	119.1	High	56.7
			N_n	2.326
			σ	6.93
			COV	14.0%
SP-SW	Average	116.0	Average	53.6
	Low	104.0	Low	41.6
	High	126.3	High	63.9
			N_n	2.059
			σ	10.82
			COV	20.0%

Bully Creek Dam

	Moist Unit Weight (pcf)		Buoyant Unit Weight (pcf)	
GP-GW	Average	124.1	Average	61.7
	Low	114.3	Low	51.9
	High	136.0	High	73.6
			N_n	2.534
			σ	8.58
			COV	14.0%
SM-ML	Average	94.9	Average	32.5
	Low	78.6	Low	16.2
	High	114.1	High	51.7
			N_n	3.173
			σ	11.20
			COV	35.0%

A summary of the ranges of *COV* determined for buoyant soil unit weights are shown in Table 5.12.

Table 5.13 - *COV* Summary for Buoyant Unit Weight

Material	Buoyant Unit Weight
GP - GW	14.0-18.0%
SM - ML	14.0-35.0%
SP - SW	20.0%

5.3 – Percentage of Fines, FC

One parameter that could vary significantly when analyzing soils for liquefaction potential is the fines content, *FC*, found within the soil. There are two potential ways by which variability in fines content could affect the liquefaction potential. First, the amount of fines could vary in a given layer across the site being evaluated. Second, there could be variability within the laboratory testing program.

Laboratory test data was collected from sieve tests performed on samples from three United States Bureau of Reclamation Dams. The three dams, Casitas Dam, Bradbury Dam, and Bully Creek Dam, were used to determine a standard deviation and *COV* for the percentage of fines in soils. Table 5.13 summarizes the number of test results available for determining both a σ and *COV*:

Table 5.14 - Summary of Available Sieve Test Results

Dam	**No. of Sieve Tests**
Casitas Dam	9
Bradbury Dam	18
Bully Creek Dam	19

The available data was broken down in groups based on unified soil classification. These groupings included GP-GW-SP-SW and SM-ML. The data used in calculating the *COV* of soil *FC* is presented in Tables 5.14 through 5.16.

As can be seen in the summary data at the bottom of Tables 5.10, 5.11, and 5.12, as the average *FC* increases, so does the range between the minimum value and maximum value within each group. Based on these results, Figure 5.1 was constructed to determine the *COV* of the *FC* parameter. Figure 5.1 is a plot of maximum fines value minus minimum fines value for each group versus the average value for each group, as follows:

Based on Figure 5.1, the following equation was obtained for the average trendline of the data set:

$$Max - Min = 1.4 \cdot Average \tag{5-1}$$

Using this equation, σ and *COV* can be calculated based on the upper and lower ranges plotted in Figure 5.1.

At an average % fines value of 20%, the range of maximum minus minimum ranges from 20% to 73%; the *COV* is calculated as follows:

$$Average = 1.4 \cdot 20 = 28.0$$

$$\sigma = \frac{(\max\ fines - \min\ fines)}{6} = \frac{(73-20)}{6} = 8.83$$

$$COV = \frac{\sigma}{average} = \frac{8.83}{28.0} = 31.5\%$$

Table 5.15 - Casitas Dam Test Results (from USBR, 1999)

Classification	% Fines	Classification	% Fines
GM	9.6	SM	14.0
SP-SM	8.2	SM	13.2
SP-SM	7.1	SM	15.1
SW-SM	2.8	SM	9.3
		SM	29.6

Max	9.6
Min	2.8
Average	6.9
Max-Min	6.8

Max	29.6
Min	9.3
Average	16.2
Max-Min	20.3

Table 5.16 - Bradbury Dam Test Results (from USBR, 1997)

Classification	% Fines	Classification	% Fines
GP	4.1	ML	63.6
GP	2.4	ML	62.3
GP	2.7	ML	72.2
GW	1.5	SM	36.2
GW	2.8	SM	39.3
SP	1.2	SM	16.1
SP	2.1	SM	17.5
SP	3.3	SM	13.9
SW	1.7	SM	14.0

Max	4.1
Min	1.2
Average	2.4
Max-Min	2.9

Max	72.2
Min	13.9
Average	37.2
Max-Min	58.3

Table 5.17 - Bully Creek Dam Test Results (from USBR, 1998)

Classification	% Fines
GM	24
GP	1
GP-GM	6
GW	2
GW	4
GW	4
GW-GM	5
SP-SM	5

Max	24
Min	1.0
Average	6.4
Max-Min	23.0

Classification	% Fines
ML	54
ML	73
ML	54
ML	67
ML	86
SM	32
SM	16
SM	46
SM	37
SM	48
CL	80

Max	86
Min	16
Average	53.9
Max-Min	70

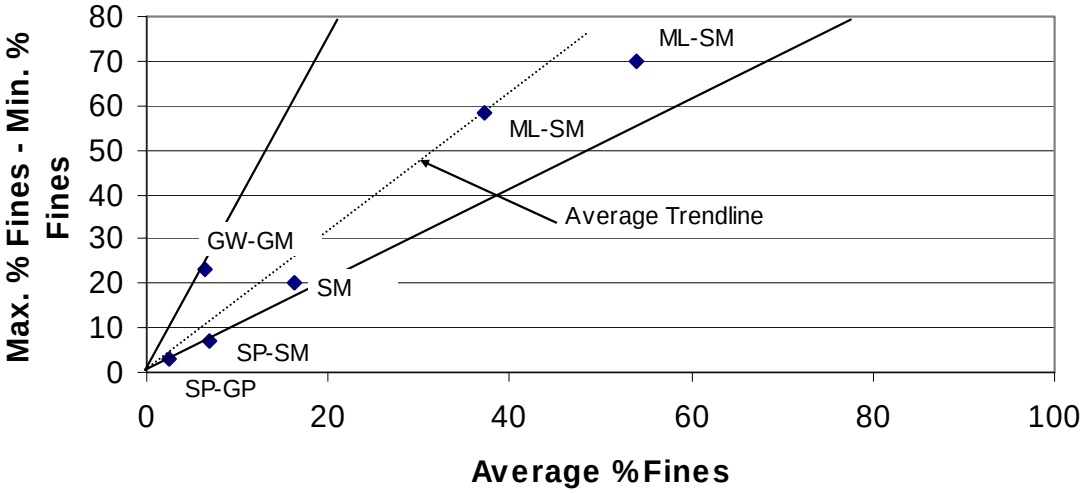

Figure 5.1 - Max. % Fines - Min. % Fines vs. Average % Fines

6 - CYCLIC STRESS RATIO (CSR) PARAMETERS

6.1 – Depth Reduction Factor, r_d

There are currently three formulations for calculating the stress reduction factor:

1) The original r_d formulation by Seed and Idriss (1971).
2) The magnitude-dependent r_d formulation by Idriss and Golesorkhi (1997).
3) The r_d formulation by Cetin and Seed (2001) based on the results of 2153 site response analyses.

<u>Seed and Idriss (1971) Stress Reduction Factor</u>

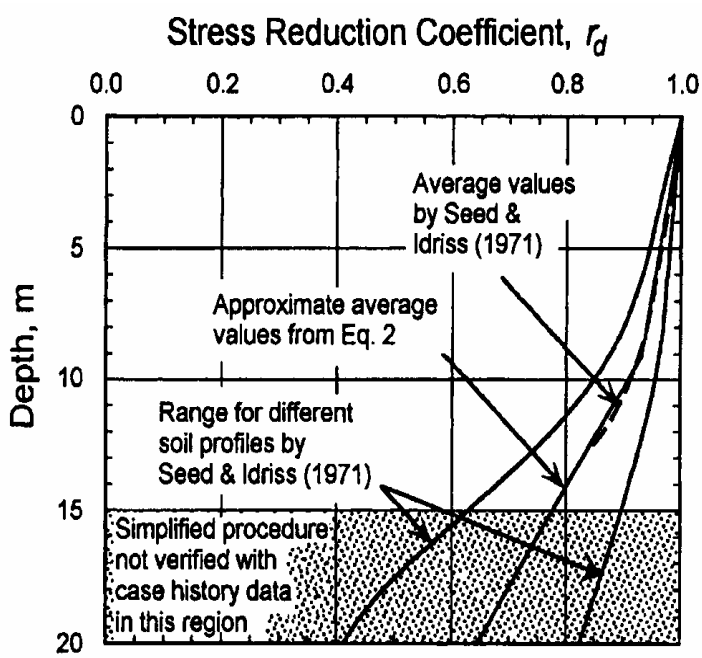

Figure 6.1 - Average and Range of r_d Values from Seed and Idris (1971)

The average, minimum and maximum values for the curves in Figure 6.1 are approximated by the following equations, where *z* is in meters:

Table 6.1 - Average, Minimum and Maximum r_d Values from Seed and Idriss (1971)

Depth	Average r_d	Minimum r_d	Maximum r_d
$z \le 10\,\text{m}$	$r_d = 1 - 0.01z$	$r_d = 1 - 0.015z$	$r_d = 1 - 0.005z$
$z > 10\,\text{m}$	$r_d = 1.15 - 0.025z$	$r_d = 1.3 - 0.045z$	$r_d = 1.075 - 0.0125z$

The approximate relations given above for the average r_d are slightly different and are simpler than the equations given by Liao and Whitman (1986), and Blake (1996). These relationships are given below:

Liao and Whitman (1986):

$$r_d = 1 - 0.00765z \text{ for } z \le 9.15\text{ m} \quad (z \text{ in m}) \tag{6-1}$$

$$r_d = 1.174 - 0.0267z \text{ for } 9.15\text{ m} \le z \le 23\text{m} \tag{6-2}$$

Blake (1996):

$$r_d = \frac{1.0 - 0.4113z^{0.5} + 0.04052z + 0.001753z^{1.5}}{1.0 - 0.4177z^{0.5} + 0.05729z - 0.00620z^{1.5} + +0.001210z^{2}} \quad (z \text{ in m}) \tag{6-3}$$

The approximations given in Table 6.1 are drawn in Figure 6.2.

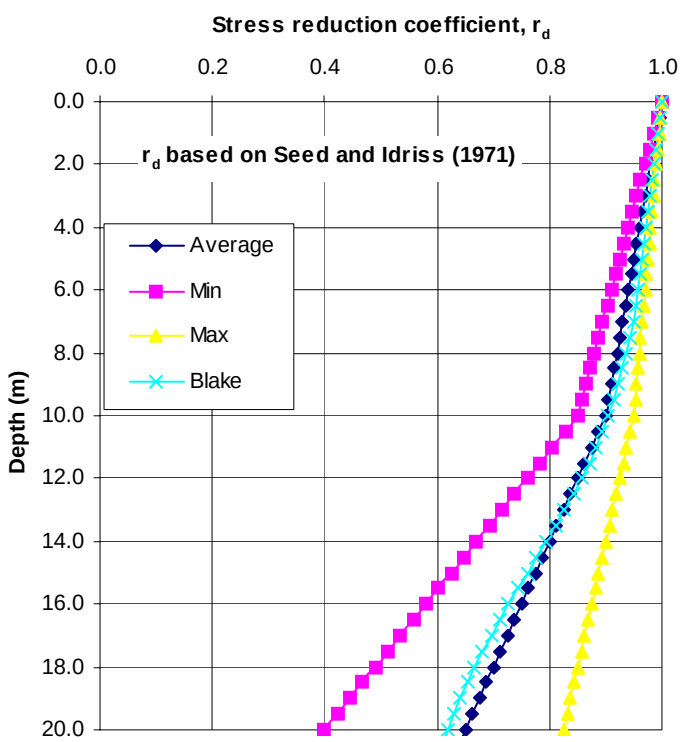

Figure 6.2 - Approximations of the Average and Range of r_d Values from Seed and Idriss (1971)

Using the average, minimum, and maximum values of r_d from Table 6.1, an estimate of the *COV* for 1-r_d is obtained from the "Three-Sigma Rule", and the calculated *COV*'s are shown in Figure 6.3.

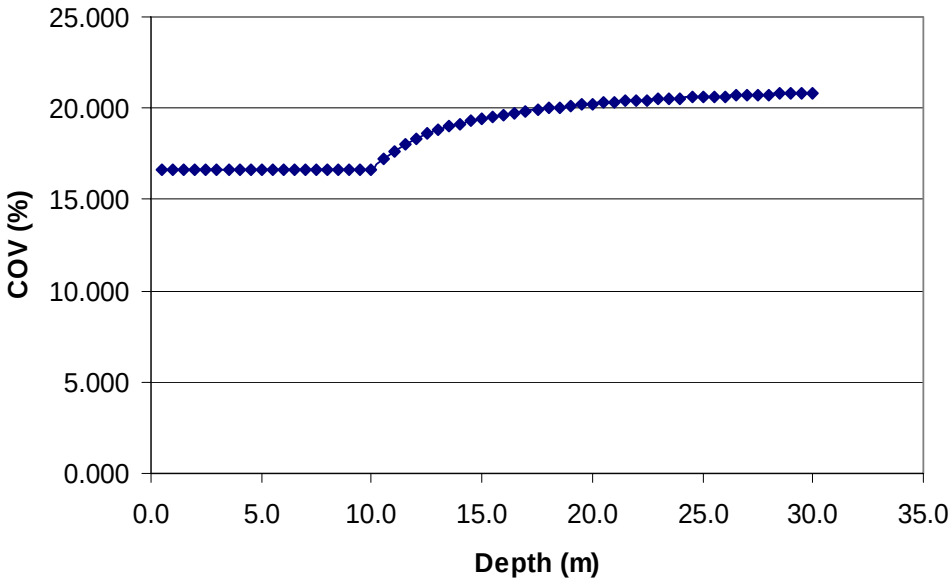

Figure 6.3 - *COV* for r_d Values from the Average and Range of r_d Values from Seed and Idriss (1971)

From Figure 6.3, an average value for *COV* for 1- r_d is estimated to be 19% based Seed and Idriss (1971) equation for average r_d.

Idriss and Golesorkhi (1997) Stress Reduction Factor

Idriss and Golesorkhi's (1997) magnitude-dependent r_d-values are given by the following expressions and are shown in Figure 6. 4.

$$\ln(r_d) = \alpha(z) + \beta(z) M_w \quad (z \text{ in ft}) \tag{6-4}$$

$$\alpha(z) = -1.012 - 1.126 \sin\left(\frac{z}{38.5} + 5.133\right) \tag{6-5}$$

$$\beta(z) = 0.106 + 0.118 \sin\left(\frac{z}{37} + 5.142\right) \tag{6-6}$$

Cetin et al. (2001) Stress Reduction Factor

The full range of r_d calculated by Cetin et al. (2001) from the results of 2153 site response analyses are shown in Figure 6.5. The average and ±1 standard deviation values shown in Figure 6.5 are curve-fitted with polynomial functions which are shown in Figure 6.6. The *COV* is calculated using equation 3-3. The calculated *COV* as function of depth *z* (in ft) for (1-r_d) is shown in Figure 6.7. From this figure, an average value of *COV* of 45% was approximated.

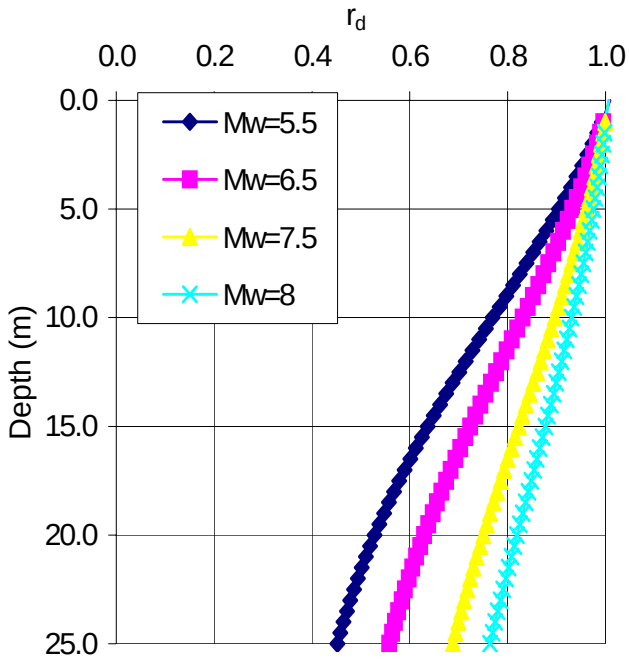

Figure 6.4 - Magnitude-Dependent r_d Values from Idriss and Golesorkhi (1997)

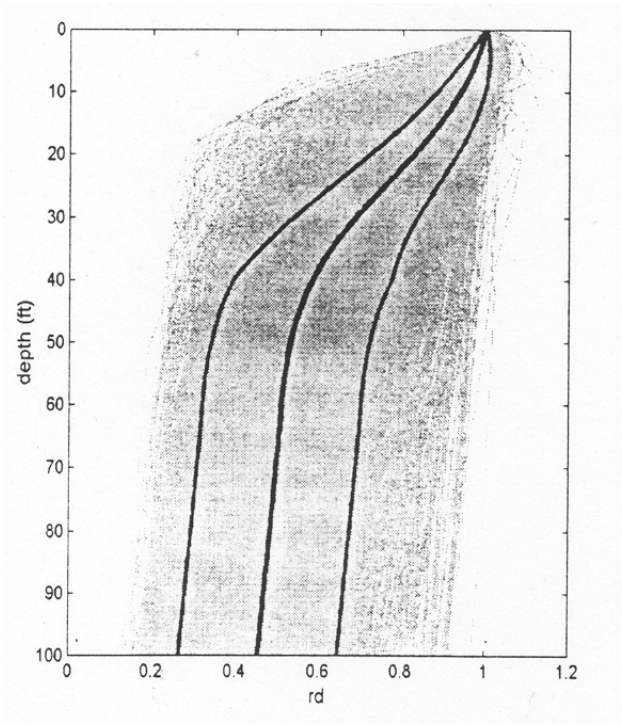

Figure 6.5 - r_d Values after Cetin et al. (2001)

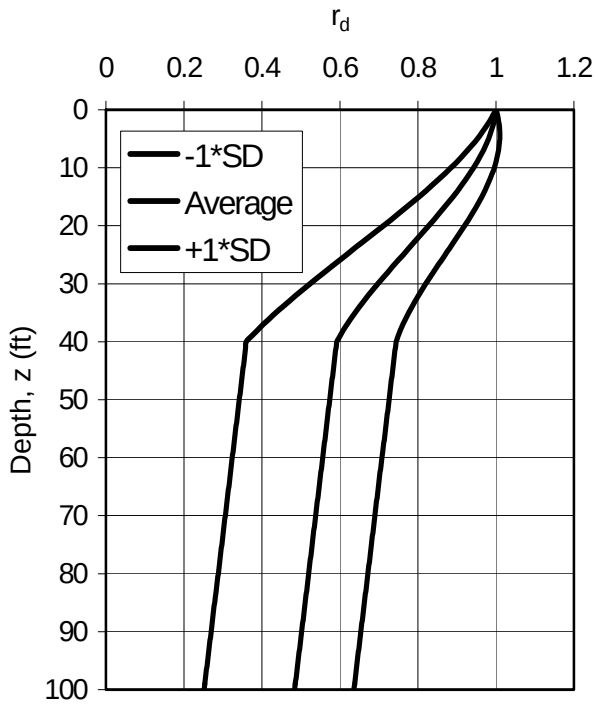

Figure 6.6 - Curve-Fitted r_d Values from Cetin et al. (2001)

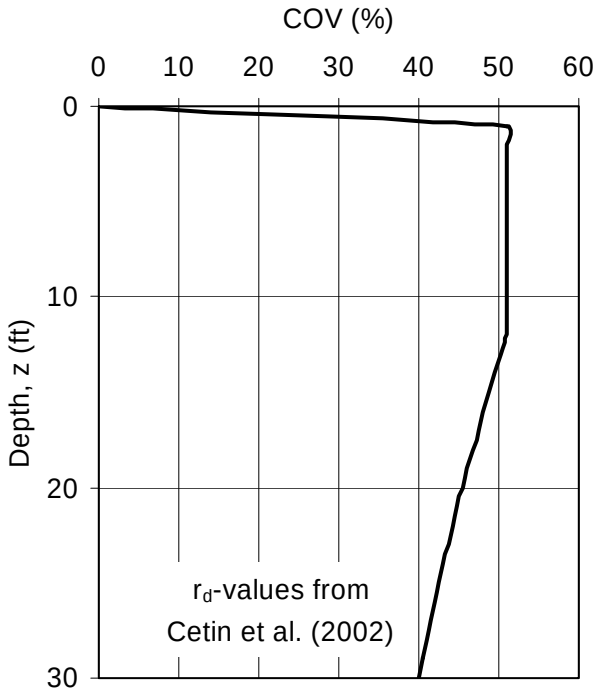

Figure 6.7 - Calculated *COV* from Cetin et al. (2001)

6.2 – Magnitude Scaling Factor, MSF

The Magnitude Scaling Factor, *MSF*, accounts for earthquake magnitudes different from M_w = 7.5. *MSF* can be calculated from the range of values recommended by the NCEER Workshop (Figure 6.8).

The lower bound, upper bound and average values of *MSF* for this recommended range can be fitted by the following equations:

Lower bound: $$MSF = \frac{10^{0.99}}{M_w^{1.13}} \quad (6\text{-}7)$$

Upper bound: $$MSF = \frac{10^{4.18}}{M_w^{4.78}} \quad (6\text{-}8)$$

Average: $$MSF = \frac{10^{2.84}}{M_w^{3.24}} \quad (6\text{-}9)$$

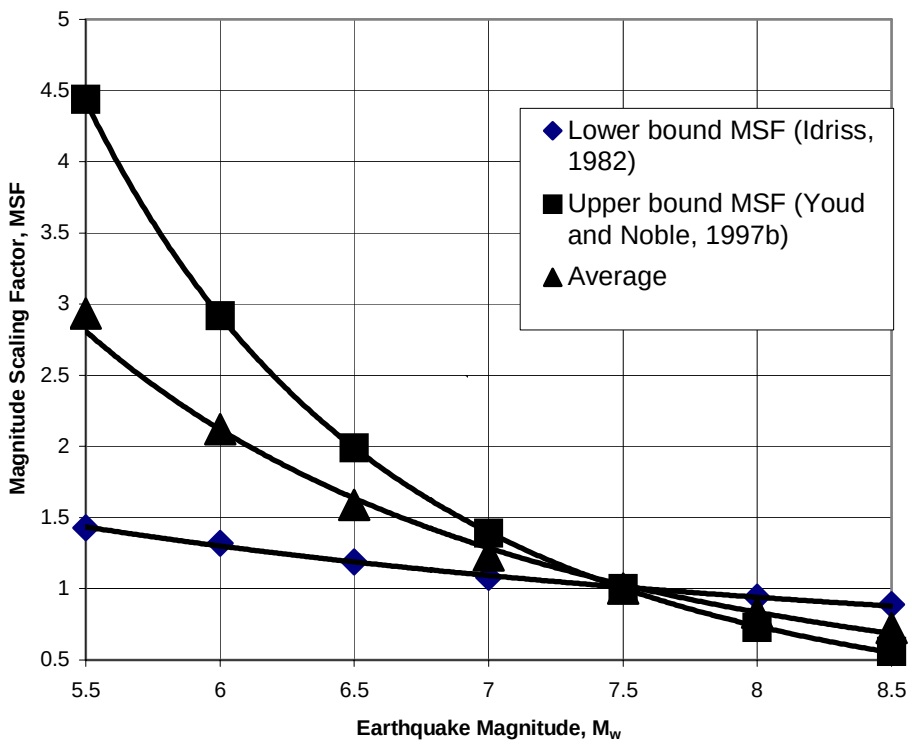

Figure 6.8 -NCEER Recommended Values of *MSF*

Based on the lower bound, upper bound and average values given in equations 6-7 to 6-9, the *COV* for $|MSF - 1|$ is calculated from:

$$COV = \frac{UpperBound - LowerBound}{6 \cdot (Average - 1)} \tag{6-10}$$

The *COV*'s calculated from equation 6-10 are shown in Figure 6.9. Based on Figure 6.9, an average value of *COV* of 22% was approximated.

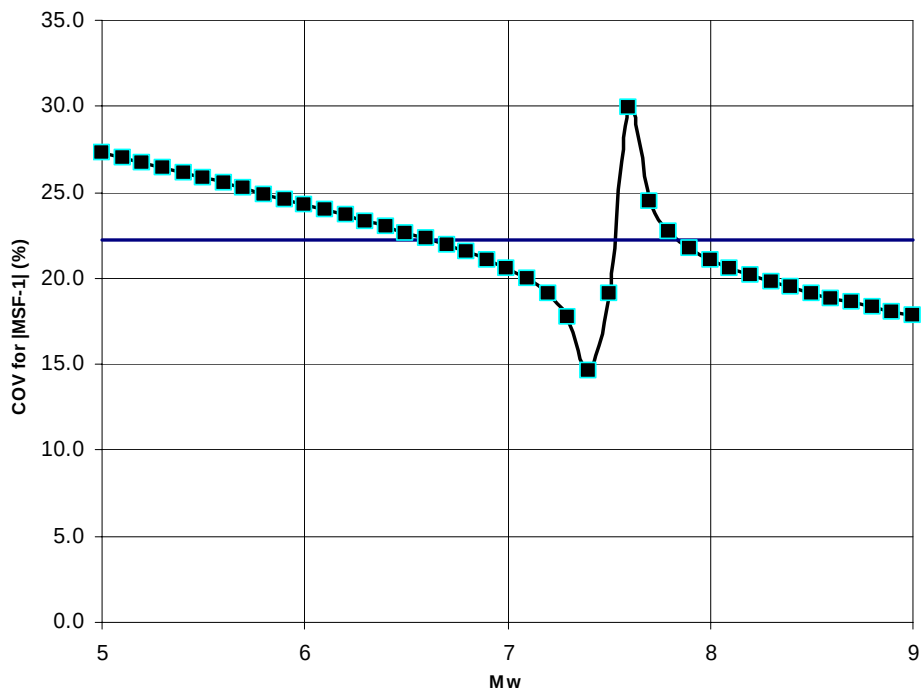

Figure 6.9 - Calculated *COV* for *MSF* Based on the NCEER Recommended Range of

6.3 – Overburden Correction Factor, K_σ, for SPT Analysis

The equation for K_σ is given as follows (Youd and Idriss et. al, 2001):

$$K_\sigma = \left(\frac{\sigma'_{vo}}{P_a} \right)^{f-1} \tag{6-11}$$

where:

$$f = 0.7 - 0.8 \text{ for } D_r = 40\text{-}60\% \tag{6-12}$$

$$f = 0.6 - 0.7 \text{ for } D_r = 60\text{-}80\% \tag{6-13}$$

There is significant uncertainty in K_σ due to the uncertainty in relative density, D_r, and there is also a wide variation in the original data from Hynes and Olsen (1999) which were used to establish equations (6-11) to (6-13). There is, however, little variation associated with correlations between D_r and $(N_1)_{60}$, thus an average deterministic $(N_1)_{60}$ vs. D_r correlation was used to estimate the *COV* for K_σ. Figure 6.10 illustrates a plot of the factor *f* against relative density, while Figure 6.11 plots *f* versus effective overburden stress.

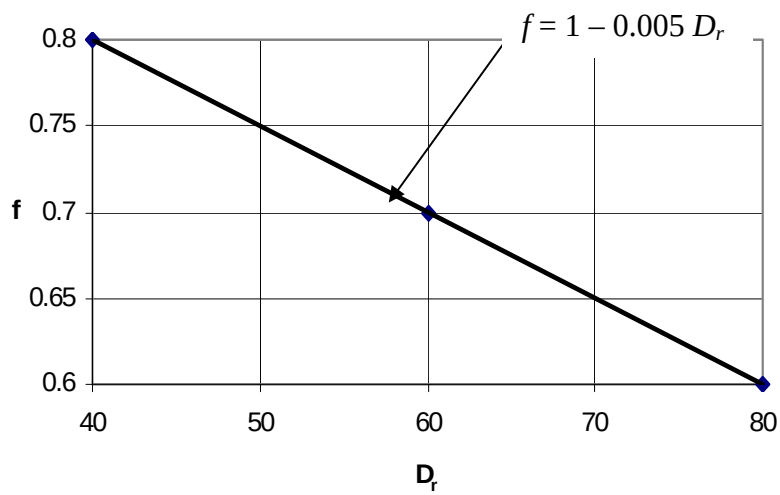

Figure 6.10 - *f* vs. D_r

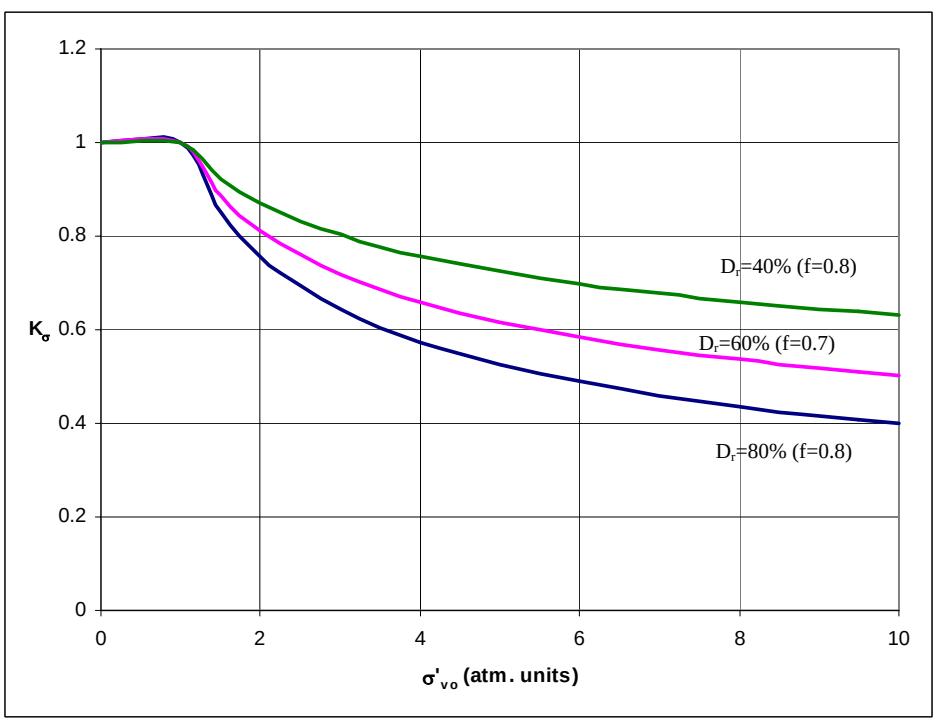

Figure 6.11 -K_σ vs. σ'_{vo}

The following equation provides the form for correlating $(N_1)_{60}$ to D_r:

$$D_r = \sqrt{\frac{(N_1)_{60}}{a\sigma'_v + b}} \tag{6-14}$$

Table 6.2 provides the results of five studies which calculated the values of constants *a* and *b* to be used in equation 6-14.

Table 6.2 - Constants *a* and *b* from Different $(N_1)_{60}$ vs D_r Correlations (σ'_v in tsf)

Constants	Gibbs and Holtz (1957)	Meyerhof (1956)	Skempton (1986)	Peck and Bazaraa (1969)	Average
A	23.3	22.4	28.7	18.5	23.2
B	17	16	30	66	32.2

The following equations combine the above referenced correlations between relative density and *N*-value with the expressions for *f* given in equations 6-17 and 6-18:

$$f = 1 - (0.005)(100)\sqrt{\frac{(N_1)_{60}}{a\sigma'_v + b}} \tag{6-15}$$

$$K_\sigma = \left(\frac{\sigma'_{vo}}{P_a}\right)^{-0.5\sqrt{\frac{(N_1)_{60}}{a\sigma'_{vo}+b}}} \tag{6-16}$$

$$\frac{(N_1)_{60}}{D_r^2} = a\sigma'_v + b \tag{6-17}$$

Next, in Figure 6.12, values of K_σ versus overburden pressure were plotted for a constant *N*=20 in order to illustrate the range of constants *a* and *b* from equation 6-14, based on the data presented in Table 6.2. Average values for *a* and *b* were established by rearranging equation 6-14 in order to plot *a* and *b* as a linear function, as in the form demonstrated in equation 6-17. Figure 6.13 plots the various recommended values of *a* and *b* from Table 6.2. From the figure, the average constants recommend for use in equation 6-14 are determined as: *a* = 23.2 and *b* = 32.3. Substituting these values of *a* and *b* in equation (6-16) gives the following equation for K_σ as function of $(N_1)_{60}$.

$$K_\sigma = \left(\frac{\sigma'_{vo}}{P_a}\right)^{-0.5\sqrt{\frac{(N_1)_{60}}{23.2\sigma'_{vo}+32.2}}} \tag{6.18}$$

This equation is plotted in Fig. 6.14.

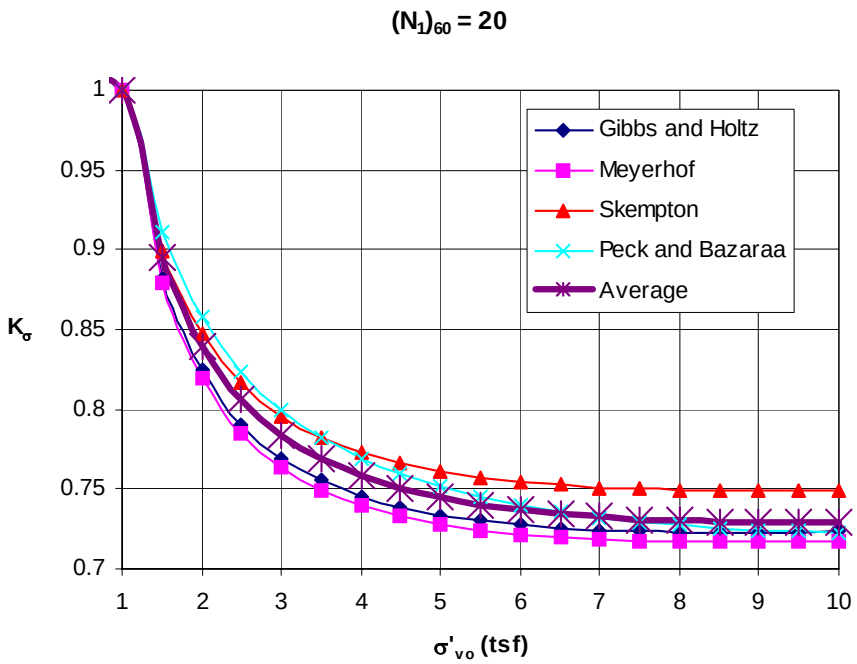

Figure 6.12 - K_σ vs. Effective Overburden Pressure for $(N_1)_{60}$ = 20.

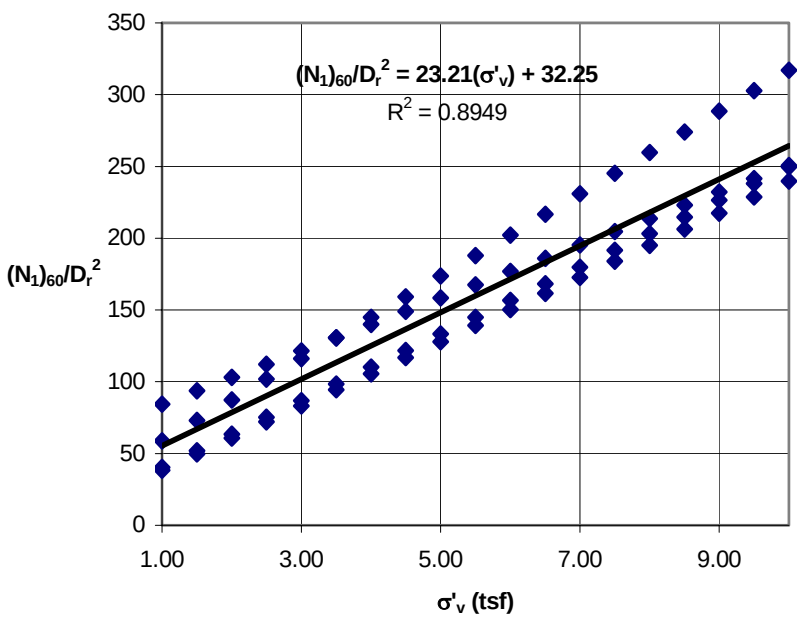

Figure 6.13 - Determination of Average *a* and *b* values

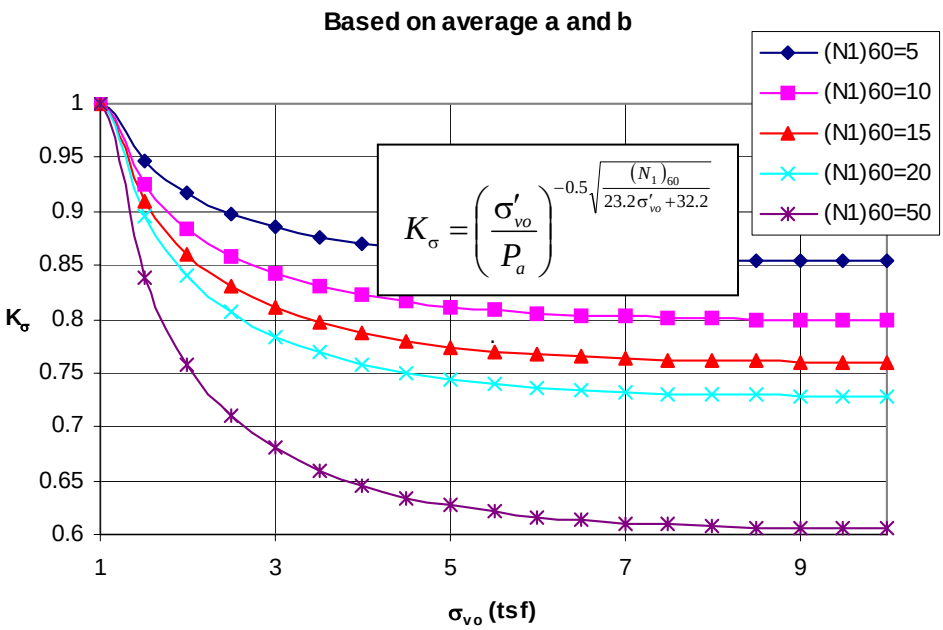

Figure 6.14 - Average Values of K_σ for Varying Corrected *N*-values

Finally, the *COV* for K_σ was estimated based upon data from Hynes and Olsen (1999) by plotting K_σ versus overburden pressure as shown in Figures 6.15 and 6.16. The maximum value of K_σ is always one, and a lower bound was estimated as shown in Figure 6.16. *COV* calculations were performed according to equation 3-3 for 1-$K_{\sigma ave}$ and established an average constant *COV* for K_σ of 33%.

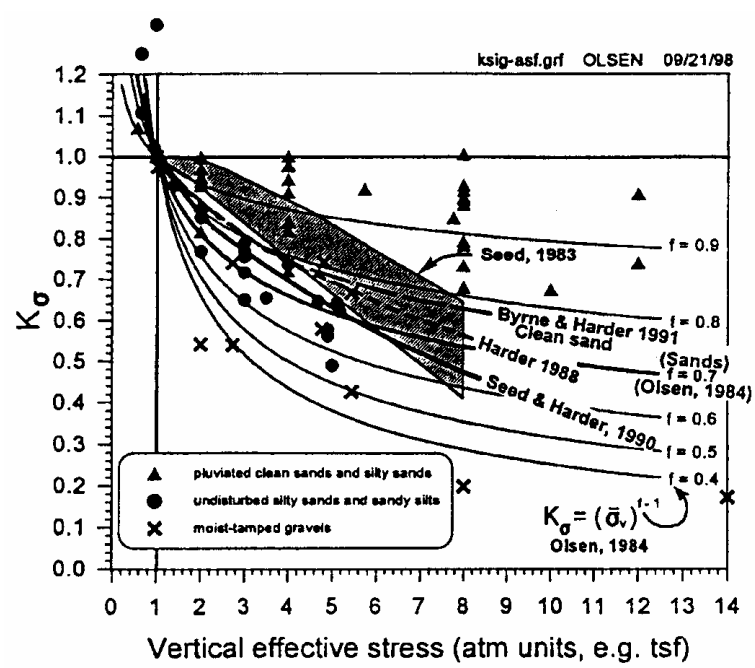

Figure 6.15 - Overburden Stress vs. K_σ (Data from Hynes and Olsen, 1999)

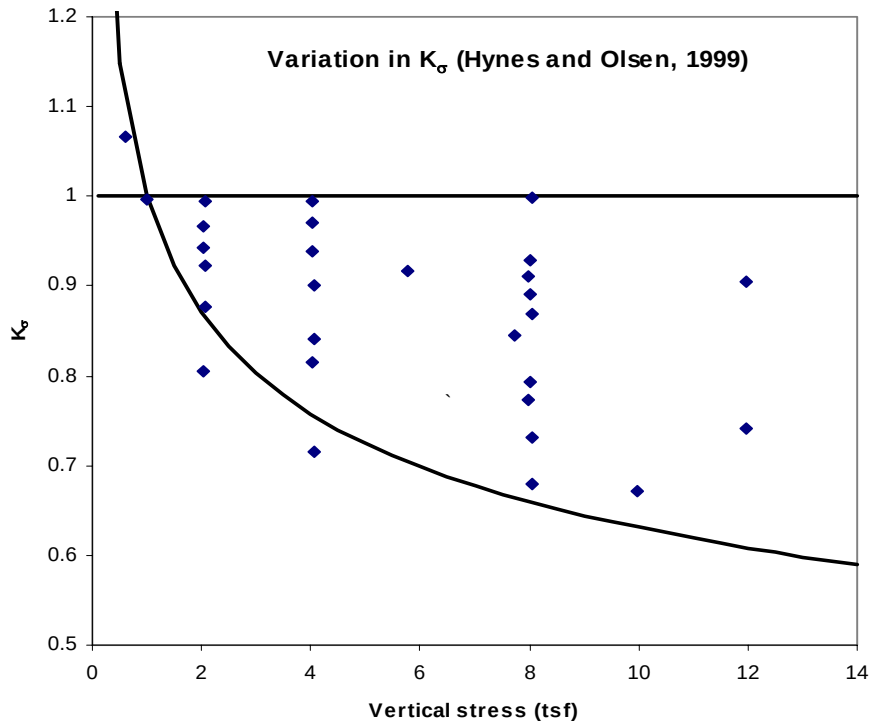

Figure 6.16 - Overburden Stress vs. K_σ (data from Hynes and Olsen, 1999)

6.4 – Overburden Correction Factor, K_σ, for CPT Analysis

The *COV* of K_σ for CPT analysis is estimated directly from the K_σ formula as prescribed by Youd and Idriss et al .(2001) assuming that the relative density is known. Equations 6-11, 6-12, and 6-13 were used to determine the *COV* of K_σ based on different relative densities. Figure 6.17 shows K_σ as a function of effective overburden stress and relative density.

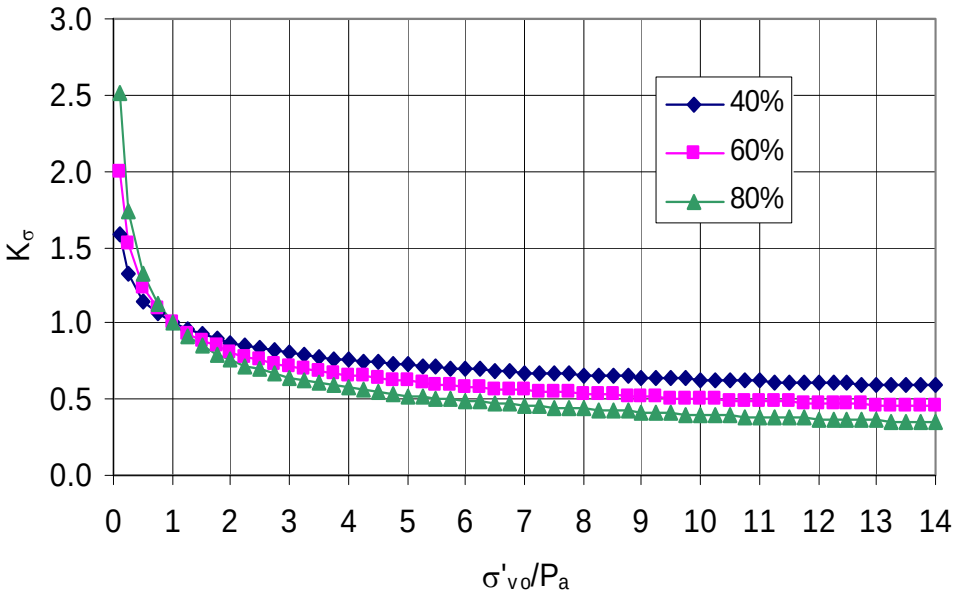

Figure 6. 17 – K_σ as a function of effective overburden stress and relative density based on the Youd and Idriss et al. (2001) formula.

Figure 6-18 shows the calculated *COV*'s for K_σ for a typical stress range along with an average line; the *COV*'s range from 0% to 9% within the stress range with an average *COV* of 6%.

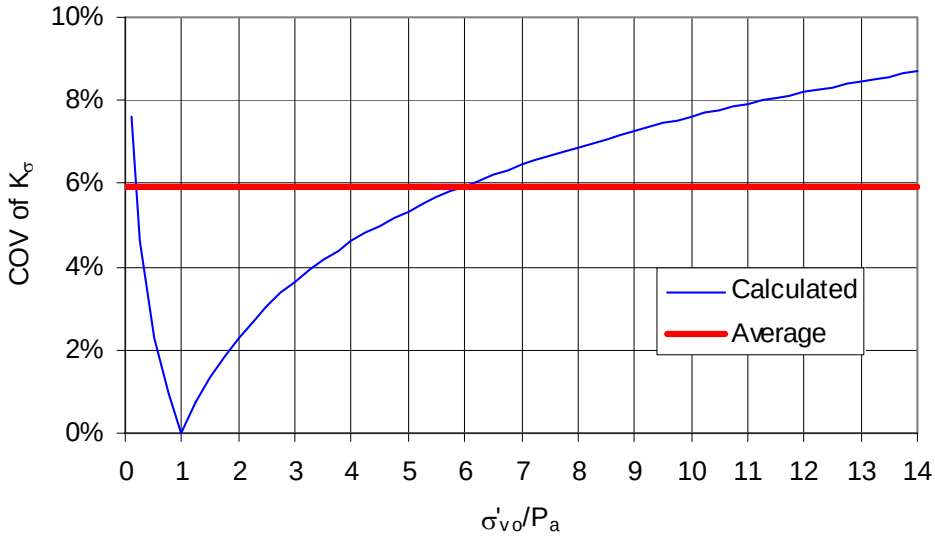

Figure 6. 18 – Calculated and average COV's for K_σ based on Youd and Idriss et al formula (2001)

The *COV* of K_σ can also be approximated as the *COV* of D_r, with D_r calculated from CPT penetration results. Figure 6.19 shows a plot and formula of relative density as a function of normalized CPT tip resistance developed by Jamiolkowski et al. (1985).

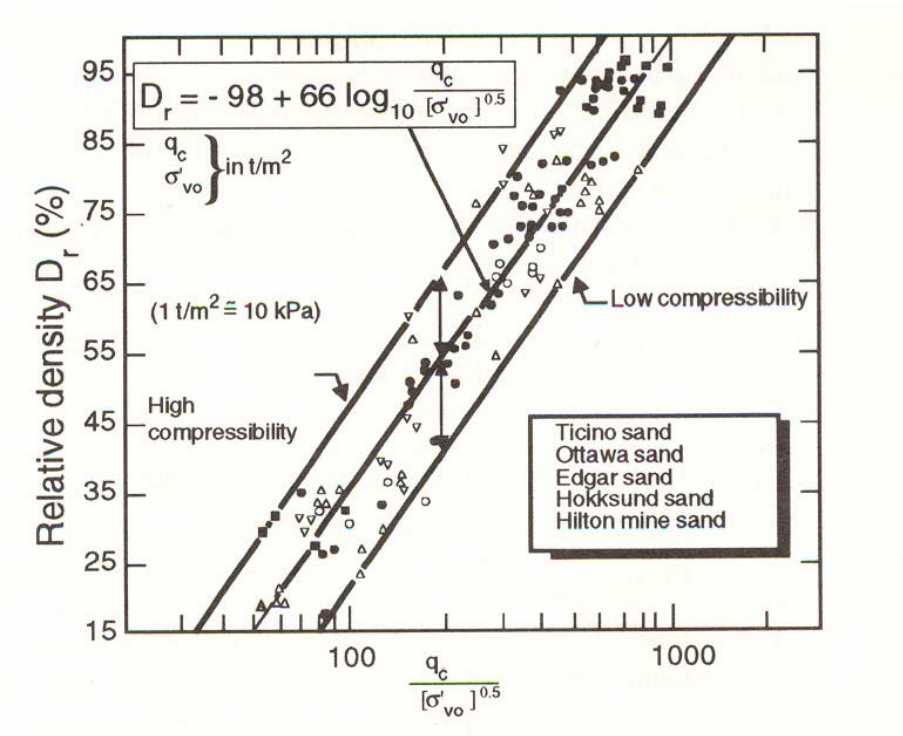

Figure 6.19 – Relative density as a function of CPT tip resistance in sands (from Lunne et al., 1997)

Figure 6.19 was used in order to estimate the *COV* of D_r when computed from CPT q_c and f_s values. Based on a $q_c/(\sigma_{vo})^{0.5}$ value of 200, the following calculations were performed to estimate the *COV* of D_r:

$$Average = \frac{(40\% + 55\% + 65\%)}{3} = 53.3\%$$

$$\sigma = \frac{(HCV - LCV)}{6} = \frac{(65\% - 40\%)}{6} = 4.2\%$$

$$COV = \frac{\sigma}{Average} = 7.9\%$$

6.5 – Correction Factor for Sloping Ground, K_α

The correction factor for sloping ground, K_α, was introduced by Seed (1983) to account for the effects of static shear stresses on liquefaction resistance. Harder and Boulanger (1997) reviewed previous publications regarding K_α, and due to the wide range of values proposed, indicated that more research is needed. Further, the 1998 NCEER committee recommended that K_α not be used by non-specialists in the geotechnical earthquake engineering field (Youd and Idriss et. al, 2001).

7 - CYCLIC RESISTANCE RATIO (CRR) FOR SPT DATA

The criterion for determining liquefaction resistance based upon SPT results is shown in the *CRR* vs. $(N_1)_{60}$ chart originally constructed by Seed et al. (1985), where $(N_1)_{60}$ is the corrected SPT *N*-value as discussed below (Figure 7.1). This chart was constructed from liquefaction case histories where SPT data was available. Youd et al. (2001) recommends the following analytical equation be used for determining the *CRR* based on SPT results:

$$CRR_{M\,7.5} = \left(\frac{1}{34-(N_1)_{60cs}}\right) + \left(\frac{(N_1)_{60cs}}{135}\right) + \left(\frac{50}{\left[10(N_1)_{60cs}+45\right]^2}\right) - \frac{1}{200} \qquad (7\text{-}1)$$

It should be noted that equation 7-1 is only valid for clean, granular sands with an $(N_1)_{60}$ less than 30 blows per foot. Sands with corrected *N*-values greater than 30 are classified as non-liquefiable.

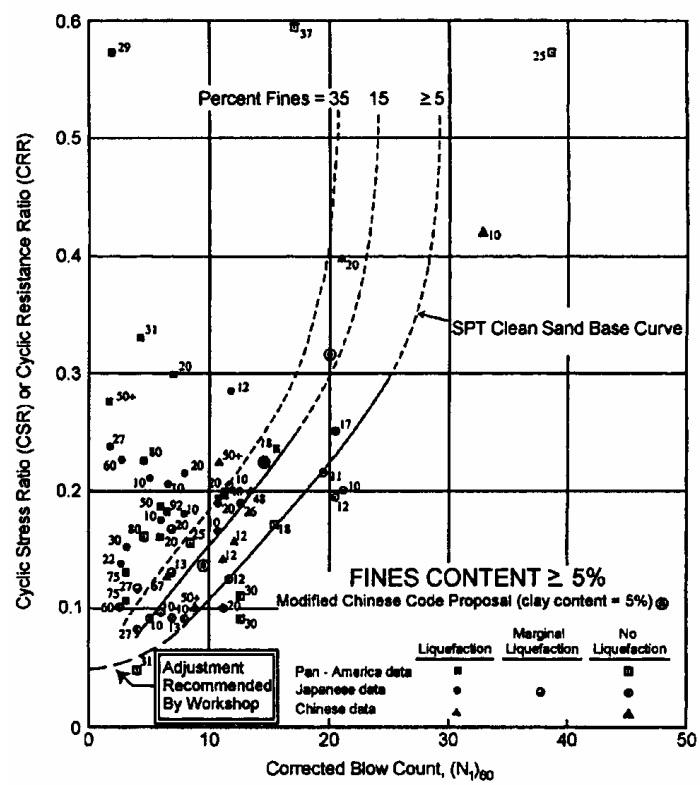

Figure 7.1 – SPT clean-sand based curve for M_w=7.5 earthquakes with data for liquefaction case histories (modified from Seed et al. 1985).

In order to obtain equivalent, clean-sand corrected *N*-values, or $(N_1)_{60cs}$, Youd et al. (2001) recommend the following equation:

$$(N_1)_{60cs} = \alpha + \beta(N_1)_{60} \qquad (7\text{-}2)$$

where α and β are given as follows:

$$\alpha = 0 \text{ and } \beta = 1 \text{ for } FC < 5.0\% \tag{7-3}$$

$$\alpha = \exp\left[1.76 - \frac{190}{FC^2}\right] \text{ and } \beta = \left[0.99 + \frac{FC^2}{1000}\right] \text{ for } 5\% < FC < 35\% \tag{7-4}$$

$$\alpha = 5 \text{ and } \beta = 1.2 \text{ for } FC > 35\% \tag{7-5}$$

The fines correction parameters α and β are treated as deterministic variables in this procedure, while the fines content *FC* is treated as a non-deterministic variable.

When determining the Standard Penetration Test *N*-value to be used as outlined in the NCEER 1997 Liquefaction Evaluation Procedure, a series of correction factors are considered. The equation used for determining the corrected *N*-value, $(N_1)_{60}$, is as follows:

$$(N_1)_{60} = N \cdot C_N \cdot C_E \cdot C_R \cdot C_S \cdot C_B \tag{7-6}$$

where N = field recorded SPT *N*-value, C_N = overburden correction factor, C_E = hammer energy correction factor, C_R = drilling rod length correction factor, C_S = sampler correction factor, and C_B = borehole diameter correction factor.

A detailed investigation of each correction factor was performed to demonstrate the effect that each has on the uncertainty of the overall corrected value. Ranges for each correction factor were obtained from published data and analyzed to determine a standard deviation and subsequently a *COV*.

The following sections outline the methods used for determining a *COV* for each correction factor, as well as describe the data used to estimate the standard deviation.

7.1 - Overburden Correction Factor, C_N

The first correction factor, C_N, normalizes the blow count to a standard overburden pressure of 1 tsf. This factor is designed to reduce the effects of increased overburden stress on the recorded blow count. The general formula for C_N as determined by Seed and Idriss (1982) is as follows:

$$C_N = \frac{2.2}{\left(1.2 + \left(\frac{\sigma'_{vo}}{P_a}\right)\right)} \tag{7-7}$$

For the purposes of estimating a standard deviation of this correction factor, a range of data based on various soil types by Castro (1995), as shown in Figure 7.2, was used.

As is shown in Figure 7.2, curves were fitted to the upper and lower bounds of the data using the general equation form:

$$C_N = \frac{x}{\left((x-1)+\left(\frac{\sigma'_{vo}}{P_a}\right)\right)} \tag{7-8}$$

where x is the variable which was altered to fit to the bounds of the data. The minimum and maximum values of x which were obtained based on the two best fit boundary curves were 0.8 and 4.3, while an average value of 2.2 from Seed and Idriss' formula was used.

Figures 7.3 and 7.4 were constructed based on data points from the minimum and maximum curves as shown above. In Figure 7.3, the ranges of overburden correction factor versus overburden pressure are plotted against one another. Because the range between the minimum and maximum recommended values of C_N decreases as the value of C_N increases, it is preferable to consider the variation in the value of 1-C_N. A subsequent plot, Figure 7.4, was constructed so that an average trend line could be determined to obtain an equation for 1-C_N. Based on this plot, the following equation was obtained:

$$1 - C_N = 0.20x - 0.14 \quad \text{for } x \geq 1 \text{ tsf} \tag{7-9}$$

where x is the overburden pressure in tsf.

Based on this average trendline, the standard deviation and *COV* can be calculated using the upper and lower ranges plotted in Figure 7.4. At an overburden pressure of 2 tsf, 1-C_N varies from 0.48 to 0.14. The *COV* is calculated as follows:

$$Average = (0.2 \cdot 2) - 0.14 = 0.26$$

$$\sigma = \frac{(0.48 - 0.14)}{6} = 0.06$$

$$COV = \frac{0.06}{0.26} = 23.1\%$$

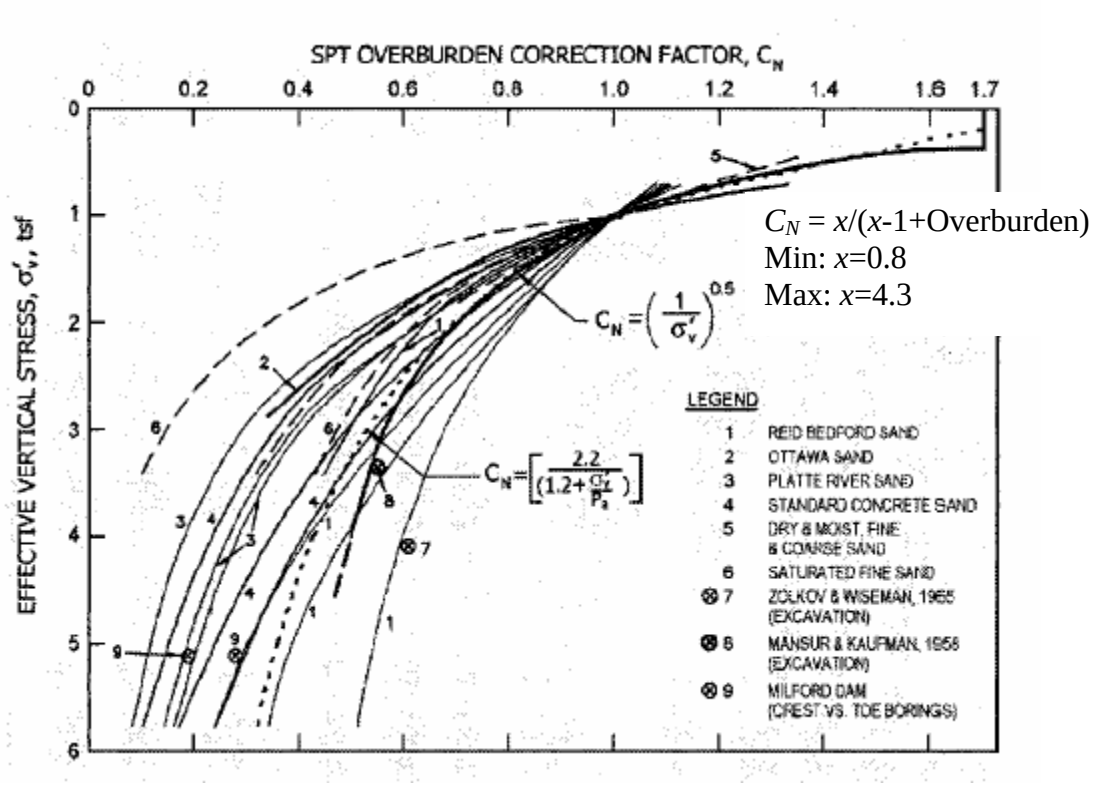

Figure 7.2 - Overburden Correction Factor vs. Vertical Effective Stress (after Castro, 1995)

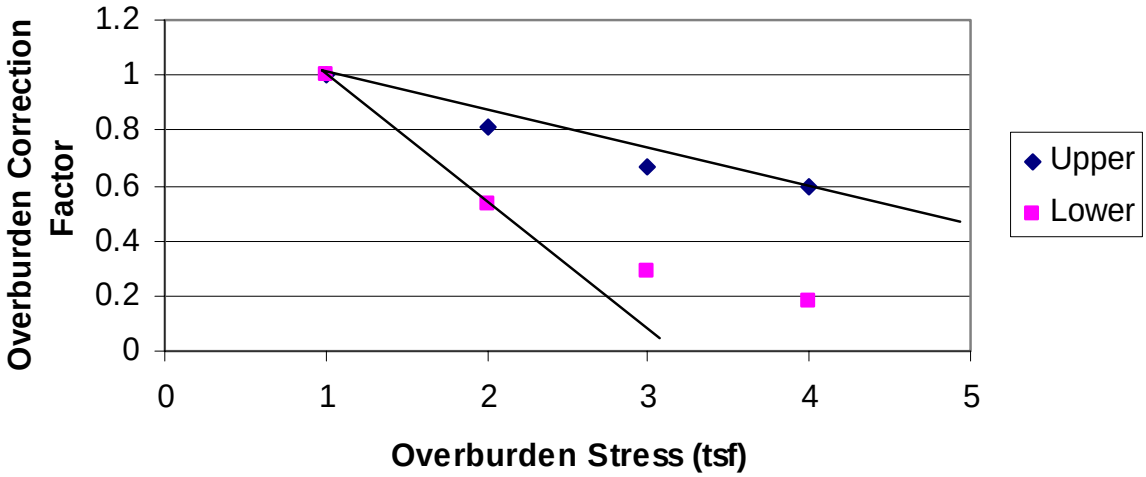

Figure 7.3 - Overburden Correction Factor vs. Overburden Pressure

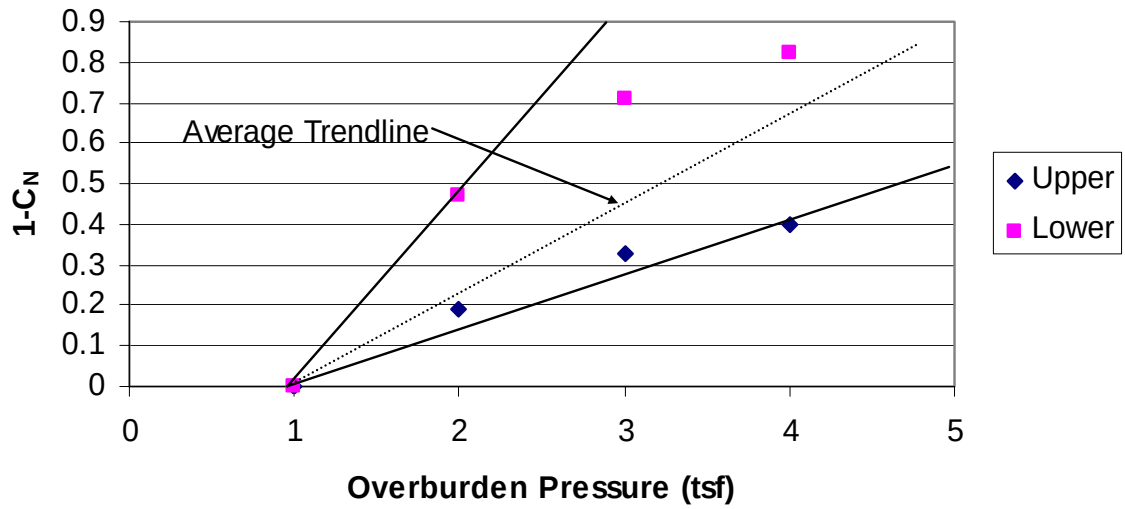

Figure 7.4 - (1-C_N) vs. Overburden Pressure

7.2 - Energy Correction Factor, C_E

The energy correction factor normalizes the blow count to a hammer which imparts 60% of its theoretical energy to the split-spoon sampler. Values vary for different types of hammers, including donut, safety, and automatic hammers. The range of values of this parameter for each of the above mentioned hammers is given in the Youd et al. (2001) as follows:

Table 7.1 - Values of C_E Based on Hammer Type (Youd and Idriss et al., 2001)

Hammer Type	C_E
Donut Hammer	0.5-1.0
Safety Hammer	0.7-1.2
Automatic Hammer	0.8-1.3

The standard deviation and coefficient of variation for each of the three hammer types was calculated as follows:

<u>Donut Hammer</u>

$$Average = 0.75$$

$$\sigma = \frac{(1.0 - 0.5)}{6} = 0.083$$

$$COV = \frac{0.083}{0.75} = 11.0\%$$

Safety Hammer

$$Average = 0.95$$
$$\sigma = \frac{(1.2 - 0.7)}{6} = 0.083$$
$$COV = \frac{0.083}{0.95} = 8.7\%$$

Automatic Hammer

$$Average = 1.05$$
$$\sigma = \frac{(1.3 - 0.8)}{6} = 0.083$$
$$COV = \frac{0.083}{1.05} = 7.9\%$$

7.3 - Rod Length Correction Factor, C_R

The next parameter is the rod length correction factor, C_R, which is needed to account for the effects of rod length above the sampling spoon. As the sampler is advanced further into the ground, the amount of energy lost in the drill rods increases. The following table provides the recommended C_R values according to the NCEER Proceedings (Youd and Idriss et. al, 2001):

Table 7.2 - Values of C_R Based on Depth (Youd and Noble et al., 2001)

Depth	C_R
<13 feet	0.75
13-20 feet	0.85
20-30 feet	0.95
>30 feet	1.0

Figure 7.5 shows the range of rod length correction factor versus depth. Again, because the range between the minimum and maximum recommended values of C_R decreases as the value of C_R increases, it is preferable to consider the variation in the value of 1-C_R. A subsequent plot, Figure 7.6, was constructed so that an average trendline could be determined to obtain an equation for 1-C_R. Based on this plot, the following equation was obtained:

$$1 - C_R = 0.36 - 0.012x \quad \text{for } x \leq 30 \text{ feet} \tag{7-10}$$

where x is the depth in feet.

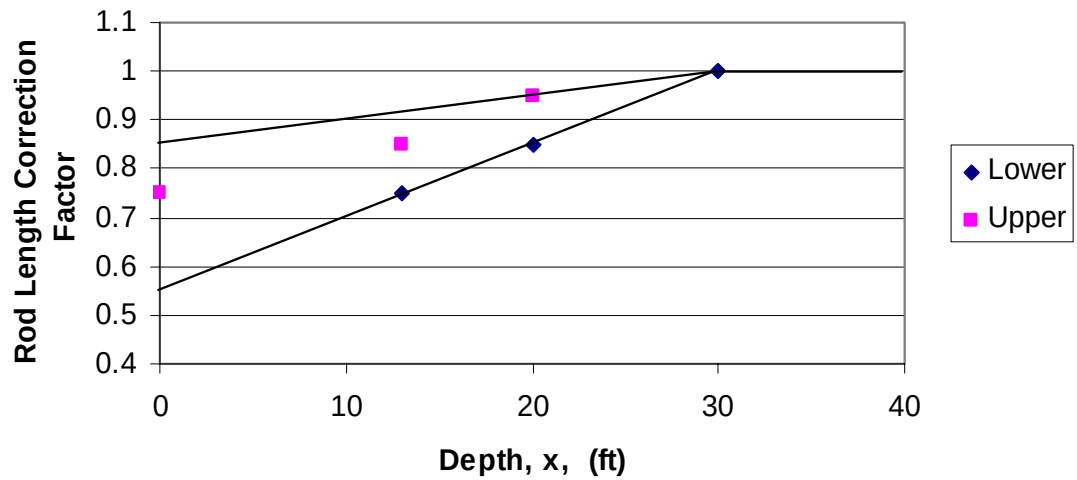

Figure 7.5 - Rod Length Correction Factor vs. Depth

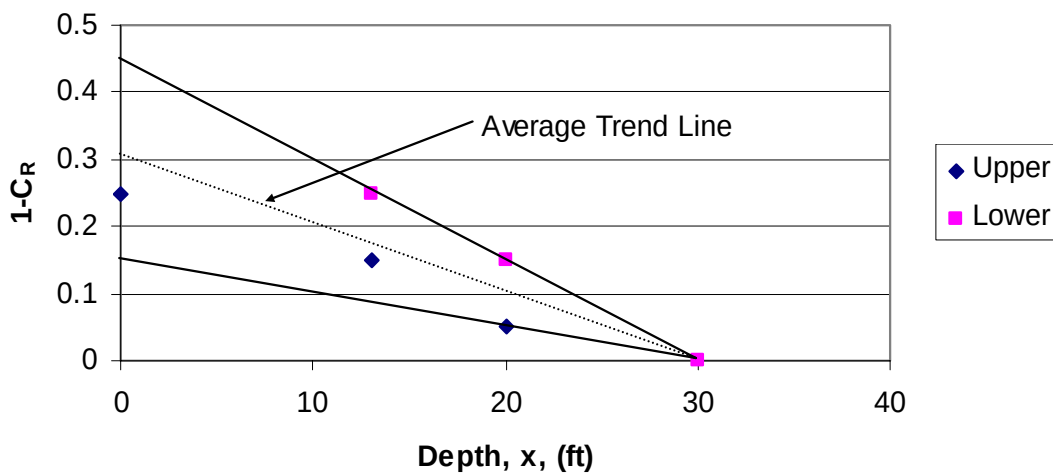

Figure 7.6 - (1-C_R) vs. Depth

Based on this average trendline, the standard deviation and *COV* can be calculated based on the upper and lower ranges plotted in Figure 7.6.

At a depth of 0 feet, 1-C_R varies from 0.45 to 0.15.

$$Average = 0.30 - (0.012 \cdot 0) = 0.036$$

$$\sigma = \frac{(0.45 - 0.15)}{6} = 0.05$$

$$COV = \frac{0.05}{0.30} = 16.7\%$$

7.4 - Sampler Correction Factor, C_S

The next correction factor to be applied is based on the type of sampler used. In samplers where there is a liner, there is a continuous 1·3/8 inch diameter within the sampler. In samplers without the liner, the interior diameter is 1·½ inches behind the drive shoe. The recommended values for C_S as proposed by the NCEER Proceedings (Youd and Idriss et al., 2001) are as follows:

Table 7.3 - Values of C_S Based on Sampler Type (Youd and Idriss et al., 2001)

Sampler	C_S
With Liner	1.0
Without Liner	1.1 to 1.3

The standard deviation and coefficient of variation were determined using the above referenced values.

<u>Sampler with Liner</u>

Since there is no spread to the standard sampler, which is the most commonly used today, the coefficient of variation was determined to be zero.

<u>Sampler without Liner</u>

$$Average = 1.2$$

$$\sigma = \frac{(1.3 - 1.1)}{6} = 0.033$$

$$COV = \frac{0.033}{1.2} = 2.8\%$$

7.5 - Borehole Diameter Correction Factor, C_B

A borehole diameter correction factor is required for diameters greater than 4.5 inches. Diameters which exceed this value could lead to stress relaxation of the soil, which would lead to lower recorded blow counts. The recommended values for this parameter are given by the Youd and Idriss et al. (2001) as follows:

Table 7.4 - Values of C_B Based on Borehole Diameter (from Youd and Idriss et al., 2001)

Borehole Diameter	**Correction Factor**
2.5 to 4.5 inches	1.0
6 inches	1.05
8 inches	1.15

The data listed in Table 7.4 are plotted in Figure 7.7. In plotting the ranges of data for borehole diameter correction, as is shown in Figure 7.7, an overall expression for C_B in terms of diameter can be derived as follows, based on an average trendline of the data:

$$C_B = 0.88 + 0.033D \tag{7-11}$$

where D is the borehole diameter in inches.

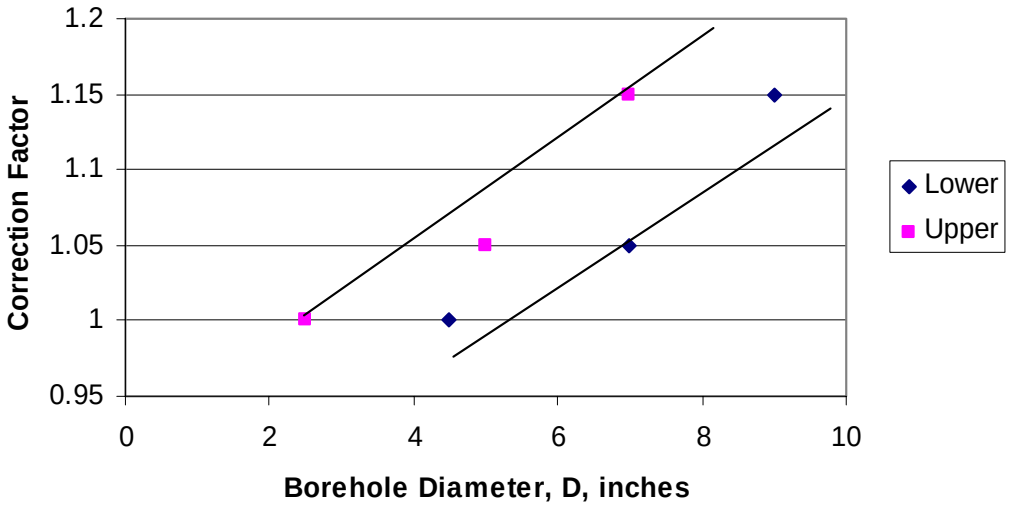

Figure 7.7 - Borehole Diameter vs. Correction Factor

Based on this average, the standard deviation and *COV* can be calculated using the upper and lower values plotted in Figure 7.7.

At 6 inches, the correction factor varies from approximately 1.12 to 1.02.

$$Average = (0.033 * 6) + 0.88 = 1.08$$

$$\sigma = \frac{(1.12 - 1.02)}{6} = 0.01$$

$$COV = \frac{0.01}{1.08} = 1.0\%$$

7.6 - Summary

Table 7.5 summarizes the results of the above calculations according to the "Three-Sigma Rule." In addition, the table also contains *COV*'s for a varying denominator in the standard deviation calculation, as discussed by Christian and Baecher (2001).

Table 7.5 - Summary of *COV* for *N*-value Correction Factors

Correction Factor	*COV (%)*			
	N_n=3*	N_n=4*	N_n=5*	N_n=6*
C_N	53.0	39.8	31.8	27.0
C_E (Donut)	22.2	16.7	13.3	11.0
C_E (Safety)	17.5	13.2	10.5	9.0
C_E (Automatic)	15.6	11.9	9.5	8.0
C_R	33.3	25	20.0	16.7
C_S (w/o liner)	5.6	4.2	3.3	3.0
C_B	2.2	1.6	1.3	1.0

* The value used in the denominator of the standard deviation expression.

8 – CRR FOR CPT DATA

The criterion for determining the liquefaction resistance based upon CPT results is shown in Figure 8.1, where q_{c1N} is the corrected CPT tip resistance as discussed below.

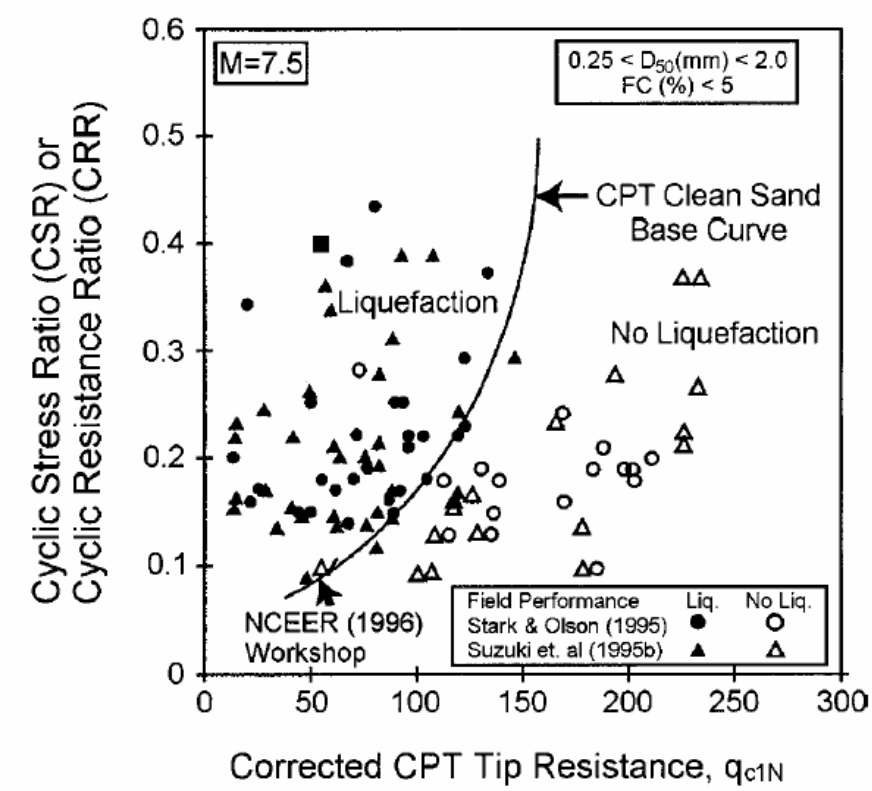

Figure 8.1 – Curve recommended for calculation of CRR based on CPT results (from Youd and Idriss et al., 2001)

Figure 8.1 was constructed from limited liquefaction case histories where CPT data was available. Youd et al (2001) recommends the following analytical equations be used for determining the *CRR* based on CPT data:

$$CRR_{7.5} = 0.833\left[\frac{(q_{c1N})_{cs}}{1000}\right] + 0.05 \quad \text{if } (q_{c1N})_{cs} < 50 \tag{8-1}$$

$$CRR_{7.5} = 93\left[\frac{(q_{c1N})_{cs}}{1000}\right] + 0.08 \quad \text{if } 50 \le (q_{c1N})_{cs} < 160 \tag{8-2}$$

where $(q_{c1N})_{cs}$ is the normalized clean-sand cone penetration resistance. It should be noted that equations 8-1 and 8-2 are only valid for clean, granular sands with a

$(q_{c1N})_{cs}$ value less than 160. Any sand with $(q_{c1N})_{cs}$-values greater than 160 is considered non-liquefiable.

In order to obtain $(q_{c1N})_{cs}$, Youd et al (2001) recommends the following equation:

$$\left(q_{c1N}\right)_{cs} = K_c q_{c1N} \tag{8-3}$$

where K_c is the correction factor for grain characteristics.

The following equations are recommended by Youd et al (2001) to calculate the K_c factor as a function of the soil behavior type index, I_c:

$$K_c = 1.0 \quad \text{for } I_c \leq 1.64 \tag{8-4}$$

$$K_c = -0.403 I_c^{\,4} + 5.581 I_c^{\,3} - 21.63 I_c^{\,2} + 33.75 I_c - 17.88 \text{ for } I_c > 1.64 \tag{8-5}$$

For values of I_c greater than 2.6, Youd et al (2001) suggests that soils in this range (plastic soils and clayey soils) are not likely to liquefy.

In order to obtain the value of I_c, Youd et al (2001) recommends the following equation:

$$I_c = \left[\left(3.47 - \log Q\right)^2 + \left(1.22 + \log F\right)^2\right]^{0.5} \tag{8-6}$$

where Q and F are the normalized cone resistance and normalized friction ratio, respectively. Q and F are determined from the following equations:

$$Q = \left[\frac{\left(q_c - \sigma_{vo}\right)}{P_a}\right]\left[\frac{P_a}{\sigma'_{vo}}\right]^n \tag{8-7}$$

$$F = 100\left[\frac{f_s}{\left(q_c - \sigma_{vo}\right)}\right] \tag{8-8}$$

where q_c = CPT tip resistance, f_s = CPT sleeve resistance, σ_{vo} = total overburden pressure, σ'_{vo} = effective overburden pressure, P_a = atmospheric pressure, and n = nonlinear stress exponent (a consistent set of units should be used for all pressures/resistances).

The apparent fines content, FC, can be estimated from the soil behavior index with the following equations:

$$FC=0\% \text{ if } I_c<1.26 \tag{8-8}$$

$$FC = 1.75 I_c^{3.25} - 3.7 \quad \text{if } 1.26 \le I_c \le 35 \tag{8-9}$$

$$FC=100\% \text{ if } I_c>35 \tag{8-10}$$

Since the apparent fines content is not used in determining the factor of safety against liquefaction, this study does not delve into its reliability. When performing a liquefaction analysis with CPT data, the fines content and soil type should be considered.

The soil behavior type index, normalized cone resistance, and normalized friction ratio are treated as deterministic parameters in this study.

When determining the CPT q_{c1N}-value to be used as outlined in the NCEER 2001 Liquefaction Evaluation Procedure, the following equation is recommended:

$$q_{c1N} = \left(\frac{q_c}{P_a}\right) C_Q \tag{8-11}$$

A detailed investigation of the non-deterministic variables was performed in order to demonstrate the effect that each has on the calculated values of $(q_{c1N})_{cs}$. These non-deterministic variables include q_c, f_s, n, C_Q, and K_c.

The following sections outline the methods used for determining COV's for each non-determinant variable mentioned above.

8.1 – CPT Tip Resistance, q_c, and Sleeve Resistance, f_s

The measured tip and sleeve resistances contribute to the overall uncertainty of a liquefaction potential evaluation using the CPT. In order to estimate this uncertainty, measured q_c- and f_s-values from calibration chamber tests (Lunne et al. 1997) were corrected to $(q_{c1N})_{cs}$ and separated into groups based on relative density, D_R. Figure 8.2, below shows the values of *COV* calculated for $(q_{c1N})_{cs}$ for different values of D_R. This study assumes that the *COV* for q_c and f_s are equal to that of $(q_{c1N})_{cs}$. The red line represents the average $(q_{c1N})_{cs}$ *COV* value. Figure 8.2 shows that the average *COV* for $(q_{c1N})_{cs}$ is approximately 21%.

In addition to the calibration chamber results, q_c- and f_s-values from thirteen CPT soundings performed at a Bureau of Reclamation dam were used to estimate site-specific *COV*'s. The q_c and f_s values were corrected to $(q_{c1N})_{cs}$ values, and these values were then subdivided into five foot intervals based on depth. The average, standard deviation, and coefficient of variation were calculated with equations 8.9, 8.10, and 8.11, respectively. Some variation was found among the *COV*'s for the different groups of data, this scatter is shown in Figure 8.3.

The *COV* for the site-specific $(q_{c1N})_{cs}$ values ranged from 15% to 50% with an average of 35%.

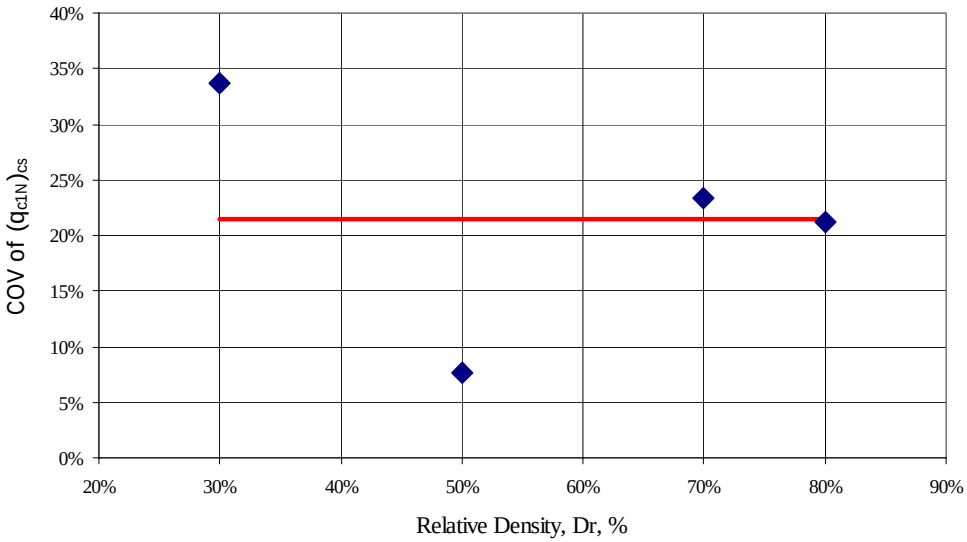

Figure 8.2 – Calibration Chamber Tests – COV's for normalized clean-sand cone penetration resistance

8.2 – Nonlinear Stress Exponent, n

The linear stress exponent *n* varies depending on the soil type. Robertson and Wride (1998) suggest using a *n*-value of 0.5 in sand type soils and 1.0 in clay type soils, their discussion recommends that an iterative procedure by used in selected the final *n*-value for the NCEER 2001 Liquefaction Evaluation Procedure.

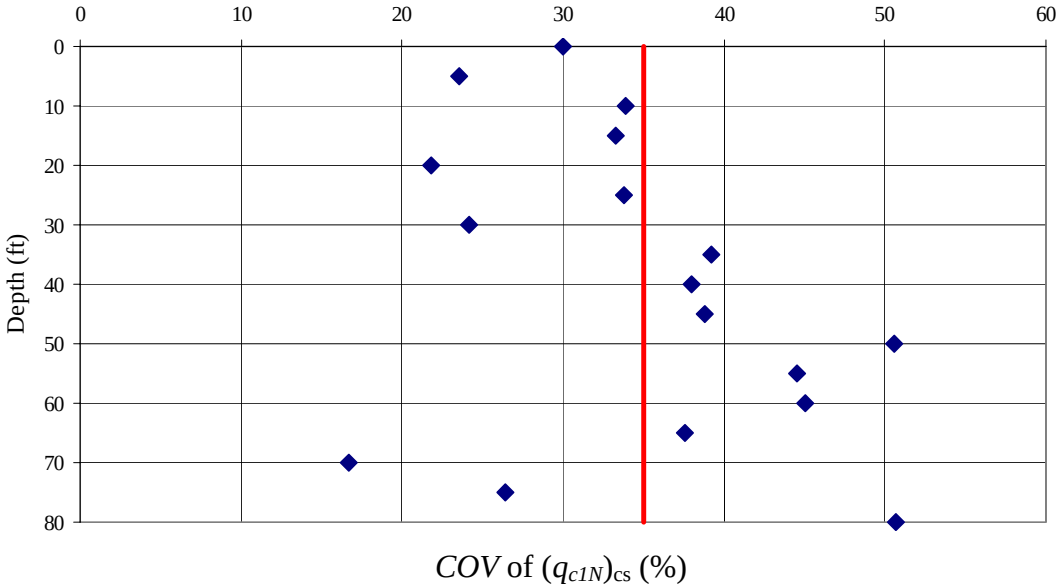

Figure 8.3 – Site-specific COV's for normalized clean-sand cone penetration resistance

In order to determine the uncertainty associated with the linear stress exponent, the following calculations were made:

$$Average = \frac{1.0 + 0.5}{2} = 0.75$$

$$\sigma = \frac{HCV - LCV}{6} = \frac{(1.0 - 0.5)}{6} = 0.083$$

$$COV = \frac{\sigma}{average} = \frac{0.083}{0.75} = 11\%$$

As shown above the *COV* for the linear stress exponent is 11%.

8.3 – Overburden Correction Factor, C_Q

The overburden correction, C_Q, normalizes the measured cone tip penetration resistance to a standard pressure. This factor is designed to reduce the effects of increased overburden stress on the recorded cone tip resistance. The general formula for C_Q recommended by Youd and Idriss et al. (2001) is as follows:

$$C_Q = \left(\frac{P_a}{\sigma'_{vo}} \right)^n \tag{8-12}$$

The overburden correction factor was normalized to its inverse logarithm, (1/log(C_Q)). This normalization was performed in an attempt to linearize C_Q as a function of the effective overburden pressure - atmospheric pressure ratio, (σ'_{vo}/P_a). Figure 8.4 shows the normalization of C_Q. Values of n ranged from 0.5 to 1.0, while σ'_{vo}-values ranged from 10 to 1400 kPa. Figure 8.4 shows normalized C_Q curves for n=0.5 and n=1.0; an average trend line was determined for calculating the *COV* associated with the overburden correction factor.

Equations 3-1 and 3-3 were used to calculate the standard deviations and coefficients of variation for the overburden correction factor. Figure 8.5 shows the calculated *COV* values of the normalized overburden correction factor. As shown in Figure 8.5, the *COV* values ranged from 6% to 19% with an average of 13%.

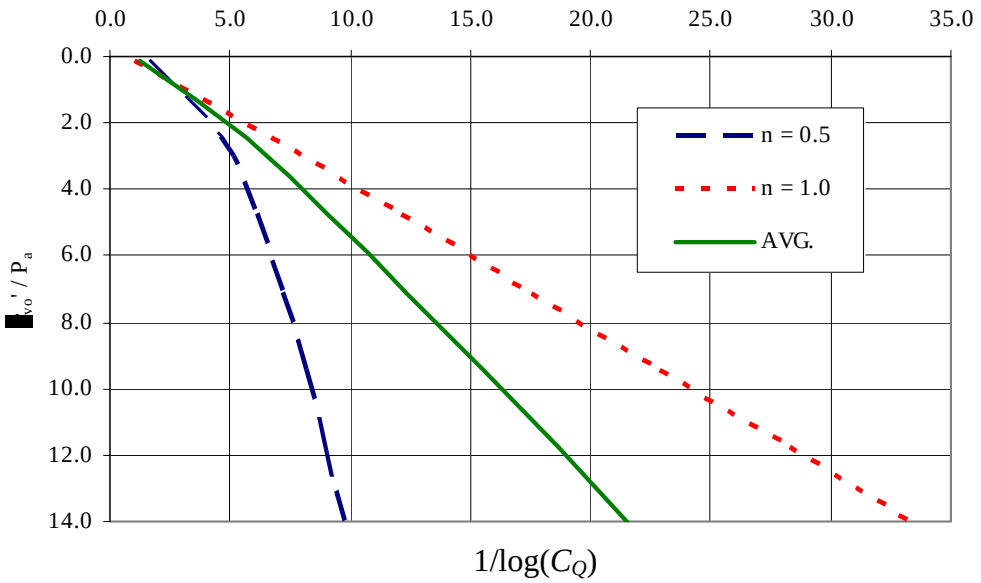

Figure 8.4 – Normalization of C_Q for the determination of the COV associated with C_Q

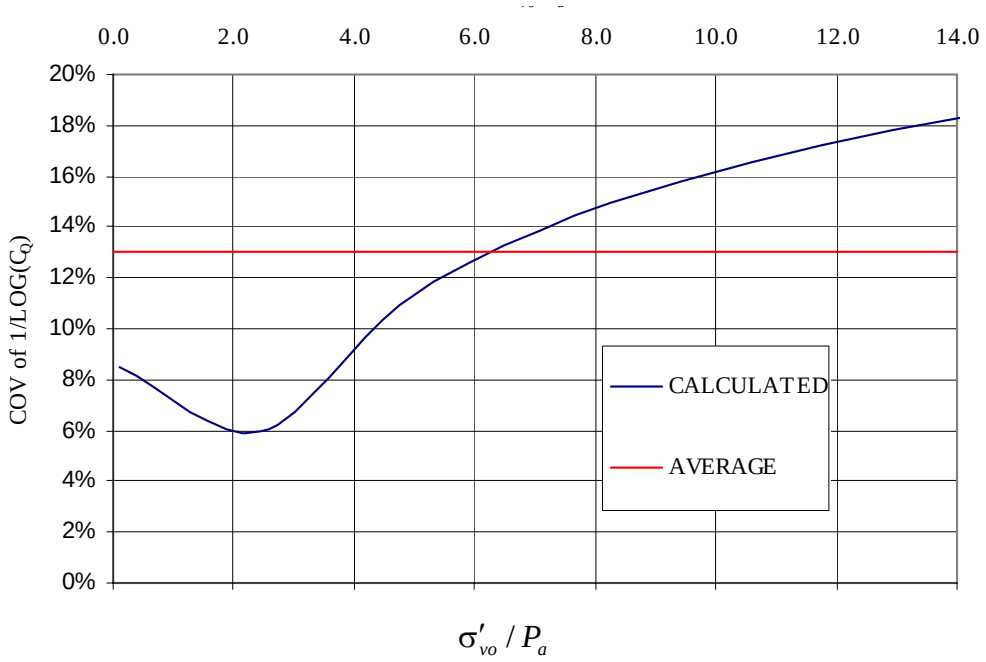

Figure 8.5 – Calculated COV's for 1/LOG(C_Q)

8.4 – CPT Grain Characteristics Correction Factor, K_c

The grain characteristics correction factor, K_c, is used to correct the normalized cone tip penetration resistance, q_{c1N}, to an equivalent clean-sand $(q_{c1N})_{cs}$-value. The equations used to determine K_c (equations 8-4 and 8-5) are among several correlations between K_c and I_c. Figure 8.6 shows a comparison of the various K_c – I_c correlations.

In order to determine the uncertainty related with K_c, Figure 8.8 was developed. Figure 8.8 shows the upper bound, lower bound, and average values selected off of Figure 8.7. The standard deviation and coefficient of variation for K_c were determined using equations 3.1 and 3.3. Figure 8.9 shows the calculated and average *COV*'s for the grain characteristic correction factor. The dotted line in Figure 8.9 shows that the average value for the *COV* of K_c is approximately 6%.

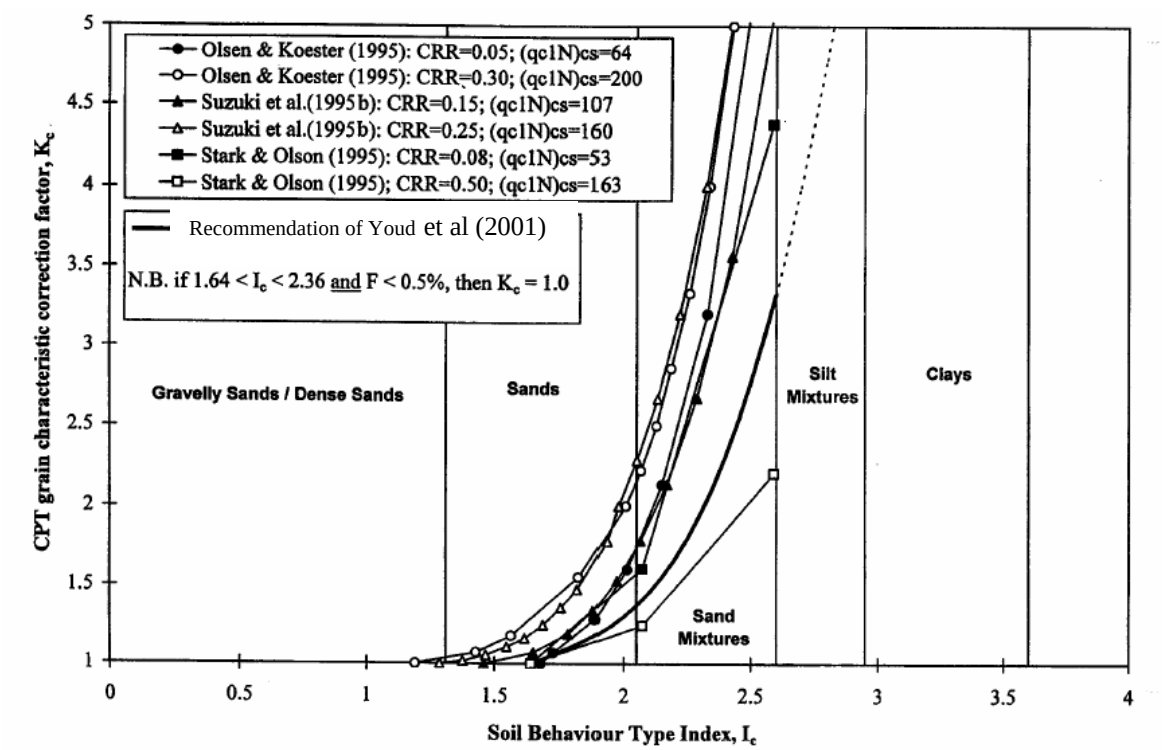

Figure 8.6 – Approximate comparison of various methods for determining K_c as a function of I_c (after Robertson and Wride, 1998)

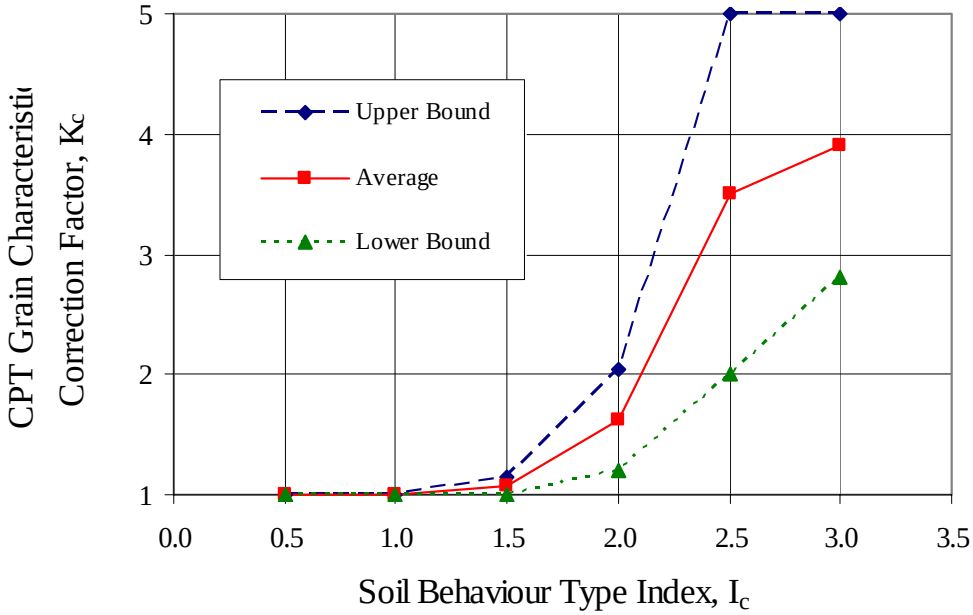

Figure 8.7 – Approximate upper, lower, and average K_c-I_c relationships used in the determination of the COV resulting from K_c

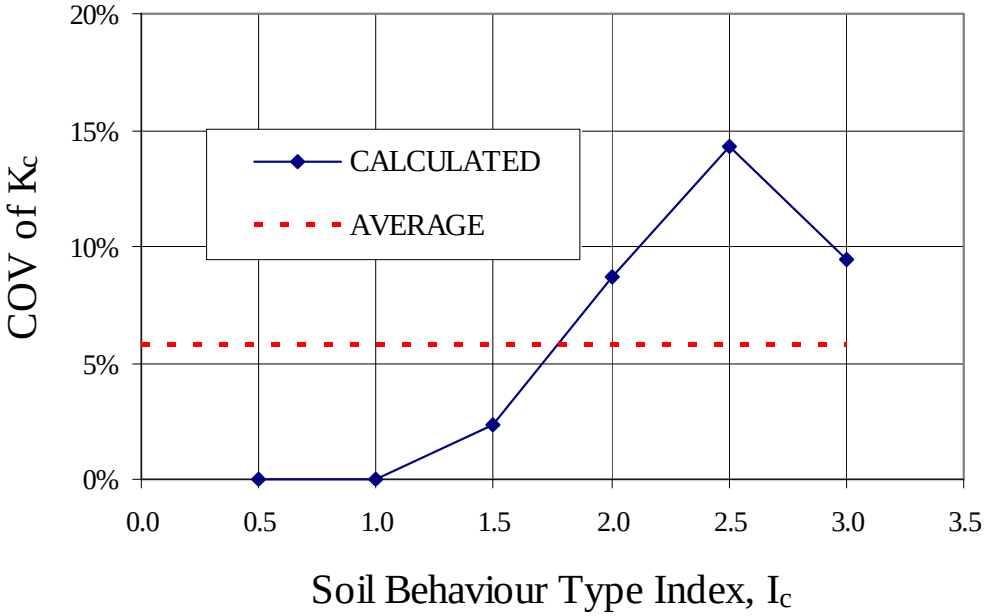

Figure 8.8 – Calculated and average COV of K_c as a function of I_c

9 – EXCEL IMPLEMENTATION

The previous sections of this report discussed in detail the various sources of uncertainties inherent to performing a liquefaction analysis with SPT and CPT testing. In order to implement the simplified reliability-based method for liquefaction evaluation, two Excel spreadsheets were developed. The spreadsheets evaluate both the factor of safety against liquefaction *FS*, and the probability of liquefaction P_L at the same points in the soil profile for SPT and CPT testing. An overview of the spreadsheets' features and capabilities are discussed below.

The parameters needed for the SPT and CPT spreadsheets are shown in Figures 9.1 and 9.2 respectively. Besides the SPT and CPT data, the input parameters include both seismic and site-specific parameters, along with the *COV*'s for these values, where applicable. Most input will be specific to the project in question. In the absence of project specific estimates of *COV*'s, values of *COV*'s are provided based on the previous discussions and findings of this report.

	A	B	C	D	E	F	G	H	I	J	K	L	M
8	**Workbook for Probability of Liquefaction Based on Standard Penetration Test**												
9													
10	**Earthquake**				Symbol	Units	Input? or computed?	Value	COV	Note: The earthquake return period and probability of exceedence determine the probability per year of the ground motion. An earthquake with a return period of 50 years and a probability of exceedence of 2% would have a probability of exceedence per year of 0.02/50 = one in 2500 years, or 4 x 10-4 per year.			
11	Return period				t	years	Input	50					
12	Probability of exceedence				P(EQ)	%	Input	2%					
13	Peak horizontal acceleration at ground surface				a_{max}/g	s	Input	0.08					
14	Moment magnitude of earthquake				M_w	s	Input	6.30					
15	Magnitude scaling factor				MSF	s	Computed	1.78	22%				
16													
17	**Stress reduction coefficient**				Symbol	Units	Input? or computed?	COV for r_d - 1					
18	Stress reduction coefficient for CSR				r_d	Dimensionless	Computed	19%	Typical value = 17% to 51%				
19													
20	**CRR correction factor K_σ**				Symbol	Units	Input? or computed?	COV for K_σ - 1					
21	Overburden correction factor for CRR				K_σ	s	Computed	33%	Typical value = 12%				
22													
23	**SPT correction factors**				Symbol	Units	Input? or computed?	Value	COV				
24	Overburden correction factor				C_N	Dimensionless	Computed - varies with σ'_{vo}		Computed	COV depends on COV of unit weight			
25	Hammer energy correction factor				C_E	Dimensionless	Input	1.05	9%	Typical value 10%			
26	Borehole diameter correction factor				C_B	Dimensionless	Input	1	1%	Typical value 1%			
27	Rod length correction factor				C_R	Dimensionless	Computed - varies with σ'_{vo}		24%	Typical value 24%			
28	Sampling method correction factor				C_S	Dimensionless	Input	1.00	0%	Typical value 3%			
29													
30	**Unit weights and depth to water table**				Symbol	Units	Input? or computed?	Value	COV				
31	Moist (total) unit weight of soil above water table				γ_{ma}	pcf	Input	110.0	8%	Typical value 9%			
32	Moist (total) unit weight of soil below water table				γ_{mb}	pcf	Input	120.0	8%	Typical value 9%			
33	Depth to water table at time of SPT				Z_{w1}	pcf	Input	6.0	Deterministic	Treated as deterministic in calculations			
34	Depth to water table expected for analysis condition				Z_{w2}	pcf	Input	6.0	Deterministic	Treated as deterministic in calculations			
35													
36	**Clean sand correction factor**								COV				
37	Add to $(N_1)_{60}$ for fines content				ΔN is computed, COV is input				32%	Typical value 31.5%			

Worksheet / Taylor's Method

Figure 9.1 - Excel SPT Probabilistic Liquefaction Workbook

	A	B	C	D	E	F	G	H	I	J	K
1	**Workbook for Probability of Liquefaction Based on Cone Penetration Test**										
2										Note: The earthquake return period and p	
3	**Earthquake parameters**				Symbol	Units	Input? or computed?	Value	COV	exceedence determine the probability per	
4	Return period				t	years	Input	50	Deterministic		
5	Probability of exceedence				P(EQ)	%	Input	2%	Deterministic	motion. An earthquake with a return peric	
6	Peak horizontal acceleration at ground surface				a_{max}/g	Dimensionless	Input	0.50	Deterministic	probability of exceedence of 2% would ha	
7	Moment magnitude of earthquake				M_w	Dimensionless	Input	7	Deterministic	exceedence per year of 0.02/50 = one in 2	
8	Magnitude scaling factor				MSF	Dimensionless	Computed	1.2	22%		
9										per year.	
10	**Stress reduction coefficient**				Symbol	Units	Input? or computed?	COV for r_d - 1			
11	Stress reduction coefficient for CSR				r_d	Dimensionless	Computed	17%	Typical value = 17% to 51%		
12											
13	**CRR correction factor K_σ**				Symbol	Units	Input? or computed?	COV			
14	Overburden correction factor for CRR				K_σ	Dimensionless	Computed	7%	Typical values = 6% to 8%		
15											
16	**CPT correction factors**				Symbol	Units	Input? or computed?	Value	COV		
17	CPT tip resistance				q_c	psi	Input	-	21%	Treated as equal to the COV of $(q_{c1N})_{cs}$	
18	CPT sleeve resistance				f_s	psi	Input	-	21%	Typical value - 15% to 50%	
19	Linear stress exponent				n	Dimensionless	Varies from 0.5 to 1.0		11%	Typical value 11%	
20	Overburden correction factor				C_σ	Dimensionless	Computed	-	13%	Typical value 13%	
21	CPT grain characteristic correction factor				K_c	Dimensionless	Computed	-	6%	Typical value 6%	
22	Normalized cone resistance				Q	Dimensionless	Computed	-	Deterministic	Treated as deterministic in calculations	
23	Normalized friction ratio				F	Percent	Computed	-	Deterministic	Treated as deterministic in calculations	
24	Soil Behaviour type index				Ic	Dimensionless	Computed	-	Deterministic	Treated as deterministic in calculations	
25	Apparent fines content				FC	Percent	Computed	-	Deterministic	Supplementary data: not used to comput	
26											
27	**Unit weights and depth to water table**				Symbol	Units	Input? or computed?	Value	COV		
28	Moist (total) unit weight of soil above water table				γ_{w1}	pcf	Input	110.0	9%	Typical value 9%	
29	Moist (total) unit weight of soil below water table				γ_{w2}	pcf	Input	125.0	9%	Typical value 9%	
30	Depth to water table at time of CPT				Z_{w1}	ft	Input	0.0	Deterministic	Treated as deterministic in calculations	
31	Depth to water table expected for analysis condition				Z_{w2}	ft	Input	0.0	Deterministic	Treated as deterministic in calculations	
32											

SPTWorksheet | CPTWorksheet

Figure 9.2 – Excel CPT Probabilistic Liquefaction Workbook

The first table requiring data input for the SPT and CPT spreadsheets deals with the seismic parameters of the analysis. These parameters include the return period for the design earthquake, the probability of exceedence for the specified time interval, the ground acceleration a_{max}, the design magnitude, and the calculated *MSF* based on this magnitude. As was previously discussed, all seismic factors listed above are treated as deterministic in the final evaluation, with the exception of the *MSF*. All of this information is obtained from the USGS website as discussed in Section 4.

Next, the *COV*'s for both r_d and K_σ need to be provided. The workbook calculates each parameter at each depth specified in the soil profile.

The third section of input for the SPT spreadsheet includes the SPT correction factors and the *COV*'s associated with them. There are recommended values programmed into the spreadsheet for values independent of depth such as hammer or sampler type, while values which vary with depth, such as C_R or C_N, are calculated for each depth when evaluating the *CRR*. The third section of input for the CPT spreadsheet includes the CPT correction factors and the *COV*'s associated with them.

Soil properties must be specified in order to calculate overburden pressures at varying depths within the soil profile. The soil properties include the unit weights, as well as the estimated *COV*'s for both unit weight and fines content as estimated in Section 5. The profile, which uses these specified properties, is the final input section. The subsurface profile input to the workbook will be specific to the project being analyzed. The SPT spreadsheet will include depth, SPT *N*-value, and percent fines. The CPT spreadsheet will

include depth, CPT q_c-value and CPT f_s-value. From this, both the total and effective overburden pressures, along with the relative density of each layer are calculated

Once all input data has been acquired and added to the workbook, the SPT and CPT spreadsheets are automated to calculate several things. In the SPT spreadsheet the first section determines the corrected *N*-values uses all the raw *N*-values and correction factors specified to calculate $(N_1)_{60}$ at each depth. In the CPT spread sheet the first section determines the appropriate linear stress exponent per Youd and Idriss et al (2001), then $(q_{c1N})_{cs}$ value is computed at each depth. Next, the *CSR* and *CRR* at each depth are calculated based on the specific soil profile, corrected SPT/CPT results, and seismic parameters inputted as described above

Final tables for both the SPT-based and CPT-based analyses calculate both the factor of safety against liquefaction and the probability of liquefaction for each layer. These tables first calculate the factor of safety against liquefaction using equation 1-1. Next, an overall *COV* is established for the factor of safety at each layer, which is then used to calculate the probability of liquefaction at each layer. These calculations are performed using the procedures outlined in Section 3.

At the completion of this report, spreadsheets for probabilistic SPT-based and CPT-based liquefaction analysis have been completed. In an effort to better illustrate and clarify any questions regarding the calculations described herein, three example projects have been worked out and are attached as Appendix B. Included in these reports are one project by Langan Engineering and Environmental Services in Newark, New Jersey, and two United States Bureau of Reclamation Dams located in California and Washington.

10 – SUMMARY AND CONCLUSIONS

A simplified reliability-based method for liquefaction evaluation was developed using Seed and Idriss (1971) "simplified procedure" for liquefaction evaluation, and the Taylor Series Reliability Method to determine the probability of liquefaction. The reliability-based method for SPT-based liquefaction evaluation was presented, but the method can also be applied to CPT and V_s-based procedures. A procedure for the determination of seismic demand using the USGS National Seismic Hazard Map was proposed. This procedure can be used in the absence of probabilistic attenuation relationships. Estimates of the Coefficients of Variation (COV) for the different parameters in the liquefaction evaluation were obtained from different sources.

The proposed procedure differs from other probabilitic procedures which treat the liquefaction criterion (Eq. 14) probabilistically. Probabilistic liquefaction criteria have been developed by Liao et al. 1988, Youd and Noble (1997), Toprak et al. 1999, and Cetin et al. 2001 based on available case histories of liquefaction. In these procedures, uncertainty in liquefaction is based on a probabilistic liquefaction criterion without regards to the different possible of sources of uncertainty and the quality of available data for the site being evaluated. In contrast, the proposed procedure treats the liquefaction criterion deterministically, but calculates the probability of liquefaction due to different sources of uncertainties in the procedure and the required parameters. The advantage of the method is that the magnitudes of the uncertainties from different components of liquefaction evaluation procedure can be clearly delineated. Another advantage is that calculation of the probability of liquefaction can be refined if *COV*s that are better than the estimates provided in the study are obtained.

Table 10.1 lists the parameters which were identified as sources of uncertainty in the simplified liquefaction analysis. Table 10.1 summarizes the findings of this report, and provides both average values and suggested values for the coefficients of variation for each parameter. From the estimates of the COVs of the different parameters, it can be seen that some of the major sources of uncertainties in estimating of liquefaction potential are procedural. In particular, estimates of the magnitude scaling factor *MSF* (COV= 22%), the stress-reduction factor r_d (COV=51%), and the rod-length correction factor C_R (COV=24%) provide three of the highest sources of uncertainties in determining CRR. In using the USGS Seismic Hazard Map to determine CSR, one very important source of uncertainty is the amplification factor F_a (with COV of as high as 52.5%). These COV estimates indicate the importance of further research in reducing the uncertainties in the procedural parameters in the simplified procedure.

Table 10.1 - Summary of Parameters

PARAMETERS	AVERAGE VALUES and *COV*'s
Seismic Parameters	
Ground Acceleration, a_{max}	• Ground motion parameters are obtained from probabilistic attenuation relationships or from the USGS Website. • All are treated "deterministically" in the conditional probability of liquefaction.
Magnitude, M_w	
Epicentral Distance, *ED*	
Site Amplification Factors, F_a	
Environmental Parameters	
Unit Weight of Soil, γ_d and γ_m	• Average values to be obtained from actual project data. Soil Type — *COV*(γ_d) — *COV*(γ_m) GP-GW — 7-13% — 7-9% SM-ML — 5-10% — 6-12% SP-SW — 6% — 9%
Buoyant Unit Weight of Soil, γ_b	• Average values to be obtained from actual project data. Soil Type — *COV*(γ_b) GP-GW — 14-18% SM-ML — 14-35% SP-SW — 20%
Percentage of Fines	• Average values to be obtained from actual project data. • *COV* = 31.5%
***CSR* Parameters**	
Depth Reduction Factor, r_d	• Average value from Seed and Idriss (1971): $r_d = 1\text{-}0.01z$ $(z \leq 10\text{m})$ $r_d = 1.15\text{-}0.025z$ $(z > 10\text{m})$ • Average *COV* = 19% • Average value from Cetin and Seed (2001): $r_d = 1\text{-}0.318\,z$ $(z \leq 2\text{m})$ $r_d = 0.546\text{-}0.006\,z$ $(z > 12\text{m})$ • Average $COV(1\text{-}r_d) = 45\%$
Magnitude Scaling Factor, *MSF*	• Average from Youd et al. (2001): $MSF = \frac{10^{2.84}}{M_w^{3.24}}$ • Average $COV(\lvert MSF\text{-}1\rvert) = 22\%$

Table 10.1 - Summary of Parameters (cont'd)

Overburden Correction Factor, K_σ	SPT: • Average value from Olsen (1984): $K_\sigma = \left(\frac{\sigma'_{vo}}{P_a}\right)^{f-1}$; $f = 1 - 0.5\sqrt{\frac{(N_1)_{60}}{23.2\sigma'_{vo} + 32.2}}$ • Average $COV(1\text{-}K_\sigma)$ = 33% CPT: • Average COV based on K_σ formula = 6% • Average COV based on D_r computed from CPT results = 8%
Sloping Ground Correction Factor, K_α	• Not recommended for use by non-experts in the field of geotechnical earthquake engineering (Youd and Idriss et al., 2001).
***CRR* Parameters for SPT**	
SPT *N*-value	• Average values to be obtained from actual project data. • COV = 15-40% (Harr, 1984; and Kulhawy, 1992).
SPT *N*-value Correction Factor C_N	• Average value from Castro (1995): $C_N = \frac{2.2}{(1.2 + \sigma'_{vo}/P_a)}$ • Average $COV(1\text{-}C_N)$ = 23%
SPT *N*-value Correction Factor C_E	• Based on Data from Youd et al. (2001): Donut Hammer: Average = 0.75 COV = 11% Safety Hammer: Average = 0.95 COV = 9% Automatic Hammer: Average = 1.05 COV = 9%
SPT *N*-value Correction Factor C_B	• Average from Youd et al. (2001): C_B = 1.07 • COV = 1%
SPT *N*-value Correction Factor C_R	• Average from Youd et al. (2001): C_R = 0.82 • COV = 24%
SPT *N*-value Correction Factor C_S	• Average from Youd et al. (2001): With Liners: Average = 1.0 COV = 0% Without Liners: Average = 1.2 COV = 3%

Table 10.1 - Summary of Parameters (cont'd)

Fines Correction Factors, α and β	• Use deterministic equations from NCEER Report to calculate α and β: α=0 and β=5.0 for $FC \leq 5\%$ $\alpha = \exp\left[1.76 - \frac{190}{FC^2}\right]$ and $\beta = \left[0.99 + \frac{FC^2}{1000}\right]$ for 5<*FC*<35% α=5 and β=1.2 for $FC \geq 35\%$
***CRR* Parameters for CPT**	
CPT q_c and f_s-value	• Average *COV* from calibration chamber data =21% • Average *COV* from site-specific testing = 35%
Linear Stress Exponent, *n*	• Average *COV* = 11%
CPT Overburden Correction Factor, C_Q	• Average *COV* based on 1/log(C_Q) normalization = 13%
CPT Grain Characteristics Correction Factor, K_c	• Average *COV* based on range presented in past studies = 6%
CPT Soil Behaviour Type Index, I_c	• Use deterministic equation from NCEER Report: $I_c = \left[\left(3.47 - \log Q\right)^2 + \left(1.22 + \log F\right)^2\right]^{0.5}$

11 - REFERENCES

Atkinsons, G.M., Finn, W.D.L., and Charlwood, R.G. (1984). "Simple Computation of Liquefaction Probability for Seismic Hazard Application." *Earthquake Spectra*, 1(1), 107-123.

Baldi, G., Bellotti, R., Ghionna, V., Jamiolkowski, M. and Pasqualini, E. (1986) "Interpretation of CPTs and CPTUs; 2nd part: drained penetration of sands". Proceedings of the Fourth International Geotechnical Seminar, Singapore, 143-56.

Blake, T.F. (1996), Personal Communication as cited in Youd et al. (2001)

Burlington, R. S., and May, D. C., Jr. (1970). *Handbook of Probability and Statistics*, McGraw-Hill, New York.

Castro, G. (1995). "Empirical methods in liquefaction evaluation." Primer Ciclo d Conferencias Internationales, Leonardo Zeevaert, Universidad Nacional Autonoma de Mexico, Mexico City.

Cetin, K.O. and Seed, R.B. (2001). "Nonlinear shear mass participation facture (r_d) for cyclic shear stress ratio evaluation", Research Report No. UCB/GT-2000/08, Univ. of California, Berkeley.

Christian, J. T., and Baecher, G. B. (2001). Discussion of "Factors of Safety and Reliability in Geotechnical Engineering" by Duncan, J. M. (2001). *J. Geotech. And Geoenvir. Engrg.*, ASCE, 126(8).

Committee on Earthquake Engineering. (1985). "Liquefaction of Soils During Earthquakes." Report No. CETS-EE-001, National Research Council (NRC), Washington D.C.

Dai, S.-H., and Wang, M.-O. (1992). *Reliability analysis in engineering applications.* Van Nostrand Reinhold, New York.

Dobry, R., Borcherdt, R.D., Crouse, C.B., Idriss, I.M., Joyner, W.B., Martin, G.R., Power, M.S., Rinne, E.E., and Seed, R.B. (2000). "New Site Coefficients and Site Classification Systems Used in Recent Building Code Provisions," *EERI Earthquake Spectra*, vol. 16, no. 1, pp. 41-67.

Duncan, J. M. (2000). "Factors of Safety and Reliability in Geotechnical Engineering." *J. Geotech. And Geoenvir. Engrg.*, ASCE, 126(4), 307-316.

Elton, D.J. and Hadj-Hamou, T. (1990). "Liquefaction Potential Map for Charleston, South Carolina." J. Geotech. Eng., ASCE, 116(2), 244-265.

Fardis, M. N. and Veneziano, D. (1982). "Probabilistic Analysis of Deposit Liquefaction." *J. Geotech. And Geoenvir. Engrg.*, ASCE, 108(3), 395-417.

Fardis, M. N. and Veneziano, D. (1981). "Statistical Analysis of Sand Liquefaction." *J. Geotech. And Geoenvir. Engrg.* ASCE, 107(10), 1361-1377.

Gibbs, H.J. and Holtz, W.G., 1957. Research on determining the density of sands by spoon penetration testing. International Conference on Soil Mechanics & Foundation Engineering., 4(1):35-39.

Girsang, C. and Gutierrez, M. (2001). "A Numerical Investigation of the Seismic Response of the Aggregate Pile Foundation System," Contract Report submitted to Geopier, Co., Inc., Blacksburg, VA.

Green, R. (2001). "Energy-based Evaluation and Remediation of Liquefiable Soils." Ph.D. Dissertation, Virginia Polytechnic Institute and State University.

Harder, L. F., Jr., and Boulanger, R. W. (1997). "Application of K_σ and K_α Correction Factors." Proc., NCEER Workshop on Evaluation of Liquefaction Resistance of Soils, Nat. Ctr. For Earthquake Engrg. Res., State Univ. of New York at Buffalo, 129-148.

Harr, M.E. (1984). Reliability-Based Design in Civil Engineering. 1984 Henry M. Shaw Lecture, Dept. of Civil Eng. North Carolina State Univ., Raleigh, NC.

Hwang, H. H. M. and Lee, C. S. (1991). Probabilistic Evaluation of Liquefaction Potential. Center for Earthquake Research and Information. Technical Report NCEER-91-0025. Memphis State University. Memphis, TN.

Hynes, M.E. and Olsen, R.S. (1999). "Influence of Confining Stress on Liquefaction Resistance." Proc. Intl. Workshop on Phys. and Mech. of Soil Liquefaction, Balkema, Rotterdam, The Netherlands, pp. 145-152.

ICBO (2003), "2003 ICC International Building Code," International Code Council.

Idriss, I.M., and Sadigh, K., and Power, M.S. (1982). Dependence of peak horizontal accelerations and velocities on earthquake magnitude at close distances to the source. Presented at the annual meeting of the Seism. Soc. Am., Anaheim, Calif., April.

Idriss, I.M. (1990). "Response of Soft Soil Sites During Earthquakes," *Proc. H.B. Seed Memorial Symp*., J.M. Duncan (ed.), UC Berkeley, May 1990, vol. 2, pp. 273-289.

Idriss, I.M. (1991), "Earthquake Ground Motions at Soft Soil Sites," *Proc. 2nd Intl. Conf.*

Recent Adv. Geotech. Earth. Eng.,March 11-15, 1991, St. Louis, Missouri, vol. III, pp. 2265-2272.

Golesorkhi (1989). "Factors influencing the computational determination of earthquake – induced shear stresses in sandy soils", PhD Thesis, University of California, Berkeley.

Jamiolkowski, M., Ladd, C.C., Germaine, J.T. and Lancelotta, R. (1985). "New developments in field and laboratory testing of soils". State-of-the art report. Proceedings of the 11th International Conference on Soil Mechanics and Foundation Engineering, San Francisco, 1, 57-153, Balkema Pub., Rotterdam.

Juang, C.H., Chen, C.J., and Jiang, T. (2001). "Probabilistic Framework for Liquefaction Potential by Shear Wave Velocity." *J. Geotech. And Geoenvir. Engrg.*, ASCE, 127(8), 670-678.

Juang, C.H., Jiang, T., and Andrus, R. D. (2002). "Assessing Probability-based Methods for Liquefaction Potential Evaluation." *J. Geotech. And Geoenvir. Engrg.*, ASCE, 128(7), 580-589.

Juang, C. H., Rosowsky, D. V., and Tang, W. H. (1999). "Reliability-Based Method for Assessing Liquefaction Potential of Soils." *J. Geotech. And Geoenvir. Engrg.*, ASCE, 125(8), 684-689.

Kavazanjian, E. Jr., Roth, R.A., and Echezuria, H. (1985). "Liquefaction Potential Mapping for San Francisco." *J. Geotech. Engr*., ASCE, 114(4), 389-410.

Kulhawy, F .H. (1992). "On the Evaluation of Soil Properties," *ASCE Geotech. Spec. Publ.* pp. 95-115.

Lew, M. (2001). "Guidelines for Analyzing and Mitigating Soil Liquefaction." Proceedings from the Ohio River Valley Soils Seminar XXXII, Louisville, KY, October 24.

Liao, S. (1985). "Statistical analysis of Liquefaction Data". Ph.D. Dissertation, Massachusetts Institute of Technology.

Liao, S.S. and Whitman, R.V., 1986. Overburden correction factors for SPT in sand. *J. Geotech. Engr*., ASCE, 112(3):373-377.

Liao, S.C., Veneziano, D., and Whitman, R. V. (1988). "Regression Models for Evaluating Liquefaction Probability." *J. Geotech. And Geoenvir. Engrg.*, ASCE, 114(4), 389-411.

Lunne, T., Robertson, P.K., and Powell, J.J.M. (1997). "Cone Penetration Testing in Geotechnical Practice." Blackie Academic and Professional, New York, 312 pp.

Martin, J.R. II (2000), Personal communication.

McGuire, R.K. and Shedlock, K.M. (1981). "Statistical Uncertainties in Seismic Hazard Evaluations in the United States," *Bull. Seism. Soc. Am.*, vol. 71., no. 4, pp. 1287-1308.

Meyerhoff, G.G., 1956. Penetration tests and bearing capacity of cohesionless soils. *J. Geotech. Engr*., ASCE, 82(1): 886/1-886/19.

Peck, R.B. and Bazaraa, A.R.S., 1969. Discussion to settlement of spread footings on sand. *J. Geotech. Engr*., ASCE, 95(3):905-909.

Rahardjo, P. P. (1989). "Evaluation of Liquefaction Potential of Silty Sand Based on Cone Penetration Test." Ph.D. Dissertation, Virginia Polytechnic Institute and State University

Rahman, M. S. and El Zahaby, K. M. (1997). "Probabilistic Liquefaction Risk Analysis including Fuzzy Variables." *Soil Dynamics and Earthquake Engineering.*, 16(1), 63-79.

Robertson, P.K. and Wride, C.E. (1998). "Evaluating cyclic liquefaction potential using the cone penetration test." Can. Geotech. J., Ottawa, 35(3), 442-459.

Seed, H.B. (1983). "Earthquake-Resistant Design of Earth Dams." Proc.Symp. Seismic Des. of Earth Dams and Caverns, ASCE, New York, 41-64.

Seed, H.B., Tokimatsu, K., Harder, L.F., and Chung, R.M., (1985). Influence of SPT procedures in soil liquefaction resistance evaluations. *J. Geotech. Engr*., ASCE, 111(12):1425-1445.

Seed, H.B. and Idriss, I.M. (1971), "Simplified Procedure for Evaluating Soil Liquefaction Potential," *J. Geotech. Engr.*, ASCE, 97(9), 1249-1273.

Seed, H. B., and Idriss, I. M. (1982). "Ground Motions and Soil Liquefaction During Earthquakes." Earthquake Engineering Research Institute Monograph, Oakland, California.

Skempton, A.W. (1986). "Standard Penetration Test Procedures and the Effects in Sands of Overburden Pressure, Relative Density, Particle Size, Aging and Overconsolidation," *Geotechnique*, 36(3), 425-447.

Todorovska, M.I. (1998). "Quick Reference Liquefaction Opportunity Map for a Metropolitan Area," Proc. 3rd ASCE Speciality Conf. Earthquake Eng. Soil Dynamics," ASCE Spl. Pub. No. 75, vol. 1, 116-127.

United States Bureau of Reclamation (USBR). Density Test Results for Casitas Dam. October 1999.

United States Bureau of Reclamation (USBR). Density Test Results for Bradbury Dam. January 1998.

United States Bureau of Reclamation (USBR). Relative Density Test Results for Mormon Island Auxiliary Dam. Date Unknown.

United States Army Corps of Engineers (USACE). (1997)."Engineering and design introduction to probability and reliability methods for geotechnical engineering," Engr. Tech. Ltr. No. 1110-2-547, U.S. Army Corps of Engrs., Dept. of the Army, Washington, D.C. (30 Sept. 1997).

United States Army Corps of Engineers (USACE). (1998). "Risk-based analysis in geotechnical engineering for support of planning studies," Engr. Tech. Ltr. No. 1110-2-554, U.S. Army Corps of Engrs., Dept. of the Army, Washington, D.C. (27 Feb. 1998).

United States Bureau of Reclamation (USBR). Density Test Results for Bully Creek Dam. February and March 1998.

Whitman, R. V. (2000). "Organizing and Evaluating Uncertainty in Geotechnical Engineering." *J. Geotech. And Geoenvir. Engrg.*, ASCE, 126(7), 583-593.

Wolff, T.F. (1994). "Evaluating the Reliability of Existing Levees." Rep. Res. Reliability of existing levees, prepared for the U.S. Army Engineers Waterways Experiment Station Geotech. Lab., Vicksburg, Miss.

Youd, T.L. and Idriss, I.M. (Chairman), (2001). "Liquefaction Resistance of Soils: Summary Report from the 1996 and 1998 NCEER/NSF Workshops on Evaluation of Liquefaction Resistance of Soils." *J. Geotech. And Geoenvir. Engrg.*, ASCE, 127(10) 817-833.

Youd, T.L., Idriss, I.M., Andrus, R.D., Arango, I., Castro, G., Christian, J.T., Dobry, R., Finn, W.D.L., Harder Jr., L.F., Hynes, M.E., Ishihara, K., Koester, J.P., Laio, S.S.C., Marcuson III, W.F., Martin, G.R., Mitchell, J.K., Moriwaki, Y., Power, M.S., Robertson, P.K., Seed, R.B., and Stokoe II, K.H. (2001), "Liquefaction Resistance of Soils: Summary Report from the 1996 and 1998 NCEER/NSF Workshops on Evaluation of Liquefaction Resistance of Soils." Journal of Geotechnical and Geoenvironmental Engineering, ASCE, 127(10) 817-833.

Youd, T.L. and Perkins, M. (1978). "Mapping Liquefaction-Induced Ground Failure Potential." *J. Geotech. Engr*., ASCE, 104(GT4), 433-446.

APPENDIX A – SPT AND CPT EXCEL WORKSHEETS

EXCEL worksheets implementing the reliability-based simplified procedure for liquefaction evaluation using SPT and CPT data can be obtained by contacting the P.I.s. for this project. Prof. Gutierrez can be reached at his e-mail address: magutier@vt.edu and telephone number: (540) 231-6357. Prof. Duncan can be at his address: jmd@vt.edu and telephone number: (540) 231-5013.

APPENDIX B– EXAMPLE PROBLEMS

Example #1 –Evaluation of SPT data
Project Location: Newark, NJ (07100 – 07199)
Project Engineer: Langan Engineering

The following example outlines the procedures required for completing the attached SPT probabilistic liquefaction analysis spreadsheet, Figures B-1a – B-1d.

1. Determine the soil profile, depth to water table, and depth to bedrock, or at least the bottom of any potentially liquefiable layers. Also, characterize the soil and rock types and determine properties needed for computation of the *CSR*.

   A layer of potentially liquefiable alluvial sands was encountered below layers of miscellaneous fill and organic clay. Table B.1 summarizes the conditions for the alluvial layer, with estimated values of fines content:

Table B.1 – Summary Data

Boring Number	Depth (ft)	Soil Classification	SPT N-value (bl/ft)	% Fines
B-3	21	Gray M-F SAND, tr. Silt	8	15
B-3	26	Dk. Gray M-F SAND, tr. Silt	7	15
B-3	31	Gravelly C-F SAND, some silt	21	30
B-3	36	Gravelly C-F SAND, tr. silt	29	15
B-5	21	Gray Silty F-SAND	3	40
B-5	26	Gray C-F SAND, some silt	17	30
B-5	31	Gray C-F SAND, tr. Silt	21	15
B-5	36	Gray C-F SAND	40	5

   Using the soil data obtained from Langan's subsurface investigation of the site, average soil unit weights were estimated for the layers above and including the potentially liquefiable layer. Table B.2 summarizes the additional soil properties and parameters pertaining to the soil profile:

Table B.2 – Unit weights and water table location

$(\gamma_m)_{avg}$ (pcf)	$(\gamma_{sat})_{avg}$ (pcf)	z_w (ft)
110	120	6

For the purposes of demonstrating calculations throughout the example, the sample located at a depth of 26 feet in boring B-5 shall be used.

2. Estimate the maximum ground surface acceleration, a_{max}.

As discussed in Section 4, the following steps would be performed for estimating the seismic parameters for the given project.

First, the Peak Ground Acceleration (*PGA*) is determined using the seismic hazard by zip code feature of the USGS geohazard website. The *PGA* corresponding to a 10% probability of exceedence in 50 years, or 500 year earthquake, is as follows:

$$PGA = 0.06g$$

where g is the acceleration of gravity.

Following the procedure for obtaining both the Earthquake Magnitude and Epicentral Distance from disaggregation data for New York City from the USGS geohazard website, the following values are obtained.

$$M_w = 6.3$$
$$ED_{PGA} = 98 \text{ km}$$

Finally, using equation 4-7 to determine the amplification effects of the site (Class D according to NEHRP classification based on SPT *N*-values) on ground motions, the following value of a_{max} are estimated for the given site:

$$a_{\max} = F_a\left(\frac{SA_{0.2}}{2.5}\right)$$
$$a_{\max} = 1.6\left(\frac{0.125}{2.5}\right) = 0.08g$$

Table B.3 shows the calculations used in determining the average seismic values *PGA* and M_w from the data obtained from the USGS website.

Table B.3 – Deaggregation for determination of Seismic Parameters

Deaggregated Seismic Hazard for PE = 2% in 50 years (PGA)
New York, New York
Latitude 40.750 N | Longitude 73.980 W

Distance (km)	Magnitude 5	5.5	6	6.5	7	7.5	Sum	Product
25	20.633	17.269	10.774	5.754	2.235	1.375	58.040	2902.000
50	3.698	5.968	6.742	5.841	3.154	2.385	27.788	2084.100
75	0.266	0.770	1.580	2.311	1.858	1.885	8.670	867.000
100	0.022	0.096	0.311	0.667	0.718	0.914	2.728	272.800
125	0.003	0.021	0.090	0.258	0.334	0.513	1.219	152.375
150	0.001	0.006	0.033	0.121	0.189	0.349	0.699	104.850
175	0.000	0.002	0.011	0.052	0.100	0.225	0.390	68.250
200	0.000	0.000	0.003	0.021	0.048	0.135	0.207	41.400
225	0.000	0.000	0.001	0.008	0.023	0.076	0.108	24.300
250	0.000	0.000	0.000	0.003	0.011	0.041	0.055	13.750
275	0.000	0.000	0.000	0.001	0.006	0.025	0.032	8.800
300	0.000	0.000	0.000	0.001	0.003	0.017	0.021	6.300
325	0.000	0.000	0.000	0.000	0.002	0.012	0.014	4.550
350	0.000	0.000	0.000	0.000	0.001	0.009	0.010	3.500
375	0.000	0.000	0.000	0.000	0.001	0.007	0.008	3.000
400	0.000	0.000	0.000	0.000	0.000	0.004	0.004	1.600
425	0.000	0.000	0.000	0.000	0.000	0.003	0.003	1.275
450	0.000	0.000	0.000	0.000	0.000	0.002	0.002	0.900
475	0.000	0.000	0.000	0.000	0.000	0.001	0.001	0.475
500	0.000	0.000	0.000	0.000	0.000	0.001	0.001	0.500
Sum	24.623	24.132	19.545	15.038	8.683	7.979		6561.725
Product	123.115	132.726	117.27	97.747	60.781	59.8425	591.4815	

For PGA

$(M_w)_{PGA}$ =	5.91	
ED_{PGA} =	65.62	km

Deaggregated Seismic Hazard for PE = 2% in 50 years ($SA_{1.0}$)
New York, New York
Latitude 40.750 N | Longitude 73.980 W

Distance (km)	Magnitude 5	5.5	6	6.5	7	7.5	Sum	Product
25	1.482	5.507	7.719	5.503	2.265	1.397	23.873	1193.650
50	0.218	1.995	5.750	6.896	3.828	2.745	21.432	1607.400
75	0.033	0.557	2.644	4.773	3.501	2.972	14.480	1448.000
100	0.005	0.148	1.035	2.489	2.205	2.048	7.930	793.000
125	0.001	0.059	0.542	1.549	1.536	1.558	5.245	655.625
150	0.001	0.035	0.378	1.225	1.317	1.466	4.422	663.300
175	0.000	0.020	0.255	0.951	1.127	1.376	3.729	652.575
200	0.000	0.011	0.161	0.684	0.909	1.197	2.962	592.400
225	0.000	0.006	0.100	0.479	0.702	0.993	2.280	513.000
250	0.000	0.003	0.061	0.326	0.518	0.786	1.694	423.500
275	0.000	0.002	0.043	0.256	0.439	0.718	1.458	400.950
300	0.000	0.001	0.033	0.218	0.404	0.712	1.368	410.400
325	0.000	0.001	0.028	0.203	0.403	0.764	1.399	454.675
350	0.000	0.001	0.024	0.189	0.401	0.811	1.426	499.100
375	0.000	0.001	0.020	0.173	0.394	0.851	1.439	539.625
400	0.000	0.000	0.014	0.138	0.335	0.766	1.253	501.200
425	0.000	0.000	0.011	0.112	0.289	0.689	1.101	467.925
450	0.000	0.000	0.008	0.092	0.223	0.562	0.885	398.250
475	0.000	0.000	0.007	0.084	0.218	0.596	0.905	429.875
500	0.000	0.000	0.005	0.061	0.166	0.487	0.719	359.500
Sum	1.740	8.347	18.838	26.401	21.180	23.494		13003.950
Product	8.700	45.909	113.028	171.607	148.260	176.205	663.708	

For PGA

$(M_w)_{PGA}$ =	6.64	
ED_{PGA} =	130.04	km

Mean Values

$(M_w)_{PGA}$ =	6.28	
ED_{PGA} =	97.83	km

3. Determine the depth reduction factor, r_d, using the average values found in table 6.1

The depth reduction factor is calculated at depths corresponding to the measured SPT *N*-values. Using the example point of 26 feet, the r_d is calculated as follows:

$$r_d = 1 - 0.00233z \quad \text{for } z < 30 \text{ feet}$$
$$r_d = 1 - 0.00233 \cdot 26 = 0.94$$
$$r_d = 0.94 \text{ at 26 feet}$$

Values of r_d calculated for the entire profile can be found in the "CSR" section of the attached spreadsheet.

4. Compute the Cyclic Stress Ratio, *CSR*, using equation 1-2.

   Like r_d, the *CSR* is calculated at the depths which correspond to the measured SPT *N*-values. The first step to calculating the *CSR*, however, is calculating both the total and effective vertical stresses at that point.

   Total and effective vertical stresses are calculated as follows:

$$\sigma_v = \gamma_t \cdot z$$
$$\sigma'_v = \gamma_t \cdot z \quad \text{for } z \le z_w$$
$$= \gamma_t \cdot z + (\gamma_t - \gamma_w)*(z - z_w) \text{ for } z > z_w$$

   At a depth of 26 feet the values for total and effective vertical stress are as follows:

$$\sigma_v = (110 \text{ pcf})\cdot(6 \text{ ft}) + (120 \text{ pcf})\cdot(20 \text{ ft}) = 3060 \text{ psf}$$
$$\sigma'_v = (110 \text{ pcf})\cdot(6 \text{ ft}) + (120\text{-}62.4 \text{ pcf})\cdot(20 \text{ ft}) = 1812 \text{ psf}$$

   Values of total and effective vertical stress for the rest of the soil profile can be found in the "Measured blow counts, percent fines, and computed values of σ_{vo}, σ'_{vo} and relative density" section of the attached spreadsheet.

   After calculating the total and effective vertical stresses for the profile, the *CSR* at each point corresponding to a SPT *N*-value is calculated as follows:

$$CSR = 0.65\left(\frac{a_{max}}{g}\right)\left(\frac{\sigma_v}{\sigma'_v}\right)r_d$$

   At a depth of 26 feet, the CSR is as follows:

$$CSR = 0.65\left(\frac{0.08g}{g}\right)\left(\frac{3060}{1812}\right)0.94 = 0.082$$

   Values of CSR calculated for the entire profile can be found in the "CSR" section of the attached spreadsheet.

5. Compute the Cyclic Resistance Ratio, CRR, for a Magnitude 7.5 earthquake using equation 7-1.

   The first step in determining the CRR is to calculate the corrected SPT N-value, $(N_1)_{60}$, at each depth. The formula for calculating $(N_1)_{60}$ is as follows:

$$(N_1)_{60} = N \cdot C_N \cdot C_E \cdot C_R \cdot C_S \cdot C_B$$

For the given project, $C_B = C_S = 1.0$, and $C_E = 1.05$ for an automatic hammer. Values for C_R and C_N are calculated at each depth corresponding to a SPT N-value, and are tabulated in the "CRR" section of the attached spreadsheet. The calculations for the latter two parameters at the example depth of 26 feet are as follows:

C_R for a depth ranging from 20-30 feet is 0.95

$$C_N = 2.2/(1.2 + (\sigma'_{vo}/P_a))$$
$$C_N = 2.2/(1.2 + (0.906/1.06)) = 1.07$$

So, the $(N_1)_{60}$ value at a depth of 26 feet in boring B-5 is as follows:

$$(N_1)_{60} = 17 \cdot 1.07 \cdot 1.05 \cdot 0.95 \cdot 1.0 \cdot 1.0 = 18 \text{ bl/ft}$$

Next, the clean sand equivalent of the SPT N-value, or $(N_1)_{60cs}$, is calculated using equation 7-2. The value of $(N_1)_{60cs}$ calculated for a depth of 26 feet in boring B-5 is as follows:

$$(N_1)_{60cs} = \alpha + \beta \cdot (N_1)_{60}$$
$$(N_1)_{60cs} = 4.71 + 1.15 \cdot 18 = 25 \text{ bl/ft}$$

Finally, calculate the CRR as follows:

$$CRR_{M7.5} = \left(\frac{1}{34 - (N_1)_{60cs}}\right) + \left(\frac{(N_1)_{60cs}}{135}\right) + \left(\frac{50}{[10(N_1)_{60cs} + 45]^2}\right) - \frac{1}{200}$$

$$CRR_{M7.5} = 0.111 + 0.185 + 0.001 - 0.005 = 0.300$$

Values of CRR calculated at each depth corresponding to a SPT sample are shown in the "CRR" Section of the attached spreadsheet.

6. Calculate the Magnitude Scaling Factor, *MSF*.

The MSF for the site is calculated using equation 6-9 based on the recommendations of Youd and Idriss et al. (2001).

$$MSF = \frac{10^{2.84}}{M_w^{3.24}}$$

$$MSF = \frac{10^{2.84}}{6.3^{3.24}} = 1.78$$

7. Calculate the Overburden Correction Factor, K_σ.

   Values of K_σ are calculated at depths corresponding to SPT N-values, as was previously done with overburden pressures, certain N-value correction factors, and the depth reduction factor, r_d. The overburden correction factor is calculated using equation 6-21, which is in terms of corrected SPT blow counts within the material. For the example point of 26 feet deep in boring B-5, K_σ is as follows:

$$K_\sigma = \left(\frac{\sigma'_{vo}}{P_a}\right)^{-0.5\sqrt{\frac{(N_1)_{60}}{23.2\sigma'_{vo}+32.2}}}$$

$$K_\sigma = \left(\frac{0.906}{1.06}\right)^{-0.5\sqrt{\frac{18}{53.22}}} = 1.00$$

8. Compute the Factor of Safety, FS, against liquefaction using equation 1-1.

$$FS = \left(\frac{CRR_{7.5}}{CSR}\right) MSF \cdot K_\sigma \cdot K_\alpha$$

$$FS = \left(\frac{0.300}{0.082}\right) \cdot 1.78 \cdot 1.00 \cdot 1.00 = 6.47$$

9. Compute the Probability of Liquefaction, P_L, as outlined in Section 3.

   Using the outline presented in Section 3 of the text, the probability of liquefaction for the site was calculated as shown in the table B.4. For the example point at 26 feet in boring B-5, the probability of liquefaction was calculated to be as follows:

$$P_L = 0\%$$

Table B.4 – Probability of liquefaction example calculation

Average Values	
N-value	17
$(N_1)_{60}$	18
CRR_{MLV}	0.300
CSR_{MLV}	0.082
F_{MLV}	6.47
Std. Dev. COV	2.98
COV	46%
β_{LN}	4.03
P_L	0%

Probability of Liquefaction Example Calculation
Example #1 - Depth = 26 ft

Deterministic Factors		
a_{max}	0.08	(%g)
M_w	6.3	

Factor	Average Value	Units	COV	Avg.$^+$	Avg.$^-$	$(N_1)_{60}^+$	$(N_1)_{60}^-$	CRR$^+$	CRR$^-$	CSR$^+$	CSR$^-$	F$^+$	F$^-$	ΔF	$(\Delta F/2)^2$
r_d	0.94		17.0%	1.10	0.78	25.00	25.00	0.30	0.30	0.097	0.069	4.85	6.83	-1.99	0.99
σ_v	1.53	(tsf)	9.0%	1.67	1.39	25.00	25.00	0.30	0.30	0.090	0.075	5.20	6.23	-1.03	0.26
σ'_v	0.91	(tsf)	15.0%	1.04	0.77	25.00	25.00	0.30	0.30	0.072	0.097	6.52	4.82	1.70	0.72
%Fines	30%		5.0%	32%	29%	25.80	25.16	0.31	0.30	0.082	0.082	5.87	5.61	0.26	0.02
C_N	1.07		15.0%	1.23	0.91	21.96	16.23	0.24	0.17	0.082	0.082	4.59	3.29	1.31	0.43
C_E	1.05		10.0%	1.16	0.95	21.01	17.19	0.23	0.18	0.082	0.082	4.34	3.48	0.87	0.19
C_R	1.00		24.0%	1.24	0.76	23.68	14.52	0.27	0.16	0.082	0.082	5.10	2.95	2.15	1.15
C_S	1.00		3.0%	1.03	0.97	19.67	18.53	0.21	0.20	0.082	0.082	4.02	3.76	0.26	0.02
C_B	1.00		1.0%	1.01	0.99	19.29	18.91	0.21	0.20	0.082	0.082	3.93	3.85	0.09	0.00
MSF	1.56		22.0%	1.90	1.22	25.00	25.00	0.30	0.30	0.082	0.082	6.96	4.45	2.51	1.58
K_σ	1.00		33.0%	1.33	0.67	25.00	25.00	0.30	0.30	0.082	0.082	7.59	3.82	3.77	3.55
														SUM =	8.90

Earthquake	Symbol	Units	Input? or computed?	Value	COV
Return period	t	years	Input	50	Deterministic
Probability of exceedence	P(EQ)	%	Input	2%	Deterministic
Peak horizontal acceleration at ground surface	a_{max}/g	Dimensionless	Input	0.08	Deterministic
Moment magnitude of earthquake	M_w	Dimensionless	Input	6.3	Deterministic
Magnitude scaling factor	MSF	Dimensionless	Computed	1.78	22%

Note: The earthquake return period and probability of exceedence determine the probability per year of the ground motion. An earthquake with a return period of 50 years and a probability of exceedence of 2% would have a probability of exceedence per year of 0.02/50 = one in 2500 years, or 4 x 10-4 per year.

Stress reduction coefficient	Symbol	Units	Input? or computed?	COV
Stress reduction coefficient for CSR	r_d	Dimensionless	Computed	17%

Typical value = 17% to 51%

CRR correction factor K_σ	Symbol	Units	Input? or computed?	COV
Overburden correction factor for CRR	K_σ	Dimensionless	Computed	33%

Typical value = 33%

SPT correction factors	Symbol	Units	Input? or computed?	Value	COV	
Overburden correction factor	C_N	Dimensionless	Computed - varies with σ'_{vo}		Computed	COV depends on COV of unit weight
Hammer energy correction factor	C_E	Dimensionless	Input	1.05	10%	Typical value 10%
Borehole diameter correction factor	C_B	Dimensionless	Input	1.00	1%	Typical value 1%
Rod length correction factor	C_R	Dimensionless	Computed - varies with σ'_{vo}		24%	Typical value 24%
Sampling method correction factor	C_S	Dimensionless	Input	1.00	3%	Typical value 3%

Unit weights and depth to water table	Symbol	Units	Input? or computed?	Value	COV	
Moist (total) unit weight of soil above water table	γ_{ma}	pcf	Input	110.0	9%	Typical value 9%
Moist (total) unit weight of soil below water table	γ_{mb}	pcf	Input	120.0	9%	Typical value 9%
Depth to water table at time of SPT	Z_{w1}	ft	Input	6.0	Deterministic	Treated as deterministic in calculations
Depth to water table expected for analysis condition	Z_{w2}	ft	Input	6.0	Deterministic	Treated as deterministic in calculations

Clean sand correction factor	Symbol	Units	Input? or computed?	Value	COV	
Add to $(N_1)_{60}$ for fines content	ΔN	Blows	Computed		32%	Typical value 31.5%

Measured blow counts, percent fines, and computed values of σ_{vo}, σ'_{vo} and relative density

Depth below ground surface - z (ft)	Measured blow count N_m	Percent fines % < #200	Total overburden pressure σ_{vo} - (psf)	Effective overburden pressure σ'_{vo} - (psf)	Relative Density %
21.0	8	15%	2460	1524	43%
26.0	7	15%	3060	1812	38%
31.0	21	30%	3660	2100	62%
36.0	29	15%	4260	2388	69%
21.0	3	40%	2460	1524	26%
26.0	17	30%	3060	1812	59%
31.0	21	15%	3660	2100	62%
36.0	40	5%	4260	2388	81%
0.0	0	0%	0	0	N/A
0.0	0	0%	0	0	N/A
0.0	0	0%	0	0	N/A
0.0	0	0%	0	0	N/A
0.0	0	0%	0	0	N/A
0.0	0	0%	0	0	N/A
0.0	0	0%	0	0	N/A
0.0	0	0%	0	0	N/A
0.0	0	0%	0	0	N/A
0.0	0	0%	0	0	N/A
0.0	0	0%	0	0	N/A
0.0	0	0%	0	0	N/A

Note: Effective overburden pressure based on water table elevation at time of SPT is used in evaluating relative density and CRR.

Figure B.1a – Example #1 SPT Spreadsheet

SPT Correction factors, $(N_1)_{60CS}$ and CRR for magnitude 7.5 earthquake

[illegible]	[illegible]	[illegible]	[illegible]	[illegible]	[illegible]	[illegible]	Fines content correction Add to $(N_1)_{60}$	Corrected clean sand blow count $(N_1)_{60CS}$	CRR for $M_w = 7.5$ $CRR_{7.5}$
21.0	1.15	1.05	1	0.89	1.00	9	2.9	12	0.127
26.0	1.07	1.05	1	0.94	1.00	7	2.9	10	0.115
31.0	1.00	1.05	1	0.98	1.00	22	8.1	30	0.457
36.0	0.94	1.05	1	1.00	1.00	29	3.9	33	V. High
21.0	1.15	1.05	1	0.89	1.00	3	5.6	9	0.103
26.0	1.07	1.05	1	0.94	1.00	18	7.5	25	0.300
31.0	1.00	1.05	1	0.98	1.00	22	3.5	25	0.298
36.0	0.94	1.05	1	1.00	1.00	40	0.0	40	V. High
0.0	1.70	1.05	1	0.71	1.00	0	0.0	0	N/A
0.0	1.70	1.05	1	0.71	1.00	0	0.0	0	N/A
0.0	1.70	1.05	1	0.71	1.00	0	0.0	0	N/A
0.0	1.70	1.05	1	0.71	1.00	0	0.0	0	N/A
0.0	1.70	1.05	1	0.71	1.00	0	0.0	0	N/A
0.0	1.70	1.05	1	0.71	1.00	0	0.0	0	N/A
0.0	1.70	1.05	1	0.71	1.00	0	0.0	0	N/A
0.0	1.70	1.05	1	0.71	1.00	0	0.0	0	N/A
0.0	1.70	1.05	1	0.71	1.00	0	0.0	0	N/A
0.0	1.70	1.05	1	0.71	1.00	0	0.0	0	N/A
0.0	1.70	1.05	1	0.71	1.00	0	0.0	0	N/A
0.0	1.70	1.05	1	0.71	1.00	0	0.0	0	N/A

Cyclic Stress Ratio - CSR

[illegible]	[illegible]	[illegible]	[illegible]	[illegible] CSR
21.0	2460	1524	0.95	0.080
26.0	3060	1812	0.94	0.082
31.0	3660	2100	0.92	0.084
36.0	4260	2388	0.88	0.082
21.0	2460	1524	0.95	0.080
26.0	3060	1812	0.94	0.082
31.0	3660	2100	0.92	0.084
36.0	4260	2388	0.88	0.082
0.0	0	0	1.00	N/A
0.0	0	0	1.00	N/A
0.0	0	0	1.00	N/A
0.0	0	0	1.00	N/A
0.0	0	0	1.00	N/A
0.0	0	0	1.00	N/A
0.0	0	0	1.00	N/A
0.0	0	0	1.00	N/A
0.0	0	0	1.00	N/A
0.0	0	0	1.00	N/A
0.0	0	0	1.00	N/A
0.0	0	0	1.00	N/A

Note: Effective overburden pressure based on water table elevation expected for analysis condition is used in evaluating relative density and CSR.

Cyclic Resistance Ratio - $CRR_{7.5}$

[illegible] below ground surface - [illegible] feet)	CRR for $M_w = 7.5$ $CRR_{7.5}$
21.0	0.127
26.0	0.115
31.0	0.457
36.0	V. High
21.0	0.103
26.0	0.300
31.0	0.298
36.0	V. High
0.0	N/A
0.0	N/A
0.0	N/A
0.0	N/A
0.0	N/A
0.0	N/A
0.0	N/A
0.0	N/A
0.0	N/A
0.0	N/A
0.0	N/A
0.0	N/A

Figure B.1b – Example #1 SPT Spreadsheet

Factors of safety and probability of liquefaction

[illegible]	[illegible]	[illegible]	[illegible]	[illegible]	Overburden correction factor K_σ	Factor of safety = (CRR / CSR) *MSF *K_σ	COV of Factor of Safety	Probability of liquefaction given design earthquake	Probability of liquefaction per year
21.0	0.127	0.080	1.78	0.79	1.00	2.82	55%	4%	1.6E-05
26.0	0.115	0.082	1.78	0.80	1.00	2.48	56%	7%	2.7E-05
31.0	0.457	0.084	1.78	0.69	1.00	9.73	56%	0%	7.9E-09
36.0	V. High	0.082	1.78	0.66	0.96	V. High	56%	V. Low	V. Low
21.0	0.103	0.080	1.78	0.80	1.00	2.30	55%	9%	3.5E-05
26.0	0.300	0.082	1.78	0.71	1.00	6.47	56%	0%	1.7E-07
31.0	0.298	0.084	1.78	0.69	1.00	6.35	56%	0%	2.1E-07
36.0	V. High	0.082	1.78	0.60	0.95	V. High	56%	V. Low	V. Low
0.0	N/A	N/A	1.78	0.60	1.00	N/A	53%	N/A	N/A
0.0	N/A	N/A	1.78	0.60	1.00	N/A	53%	N/A	N/A
0.0	N/A	N/A	1.78	0.60	1.00	N/A	53%	N/A	N/A
0.0	N/A	N/A	1.78	0.60	1.00	N/A	53%	N/A	N/A
0.0	N/A	N/A	1.78	0.60	1.00	N/A	53%	N/A	N/A
0.0	N/A	N/A	1.78	0.60	1.00	N/A	53%	N/A	N/A
0.0	N/A	N/A	1.78	0.60	1.00	N/A	53%	N/A	N/A
0.0	N/A	N/A	1.78	0.60	1.00	N/A	53%	N/A	N/A
0.0	N/A	N/A	1.78	0.60	1.00	N/A	53%	N/A	N/A
0.0	N/A	N/A	1.78	0.60	1.00	N/A	53%	N/A	N/A
0.0	N/A	N/A	1.78	0.60	1.00	N/A	53%	N/A	N/A
0.0	N/A	N/A	1.78	0.60	1.00	N/A	53%	N/A	N/A

Figure B.1c – Example #1 SPT Spreadsheet

Coefficients of variation

[illegible]	[illegible]	[illegible]	[illegible]	[illegible]	[illegible]	[illegible]	[illegible]	[illegible]	[illegible]	COV(CRR) due to fines content	COV(σ_{vo})	[illegible]	[illegible]
21.0	14%	10%	1%	24%	3%	4.2	1.2	0.139	0.111	2%	9%	14%	17%
26.0	15%	10%	1%	24%	3%	4.1	1.1	0.127	0.100	2%	9%	15%	17%
31.0	16%	10%	1%	24%	3%	9.4	5.5	V. High	0.347	0%	9%	16%	17%
36.0	16%	10%	1%	24%	3%	5.8	1.6	V. High	V. High	0%	9%	16%	17%
21.0	14%	10%	1%	24%	3%	5.6	4.9	0.103	0.097	0%	9%	14%	17%
26.0	15%	10%	1%	24%	3%	8.6	5.2	0.326	0.259	5%	9%	15%	17%
31.0	16%	10%	1%	24%	3%	5.3	1.5	0.339	0.261	6%	9%	16%	17%
36.0	16%	10%	1%	24%	3%	0.3	0.0	V. High	V. High	0%	9%	16%	17%
0.0	9%	10%	1%	24%	3%	0.0	0.0	N/A	N/A	0%	9%	9%	17%
0.0	9%	10%	1%	24%	3%	0.0	0.0	N/A	N/A	0%	9%	9%	17%
0.0	9%	10%	1%	24%	3%	0.0	0.0	N/A	N/A	0%	9%	9%	17%
0.0	9%	10%	1%	24%	3%	0.0	0.0	N/A	N/A	0%	9%	9%	17%
0.0	9%	10%	1%	24%	3%	0.0	0.0	N/A	N/A	0%	9%	9%	17%
0.0	9%	10%	1%	24%	3%	0.0	0.0	N/A	N/A	0%	9%	9%	17%
0.0	9%	10%	1%	24%	3%	0.0	0.0	N/A	N/A	0%	9%	9%	17%
0.0	9%	10%	1%	24%	3%	0.0	0.0	N/A	N/A	0%	9%	9%	17%
0.0	9%	10%	1%	24%	3%	0.0	0.0	N/A	N/A	0%	9%	9%	17%
0.0	9%	10%	1%	24%	3%	0.0	0.0	N/A	N/A	0%	9%	9%	17%
0.0	9%	10%	1%	24%	3%	0.0	0.0	N/A	N/A	0%	9%	9%	17%

Figure B.1d – Example #1 SPT Spreadsheet

Example #2 – Evaluation of SPT data with modified seismic parameters
Project Location: Newark, NJ (07100 – 07199)
Project Engineer: Langan Engineering

The SPT data and soil profile used in this example are the same as example #1. The seismic parameters were modified in this example to illustrate the occurrence of liquefaction.

1. Determine the soil profile, depth to water table, and depth to bedrock, or at least the bottom of any potentially liquefiable layers. Also, characterize the soil and rock types and determine properties needed for computation of the *CSR*.

2. Estimate the maximum ground surface acceleration, a_{max}.

   Normally the steps taken to estimate a_{max} would follow those described in section 4. For the purpose of this example assume the following values:

   $M_w = 7.5$
   $a_{max} = 0.35g$
   2% probability of exceedence
   50 year return period

3. Determine the depth reduction factor, r_d, using the average values found in Table 6.1

   The depth reduction factor is calculated at depths corresponding to the measured SPT N-values. Using the example point of 26 feet, the r_d is calculated as follows:

   $r_d = 1 - 0.00233 \cdot z$ for $z < 30$ feet
   $r_d = 1 - 0.00233 \cdot 26 = 0.94$
   $r_d = 0.94$ at 26 feet

4. Compute the Cyclic Stress Ratio, *CSR*, using equation 1-2.

   Like r_d, the CSR is calculated at the depths which correspond to the measured SPT N-values. The first step to calculating the CSR, however, is calculating both the total and effective vertical stresses at that point.

   Total and effective vertical stresses are calculated as follows:

   $\sigma_v = \gamma_t \cdot z$
   $\sigma'_v = \gamma_t \cdot z$ for $z \leq z_w$
   $= \gamma_t \cdot z + (\gamma_t - \gamma_w)*(z - z_w)$ for $z > z_w$

At a depth of 26 feet the values for total and effective vertical stress are as follows:

$$\sigma_v = (110\text{ pcf})\cdot 6\text{ ft}) + (120\text{ pcf})\cdot(20\text{ ft}) = 3060\text{ psf}$$
$$\sigma'_v = (110\text{ pcf})\cdot(6\text{ ft}) + (120\text{-}62.4\text{ pcf})\cdot(20\text{ ft}) = 1812\text{ psf}$$

After calculating the total and effective vertical stresses for the profile, the *CSR* at each point corresponding to a SPT *N*-value is calculated as follows:

$$CSR = 0.65\left(\frac{a_{\max}}{g}\right)\left(\frac{\sigma_v}{\sigma'_v}\right)r_d$$

At a depth of 26 feet, the *CSR* is as follows:

$$CSR = 0.65\left(\frac{0.35g}{g}\right)\left(\frac{3060}{1812}\right)0.94 = 0.361$$

5. Compute the Cyclic Resistance Ratio, *CRR*, for a Magnitude 7.5 earthquake using equation 7-1.

The first step in determining the *CRR* is to calculate the corrected SPT *N*-value, $(N_1)_{60}$, at each depth. The formula for calculating $(N_1)_{60}$ is as follows:

$$(N_1)_{60} = N\cdot C_N\cdot C_E\cdot C_R\cdot C_S\cdot C_B$$

For the given project, $C_B = C_S = 1.0$, and $C_E = 1.05$ for an automatic hammer. Values for C_R and C_N are calculated at each depth corresponding to a SPT N-value, and are tabulated in the "CRR" section of the attached spreadsheet. The calculations for the latter two parameters at the example depth of 26 feet are as follows:

C_R for a depth ranging from 20-30 feet is 0.95

$$C_N = 2.2/(1.2 + (\sigma'_{vo}/P_a))$$
$$C_N = 2.2/(1.2 + (0.906/1.06)) = 1.07$$

So, the $(N_1)_{60}$ value at a depth of 26 feet in boring B-5 is as follows:

$$(N_1)_{60} = 17\cdot 1.07\cdot 1.05\cdot 0.95\cdot 1.0\cdot 1.0 = 18\text{ bl/ft}$$

Next, the clean sand equivalent of the SPT N-value, or $(N_1)_{60cs}$, is calculated using equation 7-2. The value of $(N_1)_{60cs}$ calculated for a depth of 26 feet in boring B-5 is as follows:

$$(N_1)_{60cs} = \alpha + \beta\cdot(N_1)_{60}$$
$$(N_1)_{60cs} = 4.71 + 1.15\cdot 18 = 25\text{ bl/ft}$$

Finally, calculate $CRR_{7.5}$ as follows:

$$CRR_{7.5} = \left(\frac{1}{34-(N_1)_{60cs}}\right) + \left(\frac{(N_1)_{60cs}}{135}\right) + \left(\frac{50}{[10(N_1)_{60cs}+45]^2}\right) - \frac{1}{200}$$

$$CRR_{7.5} = 0.111 + 0.185 + 0.001 - 0.005 = 0.300$$

6. Calculate the Magnitude Scaling Factor, *MSF*.

   The *MSF* for the site is calculated using the following formula recommended by Youd and Idriss et al:

$$MSF = \frac{10^{2.84}}{M_w^{3.24}}$$

$$MSF = \frac{10^{2.84}}{7.5^{3.24}} = 1.01$$

7. Calculate the Overburden Correction Factor, K_σ.

   The overburden correction factor is calculated using equation 6-21, which is in terms of corrected SPT blow counts within the material. For the example point of 26 feet deep in boring B-5, K_σ is as follows:

$$K_\sigma = \left(\frac{\sigma'_{vo}}{P_a}\right)^{-0.5\sqrt{\frac{(N_1)_{60}}{23.2\sigma'_{vo}+32.2}}}$$

$$K_\sigma = \left(\frac{0.906}{1.06}\right)^{-0.5\sqrt{\frac{18}{53.22}}} = 1.00$$

8. Compute the Factor of Safety against liquefaction using equation 1-1.

$$FS = \left(\frac{CRR_{7.5}}{CSR}\right) MSF \cdot K_\sigma \cdot K_\alpha$$

$$FS = \left(\frac{0.300}{0.361}\right) \cdot 1.01 \cdot 1.00 \cdot 1.00 = 0.84$$

9. Compute the Probability of Liquefaction, P_L, as outlined in Section 3.

Using the outline presented in Section 3 of the text, the probability of liquefaction for the site at a depth of 26 feet in boring B-5, the probability of liquefaction was calculated to be as follows:

$$P_L = 73\%$$

Example #3 – Comparison of CPT Probabilistic Liquefaction analyses of Moss Landing cases during the 1989 Loma Prieta Earthquake
Project Location: Monterey Bay, California

The purpose of this example is to compare the results from the Juang et al. (1999) example and to help clarify the CPT-based procedure used in the current study. Table B-5 contains CPT test data and stress conditions for 20 different cases at Moss Landing. The stresses are not calculated in this example, rather taken from Juang et al.

Table B-5 – Total and vertical stresses along with CPT tip and sleeve resistance values for 20 case histories at Moss Landing (after Juang et al. 1999)

Case #	σ_{vo} (psf)	σ'_{vo} (psf)	q_c (psi)	f_s (psi)
UC-1	4336.8	2695.6	667.0	6.7
UC-2	864.4	816.4	1508.0	4.8
UC-3	941.7	816.4	1261.5	4.4
UC-4	941.7	816.4	1116.5	3.0
UC-4	3660.3	2265.5	3625.0	9.8
UC-6	2514.0	1605.7	2639.0	4.5
UC-7	3271.9	1969.0	623.5	11.2
UC-8	3345.0	2006.6	623.5	8.1
UC-9	1121.3	816.4	957.0	2.9
UC-10	1054.4	816.4	449.5	1.8
UC-11	1110.8	816.4	449.5	1.6
UC-12	1609.8	1146.3	899.0	8.1
UC-13	1609.8	1146.3	623.5	6.2
UC-14	1098.3	891.6	551.0	2.8
UC-15	1098.3	891.6	435.0	1.7
UC-16	822.7	816.4	957.0	4.2
UC-17	1611.9	1294.6	783.0	3.1
UC-18	1459.5	1336.3	2378.0	6.4
UC-20	1772.7	1426.1	594.5	3.4
UC-21	1582.7	1273.7	710.5	3.4

The a_{max} and M_w for this site are 0.25g and 7.1. Since no indication is given as to the return period and probability of exceedence, this example assumes that the earthquake has a 50 year return period with a 2% probability of exceedence.

The following steps outline the procedure used to calculate the factor of safety and the probability of liquefaction for Case UC-1 from table B-5 for the current study. These calculations are the same as those executed in the CPT spreadsheet (appendix A), with several exceptions: the total stress, vertical stress, and *CSR* values are taken from Juang et al. This example explicitly shows how the CPT spreadsheet determines the final *CRR* value used to determine the factor of safety and the probability of liquefaction. The *CSR* value for Case UC-1 is 0.20 (Juang et al., 1999).

1. Determine n, C_Q, Q, F, q_{c1N}, and I_c per Youd and Idriss et al (2001)

   Initially assume n is 1.0, and then calculate Q (equation 8-6), F (equation 8-7) and I_c (equations 8-8, 8-9, and 8-10). If the calculated I_c value is greater than 2.6 use n=1.0 for the remaining calculations. However, if I_c is less than or equal to 2.6 recalculate Q and I_c with n=0.5. If the recalculated I_c is less than 2.6 use n=0.5. However, if the recalculated I_c is greater than or equal to 2.6, calculate C_Q, Q, F, q_{c1N}, and I_c with n=0.7.

$$Q = [(q_c - \sigma_{vo})/P_a][(P_a/\sigma'_{vo})^n]$$

$$Q = [(667\text{psi} - (4336.8\text{psf}/144))/14.5\text{psi}][(14.5\text{psi}/(2695.6\text{psf}/144))^{1.0}] = 34.02$$

$$F = [f_s/(q_c - \sigma_{vo})]*100$$

$$F = [6.7\text{psi}/(667\text{psi} - (4336.8\text{psf}/144))]*100 = 1.05$$

$$I_c = [(3.47 - \log Q)^2 + (1.22 + \log F)^2]^{0.5}$$

$$I_c = [(3.47 - \log 34.02)^2 + (1.22 + \log 1.05)^2]^{0.5} = 2.30$$

   Because I_c is less than 2.6 recalculate Q and I_c with n=0.5:

$$Q = [(667\text{psi} - (4336.8\text{psf}/144))/14.5\text{psi}][(14.5\text{psi}/(2695.6\text{psf}/144))^{0.5}] = 38.66$$

$$I_c = [(3.47 - \log 38.66)^2 + (1.22 + \log 1.05)^2]^{0.5} = 2.25$$

   Because the re-calculated I_c is less than 2.6, the recalculated I_c is used to determine K_c. However, if the recalculated I_c had been greater than or equal to 2.6, a linear stress exponent of 0.7 would have been used to calculate Q and I_c for a third time before calculating K_c.

   With the linear stress exponent used to determine the final I_c value, compute C_Q and q_{c1N} with equations 8-15 and 8-11. Youd and Idriss et al. recommend that C_Q values less than 1.7 should not be applied.

$$C_Q = \left(\frac{P_a}{\sigma'_{vo}}\right)^n$$

$$C_Q = \left(\frac{14.5\text{psi}}{2695.6\text{psf}/144}\right)^{0.5} = 0.88$$

$$q_{c1N} = \left(\frac{q_c}{P_a}\right)C_Q$$

$$q_{c1N} = \left(\frac{667\text{psi}}{14.5\text{psi}}\right)0.88 = 40.5$$

2. Compute K_c and $(q_{c1N})_{cs}$

   K_c is calculated using either equation 8-4 or 8-5 depending on the final I_c value.

$$K_c = 1.0 \quad \text{for } I_c \le 1.64$$
$$K_c = -0.403I_c^4 + 5.581I_c^3 - 21.63I_c^2 + 33.75I_c - 17.88 \quad \text{for } I_c > 1.64$$
$$I_c = 2.25$$
$$K_c = -0.403(2.25)^4 + 5.581(2.25)^3 - 21.63(2.25)^2 + 33.75(2.25) - 17.88 = 1.81$$

   $(q_{c1N})_{cs}$ is calculated using equation 8-3:

$$(q_{c1N})_{cs} = K_c(q_{c1N})$$
$$(q_{c1N})_{cs} = 1.81 \cdot 40.5 = 73.3$$

3. Calculate the $CRR_{7.5}$ value

   $CRR_{7.5}$ can be directly read off of figure 8-1 or approximated with equations 8-1 and 8-2.

$$CRR_{7.5} = 0.833[(q_{c1N})_{cs}/1000] + 0.05 \quad \text{if } (q_{c1N})_{cs} < 50$$

$$CRR_{7.5} = 93[(q_{c1N})_{cs}/1000]^3 + 0.08 \quad \text{if } 50 \le (q_{c1N})_{cs} < 150$$

$$(q_{c1N})_{cs} = 73.3$$
$$CRR_{7.5} = 93.0[73.3/1{,}000]^3 + 0.08 = 0.12$$

4. Calculate the Magnitude Scaling Factor, (MSF).

The *MSF* for the site is calculated using the following formula recommended by Youd and Idriss et al:

$$MSF = \frac{10^{2.84}}{M_w^{3.24}}$$

$$MSF = \frac{10^{2.84}}{7.1^{3.24}} = 1.21$$

5. Calculate the Overburden Correction Factor, K_σ.

   The overburden correction factor is calculated from the f coefficient for relative density using equations 6-11. The f coefficient is obtained from equations 6-12 and 6-13. The CPT spreadsheet uses the equation on figure 6.19 to approximate the relative density based on q_c.

$$D_R(\%) = -98 + 66\log\left(\frac{q_c}{\sigma'^{0.5}_{vo}}\right)$$

$$D_R(\%) = -98 + 66\log\left(\frac{667\,psi}{(2695.6\,psf/144^{0.5}}\right) = 46\%$$

$$f = 0.7 - 0.8 \text{ for } D_r = 40\text{-}60\%$$

$$f = 0.6 - 0.7 \text{ for } D_r = 60\text{-}80\%$$

$$f = 1\text{-}0.005(46\%) = 0.77$$

$$K_\sigma = \left(\frac{(2695.6\,psf/144)}{14.5\,psi}\right)^{0.77-1} = 0.95$$

6. Compute the Factor of Safety, *FS*, against liquefaction using equation 1-1.

$$FS = \left(\frac{CRR_{7.5}}{CSR}\right) MSF \cdot K_\sigma \cdot K_\alpha$$

$$FS = \left(\frac{0.12}{0.20}\right) \cdot 1.21 \cdot 0.95 \cdot 1.00 = 0.7$$

7. Compute the Probability of Liquefaction, P_L, as outlined in Section 3.

   Using the outline presented in Section 3 of the text, the P_L for Case UC-1 was calculated as 96%.

Table B-6and Figure B.2 show values of factor of safety and probability of liquefaction for the 20 Moss Landing case histories for this study and that of Juang et al. (1999). As

can be seen, the factors of safety and probability of liquefaction calculated from the proposed simplified procedure are comparable to those calculated by Juang et al. (1999).

Table B-6 – Factors of safety and probabilities of liquefaction for 20 Moss Landing case histories.

	Factor of Safety against Liquefaction		Probability of Liquefaction, given design earthquake	
Case #	Current	Juang et al. (1999)	Current	Juang et al. (1999)
UC-1	0.7	0.6	96%	78%
UC-2	4.8	2.8	0%	0%
UC-3	2.5	2.0	7%	0%
UC-4	1.9	1.6	19%	1%
UC-4	3.4	2.7	2%	0%
UC-6	3.5	2.6	2%	0%
UC-7	0.9	0.7	82%	55%
UC-8	0.7	0.6	92%	76%
UC-9	1.2	1.0	57%	13%
UC-10	0.7	0.6	92%	75%
UC-11	0.6	0.5	94%	81%
UC-12	1.2	1.0	61%	16%
UC-13	0.9	0.7	82%	50%
UC-14	0.8	0.7	85%	56%
UC-15	0.7	0.6	91%	75%
UC-16	1.7	0.5	26%	1%
UC-17	0.9	0.7	82%	52%
UC-18	4.8	3.6	0%	0%
UC-20	0.8	0.6	88%	72%
UC-21	0.8	0.7	84%	57%

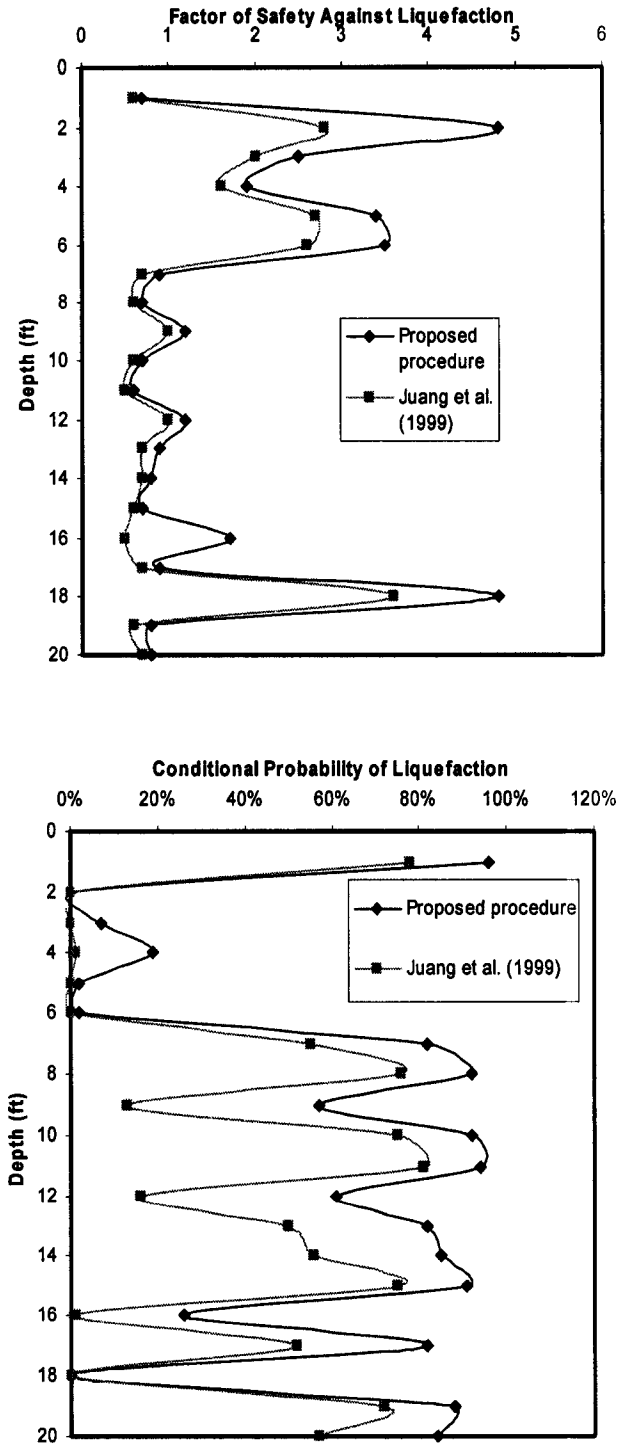

Figure B.2 - Factor of safety against liquefaction and conditional probability of liquefaction from proposed method and from Juang et al. (1999)